EUROPEAN ORGANISATION FOR NUCLEAR RESEARCH (CERN)

Submitted to: JHEP

CERN-EP-2024-218
October 24, 2024

Search for supersymmetry in final states with missing transverse momentum and charm-tagged jets using 139 fb^{-1} of proton–proton collisions at $\sqrt{s}$ = 13 TeV with the ATLAS detector

The ATLAS Collaboration

The paper presents a search for supersymmetric particles produced in proton–proton collisions at $\sqrt{s}$ = 13 TeV and decaying into final states with missing transverse momentum and jets originating from charm quarks. The data were taken with the ATLAS detector at the Large Hadron Collider at CERN from 2015 to 2018 and correspond to an integrated luminosity of 139 fb^{-1}. No significant excess of events over the expected Standard Model background expectation is observed in optimized signal regions, and limits are set on the production cross-sections of the supersymmetric particles. Pair production of charm squarks or top squarks, each decaying into a charm quark and the lightest supersymmetric particle $\tilde{\chi}_1^0$, is excluded at 95% confidence level for squarks with masses up to 900 GeV for scenarios where the mass of $\tilde{\chi}_1^0$ is below 50 GeV. Additionally, the production of leptoquarks with masses up to 900 GeV is excluded for the scenario where up-type leptoquarks decay into a charm quark and a neutrino. Model-independent limits on cross-sections and event yields for processes beyond the Standard Model are also reported.

Contents

1 Introduction

Supersymmetric (SUSY) extensions of the Standard Model (SM) of particle physics predict new particles which are partners of SM particles [1–6] – the partners of SM fermions being bosons and those of SM bosons being fermions – and provide solutions to the hierarchy problem [7–10]. R-parity-conserving SUSY models [11] are considered in this paper and predict that the supersymmetric partners of quarks (squarks) will be produced in pairs at the Large Hadron Collider (LHC) and that the lightest SUSY particle (LSP) is stable. The lightest neutralino, $\tilde{\chi}_1^0$, is considered to be the LSP and is a dark-matter candidate [12, 13].

The search described in this paper targets SUSY models where top or charm squarks ($\tilde{t}_1/\tilde{c}_1$) are the lightest squarks, with masses less than about one TeV [14]. For top squarks considered in this search, flavour-violating effects allow the top squark to decay into a charm quark and an LSP, as shown in Figure 1(a). This results in a final state with two charm quarks and missing transverse momentum from the LSPs, which escape detection. The extent of flavour-violating effects is model dependent, but when there is significant mixing between the top squark and the charm squark [15], the branching fraction of $\tilde{t}_1 \to c\tilde{\chi}_1^0$ can exceed the branching fraction of $\tilde{t} \to t^*\tilde{\chi}_1^0$, where t^* can be either an on-shell or off-shell top quark.

In supersymmetric models with minimal flavour-violating effects, charm squarks could be considerably lighter than other squarks. This motivates searches for pair production of charm squarks, with each charm squark decaying into a charm quark and an LSP as shown in Figure 1(b). Notably, the model of charm squark pair production in Figure 1(b) shares the same experimental signature and production cross-section as for the top squark pairs in Figure 1(a). The experimental signature includes jets that contain charm hadrons but no bottom hadrons and momentum imbalance caused by the two LSPs. The search discussed in this paper was optimized for the case where the branching fraction of the decay of top or charm squark into a charm quark plus the LSP is unity. However, the results of the search are also interpreted in the scenario of top squark production with a varying branching fraction of the top squark decay into a charm quark plus the LSP ranging from 0.1 to 1, with the alternative decay being to a top quark plus the LSP.

Leptoquark (LQ) models [16–24] with up-type scalar LQs (LQ^{u}) or vector LQs (vLQ) predict their pair production and subsequent decay into $c\nu c\nu$, with the same experimental signature as in top and charm squark production models (see Figure 1(c)). The following models are considered: U_1 vLQ models that couple to second-generation quarks and third-generation leptons ($\mathrm{vLQ}^{\mathrm{u}}_{23}$, where the subscript indicates the quark and lepton generations) in both the minimal and Yang–Mills coupling scenarios [25,

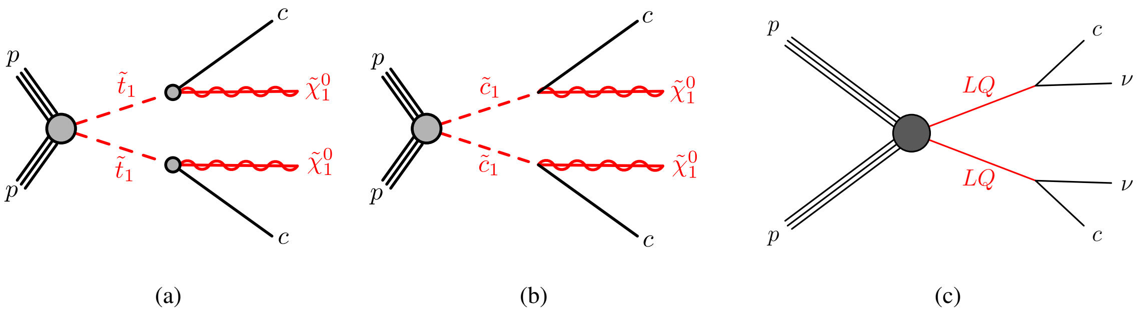

(a) (b) (c)

Figure 1: Representative diagrams for pair production of (a) top squarks ($\tilde{t}_1$) and (b) charm squarks ($\tilde{c}_1$), with subsequent decay into charm quarks and neutralinos ($\tilde{\chi}_1^0$), and (c) pair production of leptoquarks decaying into charm quarks and neutrinos.

26], assuming a branching fraction ($\mathcal{B}$) of $\mathcal{B}(\mathrm{vLQ}^{\mathrm{u}}_{23} \rightarrow c\nu_\tau) = 0.5$ in both cases with the alternative decay being $\mathrm{vLQ}^{\mathrm{u}}_{23} \rightarrow s\tau$; and models where scalar LQs couple to second-generation quarks and first- or second-generation leptons [27–29], allowing a range of $\mathcal{B}(\mathrm{LQ}^{\mathrm{u}} \rightarrow c\nu_{e/\mu})$ values (here the alternative decay is $\mathrm{LQ}^{\mathrm{u}} \rightarrow se/\mu$).

This search for top squark, charm squark, and leptoquark pair production uses pp collisions from the LHC at a centre-of-mass energy of $\sqrt{s} = 13$ TeV recorded by the ATLAS experiment from 2015 to 2018. A previous search by ATLAS [30], based on the identification of jets containing charm hadrons but no bottom hadrons (c-tagging), used 36.1 fb^{-1} of collisions and was able to probe top and charm squark masses up to 850 GeV. In addition to a larger dataset, the search herein also benefits from improvements in c-tagging and from an advanced technique, Recursive Jigsaw Reconstruction [31], which provides sensitivity to models with small mass splittings between the top squark and the LSP. Other ATLAS results also have sensitivity to the models considered in this paper: a search using final states with an energetic jet (but no c-tagging) and large missing transverse momentum [32] was particularly sensitive to models with small mass differences between the top/charm squark and the LSP, while a search for single squark production that did not utilize c-tagging [33] had good sensitivity to models with large top/charm squark masses, and a more recent search for top squark pair production focused on squarks decaying into either a top quark or charm quark plus an LSP [34]. The most recent search performed by the CMS Collaboration [35] used 137 fb^{-1} of $\sqrt{s} = 13$ TeV pp collisions from the LHC, but only considered mass differences between the top squark and the LSP of less than 80 GeV, while the present ATLAS search explores mass differences ranging from 20 GeV to about 1 TeV. Finally, for the considered leptoquark models, this paper is the first to report results from the full Run 2 dataset of an LHC experiment.

2 ATLAS detector

The ATLAS detector [36] at the LHC covers nearly the entire solid angle around the collision point.[1] It consists of an inner tracking detector surrounded by a thin superconducting solenoid, electromagnetic and hadronic calorimeters, and a muon spectrometer incorporating three large superconducting air-core toroidal magnets.

The inner-detector system (ID) is immersed in a 2 T axial magnetic field and provides charged-particle tracking in the range $|\eta| < 2.5$. The high-granularity silicon pixel detector covers the vertex region and typically provides four measurements per track, the first hit generally being in the insertable B-layer (IBL) installed before Run 2 [37, 38]. It is followed by the SemiConductor Tracker (SCT), which usually provides eight measurements per track. These silicon detectors are complemented by the transition radiation tracker (TRT), which enables radially extended track reconstruction up to $|\eta| = 2.0$. The TRT also provides electron identification information based on the fraction of hits (typically 30 in total) above a higher energy-deposit threshold corresponding to transition radiation.

The calorimeter system covers the pseudorapidity range $|\eta| < 4.9$. Within the region $|\eta| < 3.2$, electromagnetic calorimetry is provided by barrel and endcap high-granularity lead/liquid-argon (LAr)

---

[1] ATLAS uses a right-handed coordinate system with its origin at the nominal interaction point (IP) in the centre of the detector and the z-axis along the beam pipe. The x-axis points from the IP to the centre of the LHC ring, and the y-axis points upwards. Polar coordinates (r, ϕ) are used in the transverse plane, ϕ being the azimuthal angle around the z-axis. The pseudorapidity is defined in terms of the polar angle θ as $\eta = -\ln\tan(\theta/2)$ and is equal to the rapidity $y = \frac{1}{2}\ln\left(\frac{E+p_z}{E-p_z}\right)$ in the relativistic limit. Angular distance is measured in units of $\Delta R \equiv \sqrt{(\Delta y)^2 + (\Delta\phi)^2}$.

calorimeters, with an additional thin LAr presampler covering $|\eta| < 1.8$ to correct for energy loss in material upstream of the calorimeters. Hadronic calorimetry is provided by the steel/scintillator-tile calorimeter, segmented into three barrel structures within $|\eta| < 1.7$, and two copper/LAr hadronic endcap calorimeters. The solid angle coverage is completed with forward copper/LAr and tungsten/LAr calorimeter modules optimised for electromagnetic and hadronic energy measurements respectively.

The muon spectrometer (MS) comprises separate trigger and high-precision tracking chambers measuring the deflection of muons in a magnetic field generated by the superconducting air-core toroidal magnets. The field integral of the toroids ranges between 2.0 and 6.0 T m across most of the detector. Three layers of precision chambers, each consisting of layers of monitored drift tubes, cover the region $|\eta| < 2.7$, complemented by cathode-strip chambers in the forward region, where the background is highest. The muon trigger system covers the range $|\eta| < 2.4$ with resistive-plate chambers in the barrel, and thin-gap chambers in the endcap regions.

The luminosity is measured mainly by the LUCID–2 [39] detector that records Cherenkov light produced in the quartz windows of photomultipliers located close to the beampipe.

Events are selected by the first-level trigger system implemented in custom hardware, followed by selections made by algorithms implemented in software in the high-level trigger [40]. The first-level trigger accepts events from the 40 MHz bunch crossings at a rate below 100 kHz, which the high-level trigger further reduces in order to record complete events to disk at about 1 kHz.

A software suite [41] is used in data simulation, in the reconstruction and analysis of real and simulated data, in detector operations, and in the trigger and data acquisition systems of the experiment.

3 Data and simulated event samples

The data used in this analysis were recorded with a fully operational detector from stable-proton-beam collisions, and are clear of a significant amount of cosmic-ray or beam-induced background [42]. The total integrated luminosity of this dataset is 139.0 ± 2.4 fb^{-1} [43], determined using the LUCID-2 detector [44] for the primary luminosity measurements, complemented by measurements from the inner detector and calorimeters. The LHC accelerates and collides protons in bunches and there are multiple pp collisions in every bunch crossing in addition to the much less frequent hard-scattering collisions of interest. The bunch crossings happen every 25 ns. The average number of additional proton–proton interactions per bunch crossing (pileup) grew from 13 in 2015 to a value of about 38 in 2017.

Missing transverse momentum triggers were used to select the data [45] for this analysis. The triggers had thresholds of 70 GeV in 2015 and early 2016, 100 GeV in late 2016 and 2017, and 110 GeV in 2018. These triggers reach an efficiency plateau for offline missing transverse momenta greater than 200 GeV.

The predictions for signal and background contributions are obtained with Monte Carlo (MC) simulated event samples. To match the LHC beam conditions, these simulated event samples also contain pileup interactions. The simulated events were processed through the ATLAS detector simulation [46] and then subjected to the same reconstruction algorithms as the data. All samples were processed with the full Geant4 [47] detector model with the exception of the samples with leptoquarks or direct top or charm squark production which were processed with Atlfast-II detector simulations [48]. Finally, the simulated samples were corrected to improve the accuracy of the pileup modelling, jet momenta, lepton efficiency and momenta, trigger efficiencies, missing transverse momentum, and c-tagging efficiency.

Table 1: Overview of the simulated background samples. The simulated vector bosons, V, are massive W and Z bosons. The NNPDF3.0NLO [51] parton distribution functions (PDF) set is used.

Background process	Matrix element generator	PDF accuracy	Parton showering and hadronization	Underlying event tune	Cross-section calculation accuracy
$pp \to V$+jets	SHERPA 2.2.11 [49]	NNLO	SHERPA	Default	NNLO [52]
$pp \to t\bar{t}V$+jets	aMC@NLO 2.3.3 [53]	NLO	PYTHIA 8.210 [54]	A14 [55]	NLO [53]
$pp \to t\bar{t}$+jets	POWHEG BOX v2 [56]	NNLO	PYTHIA 8.230	A14	NNLO+NNLL [57–62]
$pp \to t$+jets / tW+jets	POWHEG BOX v2	NNLO	PYTHIA 8.230	A14	NNLO+NNLL [63–65]
$pp \to VV$+jets	SHERPA 2.2.1–2.2.2 [66]	NNLO	SHERPA	Default	NLO

Standard Model background samples were produced with various event generators as shown in Table 1. All samples, except the ones that use the SHERPA event generator [49], were processed with EVTGEN 1.7.0 [50] for the b- and c-hadron decays. The cross-sections, which were used to normalize the samples, were calculated separately with higher-order corrections in the strong coupling (α_s) for all samples except for the diboson production ($pp \to VV$+jets) sample, where the cross-section calculated by the SHERPA event generator was retained. For the SHERPA sample of single vector bosons produced in association with jets (V+jets), virtual electroweak loop-terms were included at next-to-leading-order (NLO) accuracy.

The SUSY event samples were generated with MADGRAPH5_aMC@NLO 2.8.1 [53] at leading order (LO) in the strong coupling constant (α_s) with up to two additional partons using the NNPDF3.0NLO [51] parton distribution function (PDF) set and were showered and hadronized with PYTHIA 8.244 [54] using the A14 set of tuned parameters (tune) in PYTHIA [55]. Samples with a small mass difference between the top squark and $\tilde{\chi}_1^0$ (up to 140 GeV) were generated with MADGRAPH5_aMC@NLO 2.9.5 and then interfaced with PYTHIA 8.306. These samples were also processed with EVTGEN 1.7.0.

The top squark and charm squark signal cross-sections were calculated from pair production of scalar coloured particles and with the gluino assumed to be massive enough to not significantly contribute to the production process. Consequently, each production cross-section depends only on the squark mass. These cross-sections are computed at approximate next-to-next-to-leading-order (NNLO) accuracy in α_s with resummation of next-to-next-to-leading logarithmic (NNLL) soft gluon terms [67–70].

The samples with pair-produced scalar LQs were generated with matrix elements calculated at NLO accuracy in α_s with MADGRAPH5_aMC@NLO 2.6.0 [53], using the method described in Ref. [27], in which NLO matrix elements [28, 29] are interfaced to PYTHIA 8.230. The total cross-sections of scalar LQ pair production were computed at approximate NNLO accuracy in α_s with resummation of NNLL soft gluon terms [67–70]. The cross-sections do not include lepton t-channel contributions, which are neglected in Ref. [27] and may lead to corrections at the percent level [71]. For vector-LQ pair production, the matrix elements were calculated at LO in α_s following the model described in Ref. [25], and events were generated using MADGRAPH5_aMC@NLO 2.9.5 in conjunction with PYTHIA 8.306. Parton luminosities were provided by the five-flavour scheme NNPDF3.0NLO PDF set and the underlying event was modelled with the A14 tune in PYTHIA. These samples were also processed with EVTGEN 1.7.0.

4 Event reconstruction

Events are required to have a primary vertex reconstructed from at least two tracks with transverse momentum $p_\text{T} > 0.5$ GeV. If more than one such vertex is found, the one with the largest sum of squares of transverse momenta of associated tracks is selected as the hard-scattering collision [72]. The other vertices are considered as pileup.

Hadronic jet candidates are reconstructed using the anti-k_t jet algorithm [73, 74] with radius parameter $R = 0.4$, using particle-flow objects (PFOs) [75] as inputs. PFOs are charged-particle tracks matched to the hard-scatter vertex with the requirement $|z_0 \sin(\theta)| < 2.0$ mm (where z_0 is the longitudinal impact parameter) and calorimeter energy clusters surviving an energy subtraction algorithm that removes the energy contributions deposited by good quality tracks from any vertex. Jet energy scale corrections, derived from MC simulation and data, are used to calibrate the average energies of jet candidates to the scale of their constituent particles [76]. Jets with $|\eta| < 4.5$ are used to calculate the missing transverse momentum [77], while jets with $p_\mathrm{T} > 20$ GeV and $|\eta| < 2.8$ are considered to be "signal" jets. Jets containing a large particle momentum contribution from pileup vertices, as measured by the jet vertex tagger (JVT) discriminant [78], are rejected if they have $p_\mathrm{T} < 60$ GeV, $|\eta| < 2.5$ and a discriminant value of JVT < 0.5.

Jets can be identified as c-tagged or b-tagged jets if they lie within the inner-detector acceptance of $|\eta| < 2.5$. To identify jets containing c-hadrons, the charm-tagging algorithm DL1r$_c$, optimized for a similar search [34], is used. The DL1r$_c$ algorithm is based on the ATLAS DL1r algorithm [79], which uses a selection of inputs including information about the impact parameters of ID tracks, the presence of displaced secondary vertices, and the reconstructed flight paths of b- and c-hadrons inside the jet. The algorithm provides three probabilities for a jet to either contain b-hadrons, c-hadrons, or light-flavor hadrons. These three probabilities are combined in a similar way to the b-tagging algorithm, but with fine-tuned parameters specifically optimized for identifying jets containing c-hadrons but not b-hadrons; the f_b parameter was set to 0.28. The DL1r b-tagging algorithm is used to identify b-jets which are no longer considered as potential c-jet candidates. The DL1r algorithm has 77% identification efficiency for b-jets and 20% and 0.9% misidentification probabilities for c-jets and light-flavor jets, respectively, evaluated in a sample of simulated SM $t\bar{t}$ events. The c-tagging algorithm (referred to as "c-tagging with b-veto") is tuned to have an efficiency of 20% by requiring that the final DL1r$_c$ discriminant be greater than 1.315. This corresponds to rejection factors of 29 for b-jets and 57 for light-flavor jets; and a τ-lepton misidentification efficiency of 15%. These efficiencies and rejections factors are determined with a sample of simulated $t\bar{t}$ events. Both the simulated c-jet identification efficiency and misidentification probabilities are corrected to match those measured in data. The approach employed is similar to that for b-tagging [80–82]. Between p_T ranges of 20 GeV and 250 GeV, the scale factors are compatible with unity for all jet-flavor corrections. For c-jets, the systematic uncertainties range from 17% for $p_\mathrm{T} < 65$ GeV to a few percent for higher-p_T jets (up to 3 TeV), while for b-jets and light-flavor jets, the uncertainties are 5-7% and approximately 13%, respectively, for all p_T ranges below 3 TeV. For b- and c-jets with $p_\mathrm{T} > 3$ TeV, the uncertainties on the scale factors are up to 30%.

Electron candidates are constructed from energy deposits in the EM calorimeter matched to an ID track. "Baseline" electron candidates, which are used to veto events with electrons, must pass a loose likelihood-based identification selection [83] and have $p_\mathrm{T} > 4.5$ GeV and $|\eta| < 2.47$. The longitudinal impact parameter of the ID track associated with a "baseline" electron is required to satisfy $|z_0 \sin(\theta)| < 0.5$ mm. Electrons used for regions rich in the dominant SM background processes with prompt electrons (i.e. W+jets and Z+jets) must meet further selection criteria: $p_\mathrm{T} > 10$ GeV, "Loose" isolation [83], $|d_0/\sigma(d_0)| < 5$ where d_0 is the transverse impact parameter and $\sigma(d_0)$ is its uncertainty, and the "Tight" likelihood-based identification selection [83]. Electrons satisfying these criteria are referred to as "signal" electrons.

Muon candidates are found by combining track segments from the inner detector and muon spectrometer or by extrapolating from the forward sections of the muon spectrometer, in the region $2.5 < |\eta| < 2.7$. "Baseline" muon candidates, which are used to veto events with muons, are required to pass "Medium" identification [84] and have $p_{\mathrm{T}} > 4$ GeV, $|\eta| < 2.7$, and $|z_0 \sin(\theta)| < 0.5$ mm. Muons passing the more stringent "Loose_VarRad" isolation [84], $|d_0/\sigma(d_0)| < 3$, and $p_{\mathrm{T}} > 10$ GeV requirements are referred to as "signal" muons.

Hadronically decaying τ-leptons are reconstructed from jets with $p_{\mathrm{T}} > 10$ GeV and either $|\eta| < 1.37$ or $1.52 < |\eta| < 2.5$ [85]. In addition, τ-lepton candidates must have $p_{\mathrm{T}} > 20$ GeV, one or three charged-particle tracks, and tracks with a total electric charge of ± 1 times the electron charge. The τ-leptons are also required to meet the "Loose" criterion of the neural-network-based identification algorithm [86].

To prevent double-counting of electrons as jets, jets within $\Delta R = 0.2$ of an electron are not considered further unless the jet is b-tagged; b-tagged jets are removed if the overlapping electron has $p_{\mathrm{T}} > 100$ GeV, otherwise the electron is removed. Muons are not counted if they are within $\Delta R = (0.04 + 10\ \mathrm{GeV}/p_{\mathrm{T}}(\mathrm{jet}))$ of a jet. This criterion is applied to remove muons from decays of b- and c-hadrons but retain high-p_{T} muons resulting from decays of high-p_{T} massive particles, which tend to be less isolated than muons from decays of low-p_{T} massive particles. Electrons that share an inner-detector track with a muon are discarded. If a τ-lepton candidate is found to overlap ($\Delta R < 0.2$) with a muon or electron, the τ-lepton is removed. Jets within $\Delta R = 0.4$ of a τ-lepton are removed. This removal of overlapping objects is only performed for baseline objects.

The missing transverse momentum $\vec{p}_{\mathrm{T}}^{\mathrm{miss}}$, with magnitude $E_{\mathrm{T}}^{\mathrm{miss}}$ [87], is calculated as the negative vector sum of the transverse momenta of jets, τ-leptons, electrons, and muons. Photons are counted as jets since they are not considered in this search. To account for the underlying event, the missing transverse momentum computation also considers tracks with $p_{\mathrm{T}} > 0.5$ GeV that are associated with the primary vertex but not with any reconstructed particle or jet.

The significance of missing transverse momentum, denoted by $E_{\mathrm{T}}^{\mathrm{miss}}$ Sig., is the ratio of $E_{\mathrm{T}}^{\mathrm{miss}}$ to its variance [88]. The variance is calculated using the p_{T} resolution of each component used to evaluate the $E_{\mathrm{T}}^{\mathrm{miss}}$. The correlation between the components is also included.

5 Event selection

The search uses simulated data to design signal regions that have sensitivity to the SUSY models of interest. Control regions that have high purity in particular background processes are used to estimate major background contributions; their normalizations are determined by the data and are extrapolated to the signal regions using simulation. The control regions are designed to not overlap with the signal regions, to have selection criteria similar to those of the signal regions so as to reduce uncertainties from the extrapolation, and to have only a small contamination from signal processes. In addition to the signal and control regions, validation regions are used to validate the background modelling before examining the recorded data in the signal regions (unblinding). Detailed descriptions of the statistical data analysis and how the SM backgrounds are constrained with a fit are provided in Section 7.

5.1 Signal regions

To maximize the discovery potential, the search uses two sets of signal regions targeting two drastically different kinematic regions: *High-Mass* and *Compressed*. The signal regions were designed using simulated event samples to maximize the expected sensitivity. The High-Mass signal regions are sensitive to leptoquark models and SUSY models with large leptoquark or top squark masses ($\gtrsim$ 600 GeV) and a large difference between the top squark and LSP masses ($\gtrsim$ 200 GeV); here $E_{\mathrm{T}}^{\mathrm{miss}}$-based variables are relied upon to separate signal events from background events. The Compressed signal regions are sensitive to SUSY models with both smaller top squark masses and compressed spectra, $\Delta m(\tilde{t}_1, \tilde{\chi}_1^0) \lesssim 175$ GeV; here the presence of high-momentum jets originating from initial-state radiation (ISR) and Recursive Jigsaw Reconstruction (RJR) [31] are used to suppress the SM background. The High-Mass and Compressed regions do not overlap because the High-Mass regions require the leading jet to be a c-tagged jet while the Compressed regions require the leading jet not to be c-tagged.

The signal models targeted in this search are expected to produce events that have significant $E_{\mathrm{T}}^{\mathrm{miss}}$ – even in the Compressed region for which additional jet activity boosts the neutralinos resulting in large $E_{\mathrm{T}}^{\mathrm{miss}}$ – so all events are required to have $E_{\mathrm{T}}^{\mathrm{miss}} > 250$ GeV. The signal processes do not produce any leptons, so events containing electrons, muons, or τ-leptons are vetoed. All regions, unless otherwise indicated, include jets with $p_{\mathrm{T}} > 20$ GeV and require at least one jet with $p_{\mathrm{T}} > 250$ GeV. For High-Mass signal regions, all jet-related variables are computed using jets with $p_{\mathrm{T}} > 40$ GeV. At least two jets must be present, and at least one must be identified as a c-tagged jet. To reject backgrounds originating from top-quark-pair ($t\bar{t}$) decays, events with b-tagged jets are discarded. Finally, the minimum azimuthal angle separation ($\Delta\phi$) between the (up to) four leading jets and the $\vec{p}_{\mathrm{T}}^{\mathrm{miss}}$ is required to be greater than 0.4 to reject multijet backgrounds, reducing them to negligible levels such that they need not be considered further in this search.

Three non-overlapping High-Mass signal regions, named SR-HM1, SR-HM2 and SR-HM3, are defined as shown in Table 2. The SUSY scenario with $\mathcal{B}(\tilde{t}_1/\tilde{c}_1 \rightarrow c + \tilde{\chi}_1^0) = 1$ and $m(\tilde{t}_1, \tilde{\chi}_1^0) = (1000, 1)$ GeV is used to optimize the selection for SR-HM1, while the scenario with $m(\tilde{t}_1, \tilde{\chi}_1^0) = (700, 400)$ GeV is used to optimize the selection for SR-HM2 and SR-HM3. All signal models are expected to produce two c-tagged jets, so all three regions require the presence of at least two c-tagged jets. Additionally, the signal models which are used to optimize the High-Mass signal regions are expected to have highly energetic c-tagged jets, motivating the requirement that the leading jet be c-tagged and that the subleading jet have a p_{T} ($p_{\mathrm{T}}(j_2)$) of at least 150 GeV. Standard Model background contributions with two c-tagged jets originating from real charm quarks are expected to be produced from $g \rightarrow c\bar{c}$, where g is a gluon, and m_{cc}, the invariant mass of the two highest-p_{T} c-tagged jets, is expected to have a falling spectrum. Thus, SR-HM1, SR-HM2, and SR-HM-3 require m_{cc} to be at least 200 GeV. Different m_{cc} requirements are made in SR-HM2 and SR-HM3 to target signal samples with $\Delta m(\tilde{t}_1, \tilde{\chi}_1^0) \sim 300$ GeV and ~ 400 GeV, respectively. An upper bound on m_{cc} was added to SR-HM3 to reject V+jets backgrounds where m_{cc} falls less steeply than in the signal samples above $m_{cc} \sim 600$ GeV. The minimum transverse mass $m_{\mathrm{T}}^{\mathrm{min}}(c)$, where $m_{\mathrm{T}}(c) = \sqrt{2 p_{\mathrm{T}}(c) \times E_{\mathrm{T}}^{\mathrm{miss}} \times (1 - \cos\Delta\phi(c, \vec{p}_{\mathrm{T}}^{\mathrm{miss}}))}$ is calculated for each c-tagged jet, is required to be at least 250 GeV to reject $W(\rightarrow \tau\nu)$ + jets backgrounds containing hadronically decaying τ-leptons misidentified as c-tagged jets. Finally, various $E_{\mathrm{T}}^{\mathrm{miss}}$ Sig. requirements are imposed to target signal models which are expected to have different kinematics. In addition to SR-HM1, SR-HM2, and SR-HM3, a signal region SR-HM-Disc with less stringent requirements is defined and is only used to set model-independent cross-section limits.

Four Compressed signal regions, named SR-Comp1, SR-Comp2, SR-Comp3 and SR-Comp-1c, are defined as shown in Table 3. All Compressed signal regions are orthogonal to the High-Mass signal regions as the leading jet is required to not be c-tagged. The most compressed SUSY scenarios, with $\Delta m(\tilde{t}_1, \tilde{\chi}_1^0) \approx 20-50$ GeV, are targeted with SR-Comp1 and SR-Comp-1c. SUSY scenarios with $\Delta m(\tilde{t}_1, \tilde{\chi}_1^0) \approx 80$ GeV are targeted with SR-Comp2, and a looser, more general signal region, SR-Comp3,

Table 2: Requirements of the SR-HM1–3 High-Mass regions, which are aimed at signal models with high top squark mass ($\gtrsim 600$ GeV), and SR-HM-Disc which is aimed at a broad range of models.

Variable	**SR-HM1**	**SR-HM2**	**SR-HM3**	**SR-HM-Disc**
Number of c-tagged jets	≥ 2			
Leading jet is c-tagged	yes			
$m_{\mathrm{T}}^{\mathrm{min}}(c)$ [GeV]	> 300			
$p_{\mathrm{T}}(j_2)$ [GeV]	> 200	> 150		
m_{cc} [GeV]	> 200	$200-400$	$400-600$	> 200
$E_{\mathrm{T}}^{\mathrm{miss}}$ Sig.	> 22	$15-22$		> 15

Table 3: Requirements of the Compressed signal regions that target signal models with top-squark–neutralino mass differences between 20 GeV and 175 GeV.

Variable	**SR-Comp1**	**SR-Comp2**	**SR-Comp3**	**SR-Comp-1c**
Number of c-tagged jets	≥ 2			$= 1$
Leading jet is c-tagged	no			
$m_{\mathrm{T}}^{\mathrm{min}}(c)$ [GeV]	–	> 80	> 120	< 250
m_{cc} [GeV]	–		> 100	–
$p_{\mathrm{T}}^{\mathrm{CM}}$ [GeV]	–			< 10
m_{V} [GeV]	–			< 80
$\Delta\phi(\vec{p}_{\mathrm{T}}^{\mathrm{miss}}, j_1)$	–			> 2
$N_{c\text{-jets}}^{\mathrm{S}}$	≥ 2			$= 1$
$p_{\mathrm{T}}^{\mathrm{ISR}}$ [GeV]	> 550	> 500	> 400	> 700
R_{ISR}	> 0.85	$0.75-0.85$	> 0.65	$0.9-1.0$

is designed to target a wide range of larger mass splittings $50\,\mathrm{GeV} \lesssim \Delta m(\tilde{t}_1, \tilde{\chi}_1^0) \lesssim 175\,\mathrm{GeV}$. At least two c-tagged jets are required for SR-Comp1, while only one is required for SR-Comp-1c to increase signal contributions for the low-p_{T} regime where the c-tagging efficiency decreases. SR-Comp-1c also has a requirement of $\Delta\phi(\vec{p}_{\mathrm{T}}^{\mathrm{miss}}, j_1) > 2$ on the azimuthal angle separation between the leading jet and the $\vec{p}_{\mathrm{T}}^{\mathrm{miss}}$. In SR-Comp3, selections on $m_{\mathrm{T}}^{\mathrm{min}}(c)$ and m_{cc} improve background rejection, with the latter serving to reduce background contributions from $g \to c\bar{c}$. There is some overlap between the Compressed signal regions: SR-Comp3 overlaps with SR-Comp1 and SR-Comp2, but SR-Comp1, SR-Comp2, and SR-Comp-1c are all orthogonal to one another, and SR-Comp-1c is orthogonal to SR-Comp3. Recursive Jigsaw Reconstruction [89] is used in the Compressed signal regions to enhance background rejection. In the presence of an ISR system, which consists of one or more jets produced by initial-state radiation, the $\tilde{t}_1\tilde{t}_1$ or $\tilde{c}_1\tilde{c}_1$ system is boosted in the transverse plane. Kinematic variables are then defined appropriately for the assignment of objects to either the ISR system or the sparticle (squarks plus LSPs) system. This method is equivalent to grouping the event objects according to the axis of maximum back-to-back p_{T} in the event's centre-of-mass (CM) frame, where the p_{T} of all objects sums vectorially to zero. The technique provides a suite of variables which are leveraged in the Compressed signal regions and include R_{ISR}, which is the projection of the invisible system's p_{T} direction vector onto the ISR system's p_{T} direction vector. The ISR and sparticle systems tend to be approximately back-to-back in compressed SUSY events, resulting in R_{ISR} values close to unity, while SM backgrounds tend to populate a wider range of R_{ISR} values. The vector sum of the jets' transverse momenta in the ISR frame, $p_{\mathrm{T}}^{\mathrm{ISR}}$, is also used to reject background. For SM backgrounds, $p_{\mathrm{T}}^{\mathrm{ISR}}$ has a smoothly falling distribution, while for compressed SUSY signal models, a peak at higher $p_{\mathrm{T}}^{\mathrm{ISR}}$ is seen, with the location of the peak typically being related to the mass of the parent SUSY particle. The number of c-tagged jets assigned to the sparticle (S) frame of the ISR decay tree, $N_{c\text{-jets}}^{\mathrm{S}}$, is also utilized as a discriminating variable. To suppress the increased SM contributions, SR-Comp-1c requires more stringent selections on R_{ISR} and $p_{\mathrm{T}}^{\mathrm{ISR}}$, and additional selections are also imposed on $p_{\mathrm{T}}^{\mathrm{CM}}$, the transverse momentum of the CM frame as evaluated in the laboratory frame, and m_{V}, the invariant mass of objects assigned to the visible (V) system.

Model-independent cross-section limits are set in the signal regions with the least stringent requirements (SR-HM1, SR-Comp3, and SR-HM-Disc) to search for any "beyond the Standard Model" (BSM) contributions. SR-HM-Disc has requirements similar to those in the other SR-HM regions, but it has a less stringent requirement on m_{cc} ($m_{cc} > 200$ GeV) and lacks the upper bound on $E_{\mathrm{T}}^{\mathrm{miss}}$ Sig. applied in SR-HM2 and SR-HM3 (see Table 2).

5.2 Background estimation and the control regions

The dominant backgrounds in all the signal regions are from processes with W or Z bosons produced in association with jets, with the bosons decaying as $W \rightarrow \ell\nu$ or $Z \rightarrow \nu\nu$ and producing real missing transverse momentum. The Z+jets background has similar contributions from $Z + c\bar{c}$, $Z + cj$, and $Z + jj$ (where j indicates a non-charm quark) in all signal regions except SR-Comp-1c, where the $Z + jj$ background dominates. The W+jets background has larger contributions from the $W + cj$ and $W + jj$ components than from $W + c\bar{c}$. To reduce the systematic uncertainties, these backgrounds are estimated by extrapolating production-rate correction factors from the control regions (CRs) to the signal regions using the simulated samples. The extrapolation is performed in lepton multiplicity as illustrated in Figure 2 while other requirements in the CRs are made to be as close as possible to those in the signal regions. The normalization of the Z+jets and W+jets backgrounds is performed *in situ* with the two-lepton (CRZ) and one-lepton (CRW) control regions, respectively. Three groups of CRs are designed for each background contribution: one set of CRs for the High-Mass signal regions, one set for the Compressed signal regions with two c-tagged jets, and one set for the Compressed signal region with one c-tagged jet. Contamination from signal processes was checked and found to be negligible in the defined CRs. Background processes that contribute less significantly are not normalized using control regions but using calculated cross-sections and include processes involving top quarks and multiple vector bosons. These processes are grouped together and referred to as "Other" processes in the remainder of this document.

The data for the Z+jets control regions (CRZ) were collected with the lowest unprescaled single-electron and single-muon triggers. These triggers have nearly constant efficiency for leptons with a p_{T} ($p_{\mathrm{T}}(\ell_1)$) greater than 27 GeV. To ensure a high-purity sample of Z+jets events, the invariant mass of the two signal leptons is required to be consistent with the mass of the Z boson ($76\,\mathrm{GeV} < m_{\ell\ell} < 106\,\mathrm{GeV}$). Further details of the CRZ selection are shown in Table 4.

For all the Z+jets control regions, $E_{\mathrm{T}}^{\mathrm{miss}}$ and all the other variables that use it (including $E_{\mathrm{T}}^{\mathrm{miss}}$ Sig.) treat the leptons as invisible by subtracting their contribution from the $\vec{p}_{\mathrm{T}}^{\mathrm{miss}}$ computation; these variables are

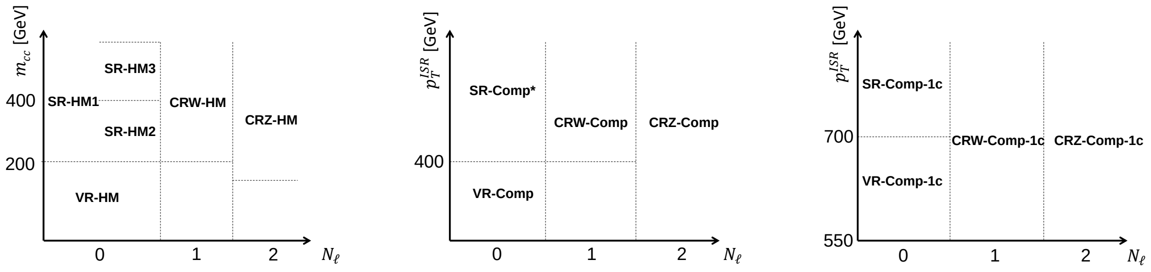

(a) (b) (c)

Figure 2: Phase-space partitioning between the signal, control, and validation regions for the (a) High-Mass signal regions, (b) Compressed signal regions SR-Comp1, SR-Comp2 and SR-Comp3, and (c) SR-Comp-1c. Control regions differ from the signal and validation regions by the electron and muon multiplicities (exactly one electron or muon in the W+jets control regions and two electrons or muons in the Z+jets regions) while the validation regions veto events with leptons as in the signal regions. The asterisk in "SR-Comp*" is a wildcard character to denote all the Compressed signal regions which require two c-tagged jets.

indicated with a prime ($'$). The treatment of the two leptons as invisible particles emulates the dominant contribution from $Z \to \nu\nu$ decays. To avoid significant extrapolation uncertainties between signal and control regions related to jet flavour composition, the requirements on the number of c-tagged jets ($= 1$ or ≥ 2) and on $m_{\mathrm{T}}^{\mathrm{min}'}(c)$ are kept as close as possible to those in the Compressed signal regions while also ensuring that the CRs provide sufficiently small statistical uncertainty in the Z+jets production rate. Distributions of selected kinematic observables are shown in Figure 3. These distributions illustrate the accuracy of the simulated samples' modelling of the data.

The W+jets control regions (CRW) require exactly one signal electron or muon. To keep the kinematic selection in the CRWs and the corresponding signal regions similar, all the CRWs require events to pass the $E_{\mathrm{T}}^{\mathrm{miss}}$ trigger and to have $E_{\mathrm{T}}^{\mathrm{miss}} > 250\,\mathrm{GeV}$. To ensure a high purity of W+jets background and to avoid contamination from $t\bar{t}$ processes, CRW-Comp includes a veto on events that include a τ-lepton. CRW-Comp has a higher contamination from $t\bar{t}$ than is seen in CRW-HM because of the former's lower $m_{\mathrm{T}}^{\mathrm{min}}(c)$ requirement, which is made to match the requirements in SR-Comp. CRW-Comp-1c contains events that have different kinematics due to its one-c-tag and high-p_{T}-ISR requirements, and thus does not require additional $t\bar{t}$ rejection from a τ-lepton veto. A detailed description of all the CRW selections is shown in Table 5. Figure 4 shows the distributions of the main kinematic variables used for extrapolation from the CRWs to the Compressed signal regions.

5.3 Validation of background estimates

The validation regions are used to test the accuracy of the procedure used to extrapolate the background from the control region to the signal regions before unblinding data in the signal regions. The parameter used in the extrapolation between the control and signal regions is the electron and muon multiplicity. Therefore, the validation regions veto events with leptons as do the signal regions. The validation regions are designed to have a background composition that consists of the dominant background processes expected in the signal regions, i.e. Z+jets and W+jets. The validation regions are orthogonal to the signal regions and control regions and have sufficient event yields to test the extrapolation procedure with reasonable accuracy.

Table 4: Requirements of the Z+jets control regions for SR-HM1, SR-HM2, and SR-HM3 (CRZ-HM), SR-Comp1, SR-Comp2, and SR-Comp3 (CRZ-Comp), and SR-Comp-1c (CRZ-Comp-1c). Variables that are calculated using $E_{\mathrm{T}}^{\mathrm{miss}}$ (including $E_{\mathrm{T}}^{\mathrm{miss}}$ Sig.) use an $E_{\mathrm{T}}^{\mathrm{miss}}$ variant that includes contributions from electrons/muons that are treated as invisible, and are indicated by a prime ($'$).

Variable	**CRZ-HM**	**CRZ-Comp**	**CRZ-Comp-1c**
Used for	SR-HM	SR-Comp	SR-Comp-1c
$p_{\mathrm{T}}(j_1)$	> 250 GeV		> 350 GeV
Number of c-tagged jets	≥ 2		= 1
Leading jet is c-tagged	yes	no	
Number of signal muons/electrons	= 2		
Passed single-electron/muon triggers	yes		
$p_{\mathrm{T}}(\ell_1)$ [GeV]	> 30		
$m_{\ell\ell}$ [GeV]	76−106		
$E_{\mathrm{T}}^{\mathrm{miss}}$ [GeV]	< 200		
$E_{\mathrm{T}}^{\mathrm{miss}'}$ [GeV]	> 200		
m_{cc} [GeV]	> 150	–	
$m_{\mathrm{T}}^{\mathrm{min}'}(c)$ [GeV]	> 150	–	< 250
$E_{\mathrm{T}}^{\mathrm{miss}'}$ Sig.	> 10	–	
$N_{c\text{-jets}}^{\mathrm{S}'}$	–	≥ 1	= 1
R'_{ISR}	–	> 0.75	0.9−1.0
$p_{\mathrm{T}}^{\mathrm{ISR}'}$ [GeV]	–		> 550
$\Delta\phi(\vec{p}_{\mathrm{T}}^{\mathrm{miss}'}, j_1)$	–		> 2

The validation regions are also designed to avoid a large contamination from signal scenarios, with less than 20% contamination seen for the models not excluded by the previous ATLAS search.

To validate the extrapolation of the backgrounds from the control regions CRW-HM and CRZ-HM to the High-Mass signal regions SR-HM1, SR-HM2 and SR-HM3, a single validation region VR-HM is used, with an expected Z+jets and W+jets contribution of 45% and 26%, respectively. The requirements for VR-HM are the same as in the signal region, except for a reversal of the m_{cc} requirement, an absence of $E_{\mathrm{T}}^{\mathrm{miss}}$ Sig. and $p_{\mathrm{T}}(j_2)$ requirements, and a less stringent requirement of $m_{\mathrm{T}}^{\mathrm{min}}(c) > 200$ GeV (as compared to $m_{\mathrm{T}}^{\mathrm{min}}(c) > 300$ GeV in the signal regions).

The normalization procedure for Compressed regions that require at least two charm-tagged jets, i.e. SR-Comp1, SR-Comp2, and SR-Comp3, is validated in one region, VR-Comp. This region is orthogonal to the signal regions because it has a reversed $p_{\mathrm{T}}^{\mathrm{ISR}}$ requirement ($p_{\mathrm{T}}^{\mathrm{ISR}} < 400$ GeV). The other requirements, including the veto on events with leading c-tagged jets that makes the Compressed regions orthogonal to the High-Mass regions, are kept the same as in the signal regions, with the following four exceptions. The

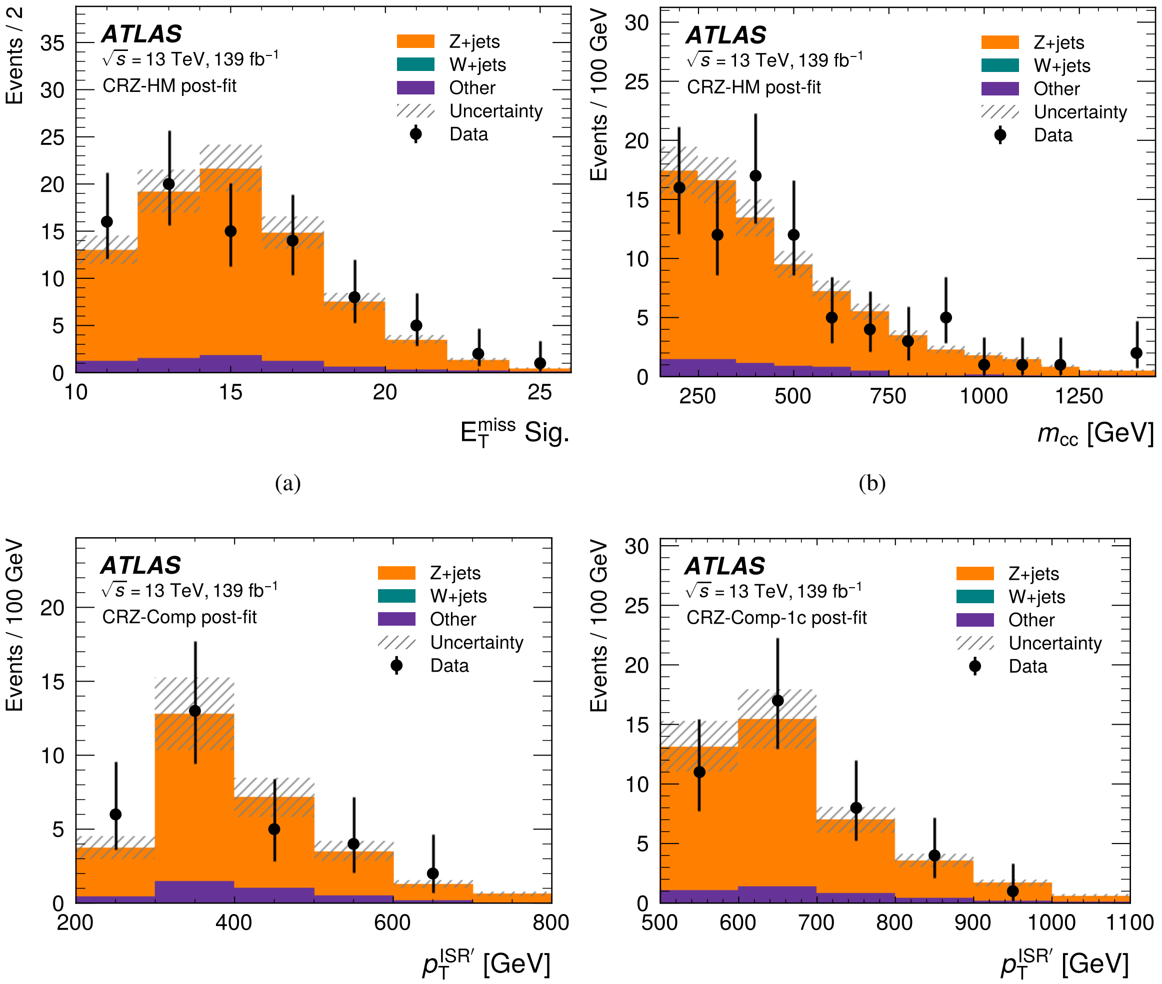

(a) (b) (c) (d)

Figure 3: Distributions showing the level of agreement the between data (points) and the SM expectation (stacked histograms, after simultaneously fitting the Z+jets and W+jets backgrounds) in the Z+jets control regions for some variables which have different selection criteria in the signal regions: (a) E_T^{miss} Sig. in CRZ-HM, (b) m_{cc} in CRZ-HM, (c) $p_T^{\text{ISR}'}$ in CRZ-Comp, and (d) $p_T^{\text{ISR}'}$ in CRZ-Comp-1c. The hatched uncertainty band around the total SM expectation includes theory-based and detector-related systematic uncertainties and MC statistical uncertainties. Processes with top quarks and multiple vector bosons are included in “Other”. The W+jets background contribution is negligible and not visible in the plots. The right-most bin in each histogram does not include the overflow entry but the x-axis range is chosen to include all observed data.

c-tagged jet multiplicity in the sparticle frame, $N^{\text{S}}_{c\text{-jets}}$, is loosened to be greater than or equal to one (rather than two in the signal regions). The requirement on R_{ISR} is also less stringent in VR-Comp ($R_{\text{ISR}} > 0.65$) than in SR-Comp1 ($R_{\text{ISR}} > 0.85$) and SR-Comp2 ($0.75 < R_{\text{ISR}} < 0.85$) but is the same as in SR-Comp3. Additionally, $m_{\text{T}}^{\text{min}}(c)$ is required to be greater than 80 GeV in VR-Comp, whereas there is no requirement on $m_{\text{T}}^{\text{min}}(c)$ in SR-Comp1. SR-Comp2 also requires a minimum of 80 GeV, and SR-Comp3 requires $m_{\text{T}}^{\text{min}}(c) > 120$ GeV. Finally, no requirement is made on m_{cc} in VR-Comp, as is the case in SR-Comp1 and SR-Comp2, but which differs from the $m_{cc} > 100$ GeV requirement in SR-Comp3.

Table 5: Requirements of the W+jets control regions for SR-HM1, SR-HM2, and SR-HM3 (CRW-HM), SR-Comp1, SR-Comp2, and SR-Comp3 (CRW-Comp), and SR-Comp-1c (CRW-Comp-1c).

Variable	**CRW-HM**	**CRW-Comp**	**CRW-Comp-1c**
Used for	SR-HM	SR-Comp	SR-Comp-1c
$p_{\mathrm{T}}(j_1)$ [GeV]	> 250		> 350
Number of c-tagged jets	≥ 2		$= 1$
Number of signal muons/electrons	$= 1$		
Passed $E_{\mathrm{T}}^{\mathrm{miss}}$ trigger	yes		
$E_{\mathrm{T}}^{\mathrm{miss}}$ [GeV]	> 250		
m_{cc} [GeV]	> 200	–	
$m_{\mathrm{T}}^{\mathrm{min}}(c)$ [GeV]	> 200	> 120	< 250
$E_{\mathrm{T}}^{\mathrm{miss}}$ Sig.	> 14	–	
Leading jet is c-tagged	yes	no	
$N_{c\text{-jets}}^{\mathrm{S}}$	–	≥ 1	$= 1$
$p_{\mathrm{T}}^{\mathrm{ISR}}$ [GeV]	–	> 400	> 550
R_{ISR}	–	> 0.65	$0.9-1.0$
τ veto	–	yes	–
$\Delta\phi(\vec{p}_{\mathrm{T}}^{\mathrm{miss}}, j_1)$	–		> 2

The one-c-tag validation region is identical to SR-Comp-1c with the exception of the defining reversal of the $p_{\mathrm{T}}^{\mathrm{ISR}}$ requirement relative to the signal region and the widening of the R_{ISR} window from $0.9 < R_{\mathrm{ISR}} < 1.0$ in SR-Comp-1c to $0.85 < R_{\mathrm{ISR}} < 1.05$. The full set of selections for all validation regions is shown in Table 6, while distributions of the main kinematic variables that differ between the validation regions and the signal regions are shown in Figure 5.

6 Systematic uncertainties

The effect of systematic uncertainties is taken into account for the limited accuracy of the background and signal predictions. To properly treat correlations of uncertainties across the signal and control regions, the uncertainties are separated by source. There are uncertainties for the simulated detector response, integrated luminosity [43], number of simulated events, predicted cross-sections, parton distribution functions, underlying event and minimum-bias pp collisions, parton hadronization models, limited accuracy of matrix element and parton shower calculations, and experimental effects. Below is a discussion of the most relevant sources of uncertainty affecting the search.

The uncertainty in the measured c-tagging efficiency is one of the dominant sources of uncertainty because all the signal and control regions require events with one or more c-tagged jets. The simulated event

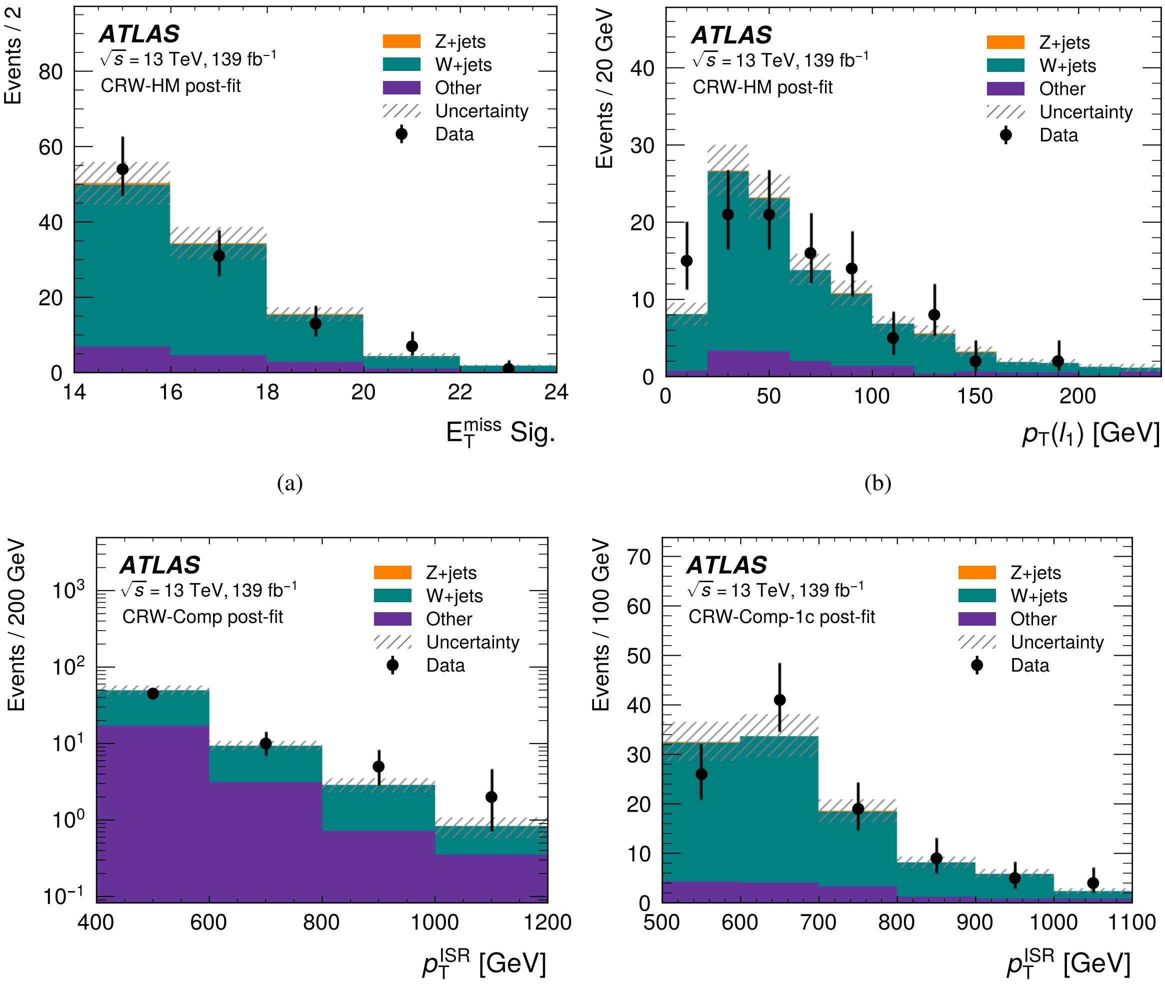

(a) (b)

(c) (d)

Figure 4: Distributions showing the level of agreement between the data (points) and the SM expectation (stacked histograms, after simultaneously fitting the Z+jets and W+jets backgrounds) in the W+jets control regions for some variables which have different selection criteria in the signal regions: (a) $E_{\mathrm{T}}^{\mathrm{miss}}$ Sig. in CRW-HM, (b) p_{T} of leading lepton in CRW-HM, (c) $p_{\mathrm{T}}^{\mathrm{ISR}}$ in CRW-Comp, and (d) $p_{\mathrm{T}}^{\mathrm{ISR}}$ in CRW-Comp-1c. The hatched uncertainty band around the total SM expectation includes theory-based and detector-related systematic uncertainties and MC statistical uncertainties. Processes with top quarks and multiple vector bosons are included in “Other”. The Z+jets background contribution is negligible and not visible in the plots. The right-most bin in each histogram does not include the overflow entry but the x-axis range is chosen to include all observed data.

samples are reweighted so that the predicted and measured identification efficiencies of c-tagged jets are identical and so the uncertainties are propagated. The uncertainty in the c-tagging efficiency also depends on the jet p_{T} and whether the tagged jet is initiated by a b-quark, c-quark, or light quark [80–82].

The uncertainties in the predicted jet energies are driven by the accuracy of the measured jet energies and resolution [76]. There is an uncertainty in the contribution from jets that originate from the overlapping pp interactions but are mistakenly counted as coming from the hard scatter [78]. This includes the efficiency of identifying jets originating from secondary pp interactions and the accuracy of simulated minimum-bias

Table 6: Requirements of the validation regions.

Variable	**VR-HM**	**VR-Comp**	**VR-Comp-1c**
Validates backgrounds in	SR-HM	SR-Comp	SR-Comp-1c
Number of c-tagged jets	≥ 2		$= 1$
Passed $E_{\mathrm{T}}^{\mathrm{miss}}$ trigger	yes		
$E_{\mathrm{T}}^{\mathrm{miss}}$ [GeV]	> 250		
m_{cc} [GeV]	> 200	–	
$m_{\mathrm{T}}^{\mathrm{min}}(c)$ [GeV]	> 200	> 80	> 100
Leading jet is c-tagged	yes	no	
$N_{c\text{-jets}}^{\mathrm{S}}$	–	≥ 1	$= 1$
$p_{\mathrm{T}}^{\mathrm{ISR}}$ [GeV]	–	< 400	
R_{ISR}	–	> 0.65	$0.85-1.05$
τ veto	yes		
$\Delta\phi(\vec{p}_{\mathrm{T}}^{\mathrm{miss}}, j_1)$	–		> 2
$p_{\mathrm{T}}^{\mathrm{CM}}$ [GeV]	–		< 10
m_{V} [GeV]	–		< 80

interactions.

The theoretical uncertainties for the W+jets and Z+jets backgrounds are estimated with Sherpa. Uncertainties due to inaccuracies in the matrix element calculation and parton showering are estimated by varying the generator's parameters. The envelope of the associated predicted distributions is taken as the uncertainty. The matrix element matching scale is varied between 15 GeV and 30 GeV. Its nominal value is 20 GeV. The renormalization and factorization scales are varied by factors of 0.5 and 2 independently. The impact of the PDF uncertainties is taken into account in addition to the generator uncertainties.

The secondary backgrounds such as top-quark pairs produced in association with jets [90] and vector-boson pairs produced in association with jets, labeled as "Other" in the figures and tables, have a minor effect on the total background estimate. A normalization uncertainty of 25% is assigned and treated as fully correlated across regions. This uncertainty estimate, is meant to cover cross-section normalization and modeling uncertainties and does not contribute significantly to the total uncertainty. Treating the uncertainty uncorrelated between regions was found to increase the total expected background contribution by at most one standard deviation in SR-Comp2 and SR-Comp3 with a negligible effect on the final result.

Additionally, for signal predictions (i.e. SUSY and LQ), theoretical uncertainties are taken as an envelope of the results obtained when varying the factorization and renormalization scales independently by factors of 0.5 and 2. The Var3c parameter (which corresponds to the strong coupling parameter, α_{s}, used for ISR) of the A14 underlying-event tune is also varied. The contribution from these uncertainties is largest in the compressed regions, where it reaches 20%.

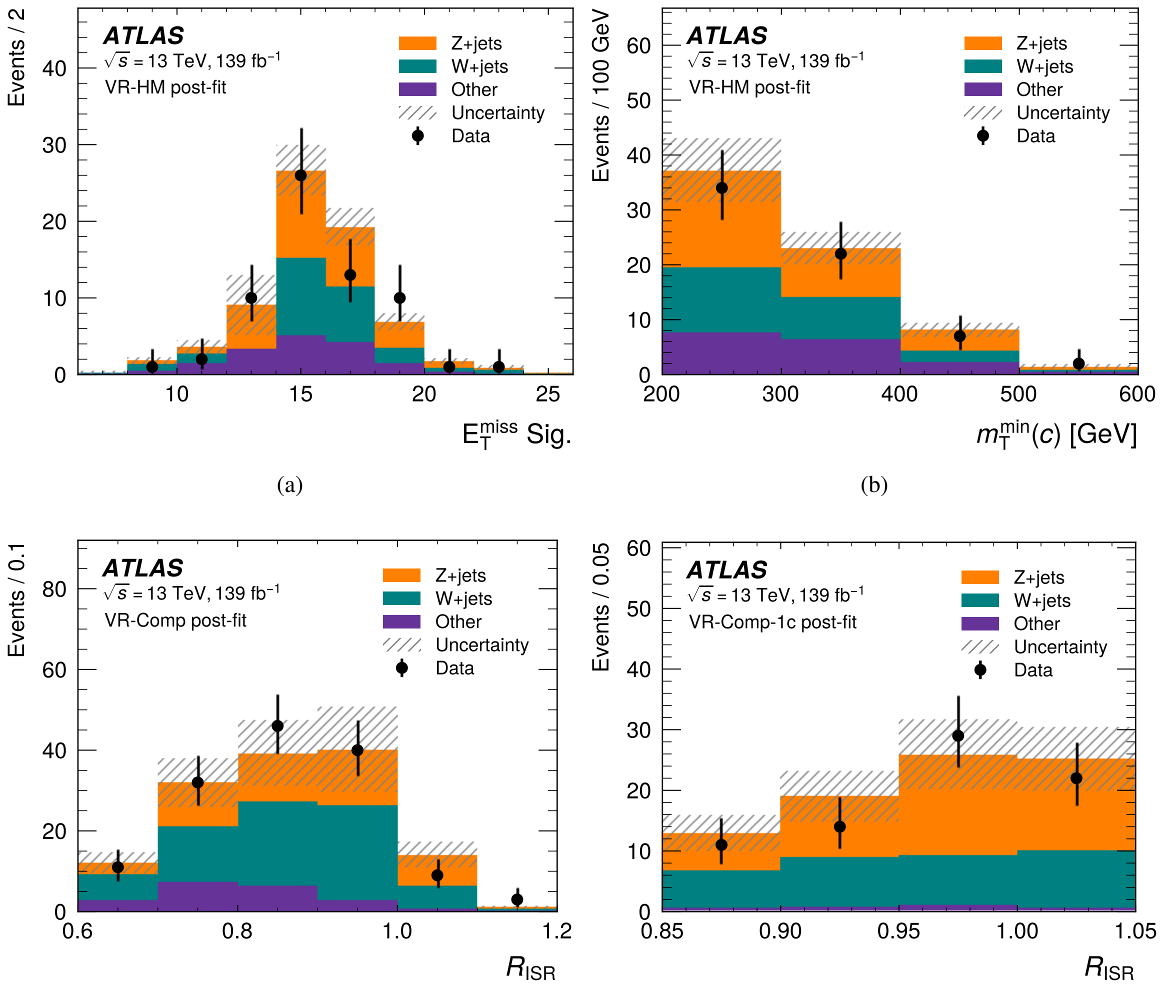

(a)

(b)

(c)

(d)

Figure 5: Distributions, in various validation regions, showing the level of agreement between the data (points) and the SM expectation (stacked histograms, after simultaneously fitting the Z+jets and W+jets backgrounds) for variables which have different selection criteria in the signal regions: (a) $E_{\mathrm{T}}^{\mathrm{miss}}$ Sig. in VR-HM, (b) $m_{\mathrm{T}}^{\mathrm{min}}(c)$ in VR-HM, (c) R_{ISR} in VR-Comp, and (d) R_{ISR} in VR-Comp-1c. The hatched uncertainty band around the total SM expectation includes theory-based and detector-related systematic uncertainties and MC statistical uncertainties. Processes with top quarks and multiple vector bosons are included in “Other”. The right-most bin in each histogram does not include the overflow entry but the x-axis range is chosen to include all observed data.

7 Results and interpretation

A statistical analysis of the data is performed with a simultaneous likelihood fit [91] that includes the effects of systematic uncertainties on the number of fitted signal and background events through nuisance parameters that change the expected contributions in the control and signal (or validation) regions in a correlated manner. The likelihood probability is calculated by combining Poisson probabilities for the signal, validation, and control regions with a Gaussian probability distribution for each systematic uncertainty. The fit is performed simultaneously across all signal (or validation) and control regions, extracting free-floating normalization factors for the W+jets and Z+jets background contributions, with three normalization factors for each (i.e. for High-Mass, Compressed, and one-c-tag regions).

A "background-only" fit is performed for the High-Mass (CRZ-HM, CRW-HM), Compressed (CRZ-Comp, CRW-Comp), and one-c-tag (CRZ-Comp-1c, CRW-Comp-1c) regions using the likelihood in the control regions and extrapolating the normalization of Z+jets and W+jets contributions into the validation or signal regions (thus not considering the data yield in the signal and validation regions). The fitting strategy reduces systematic uncertainties in the signal regions because the control regions are chosen to minimize the extrapolation uncertainties. Thus the effect on the W+jets and Z+jets background estimates due to systematic uncertainties is similar in the control and signal regions and partially cancels out. This strategy is especially effective in the High-Mass regions, where the total uncertainty of the SM backgrounds is reduced from 30%–37% to 13%–17%. The systematic uncertainties that contribute the most to the total post-fit uncertainty are related to c-tagging and V+jets theoretical uncertainties. Theoretical systematic uncertainties are dominated by the variations of the scales, with contributions to the total uncertainty ranging from 14% to 36%, while the largest contributions from c-tagging-related systematic uncertainties to the total uncertainty of the background estimate in the signal regions range from 8% to 14%.

No significant excesses over the expected SM backgrounds in the validation and signal regions are observed when considering all statistical and systematic (experimental and theory) uncertainties, as shown in Tables 7 and 8 and Figure 6. The extracted normalization factors for the W+jets and Z+jets backgrounds are shown in Table 9 and are generally consistent with unity given their associated uncertainties, with the normalization factors for W+jets background being larger across all control regions. Selected kinematic distributions in the signal regions are shown in Figure 7.

The exclusion fit is performed for each signal model individually, using the signal and control regions. For SUSY models, the two statistical combinations considered use the three High-Mass signal regions with non-overlapping Compressed signal regions: the first combines SR-HM1, SR-HM2, SR-HM3, SR-Comp1, SR-Comp2, and SR-Comp-1c, while the second combines SR-HM1, SR-HM2, SR-HM3, SR-Comp3, and SR-Comp-1c. For both combinations, all six control regions are used to estimate the background contributions. To maximize the exclusion power of the two configurations, the combination with the lowest expected $\mathrm{CL_S}$ [93] value is chosen for the final result. The expected sensitivity is calculated by generating pseudo-experiments that assume an absence of BSM signals. Exclusion limits are set at 95% confidence level (CL) and are shown for the considered SUSY models in Figure 8. The expected exclusion limits from this search exceed those from the previous ATLAS search that used c-tagging [30] (grey-filled contour and dashed line in Figure 8), while being complementary to an ATLAS search for single squark production that did not utilize c-tagging [33] (green-filled contour and dashed line in **??**) for $m_{\tilde{t}_1/\tilde{c}_1} \lesssim 920$ GeV and $m(\tilde{\chi}_1^0) \gtrsim 400$ GeV, and is also complementary to an ATLAS single-jet search [32] (cyan-filled contour and dashed line in **??**) for $\Delta m(\tilde{t}_1, \tilde{\chi}_1^0) \gtrsim 30$ GeV.

Table 7: Post-fit event yields for the High-Mass control, validation, and signal regions. The Z+jets and W+jets backgrounds are normalized by fits within the control regions. Processes with top quarks and multiple vector bosons are included in “Other”. Pre-fit event yields for a representative signal point for each of the signal regions are also shown.

	CRW-HM	CRZ-HM	VR-HM
Z+jets	0.66 ± 0.12	74 ± 9	31 ± 5
W+jets	90 ± 11	0.030 ± 0.009	22 ± 4
Other	15 ± 4	6.6 ± 1.8	17 ± 5
Total SM	106 ± 10	81 ± 9	70 ± 8
Observed	106	81	65

	SR-HM1	SR-HM2	SR-HM3	SR-HM-Disc
Z+jets	5.2 ± 1.3	12.3 ± 3.4	14.7 ± 2.7	58 ± 9
W+jets	3.2 ± 0.7	9.8 ± 1.7	12.5 ± 2.1	43 ± 6
Other	0.88 ± 0.33	1.6 ± 0.6	2.2 ± 0.7	9.0 ± 2.5
Total SM	9.3 ± 1.6	24 ± 4	29 ± 4	110 ± 12
Observed	13	31	27	133
$m(\tilde{t}_1, \tilde{\chi}_1^0)$=(1000, 1) GeV	6.6 ± 1.0	12.7 ± 2.1		12.7 ± 2.1
$m(\tilde{t}_1, \tilde{\chi}_1^0)$=(750, 450) GeV		17.3 ± 2.6	12.6 ± 2.1	41 ± 7

Exclusion limits are also presented in Figure 9 for an alternative interpretation in which top squarks are pair produced and each decays into a neutralino and either a top or a charm quark, with $\mathcal{B}(\tilde{t}_1 \rightarrow c + \tilde{\chi}_1^0)$ being varied between 0.1 and 1. Due to the b-jet veto imposed, none of the signal and control regions are sensitive to the decay pathway producing a top quark; nonetheless these decay modes are included in the simulated signal samples. Two cases are studied: the mass of the neutralino is fixed to either 1 GeV or 200 GeV. The strongest limits are set when the top squark decays only via the $c + \tilde{\chi}_1^0$ channel, as expected, with top squark masses up to approximately 900 GeV being excluded at 95% CL in both cases. The scenario in which $m(\tilde{\chi}_1^0) = 1$ GeV presents a boosted decay topology over the entire range of top squark masses considered, and as such, the major constraining power comes from the High-Mass signal regions. A monotonic decrease in sensitivity is observed with decreasing branching fraction to $c + \tilde{\chi}_1^0$. For $m(\tilde{\chi}_1^0) = 200$ GeV neutralinos, the Compressed signal regions gradually become more sensitive as the top squark mass decreases, causing the change in behaviour near $m(\tilde{t}_1) = 500$ GeV.

Additional limits are set in terms of LQ models after performing a combined fit of the LQ signals using only the High-Mass regions because of similarities in kinematics in the scenario where the LSP is massless. In the case of scalar-LQ models, events were reweighted to span the full range of branching fractions of the LQ decay into $c\nu$. Expected and observed exclusion limits on the $\mathcal{B}(\mathrm{LQ}^{\mathrm{u}} \rightarrow c\nu_e)$ and $\mathcal{B}(\mathrm{LQ}^{\mathrm{u}} \rightarrow c\nu_\mu)$ at 95% CL are presented in Figure 10 as a function of the leptoquark mass, with the observed upper limit on the production cross-section shown on the z-axis. Leptoquarks with masses up to approximately 900 GeV are excluded.

Vector-LQ models are excluded at 95% CL up to masses of 950 GeV in the minimal coupling scenario, and 1150 GeV for the Yang–Mills case, for an assumed branching fraction of $\mathcal{B}(\mathrm{vLQ}_{23}^{\mathrm{u}} \rightarrow c\nu_\tau) = 0.5$. Upper

Table 8: Post-fit event yields for the Compressed control, validation, and signal regions. The Z+jets and W+jets backgrounds are normalized by fits within the control regions. Processes with top quarks and multiple vector bosons are included in "Other". Pre-fit event yields for a representative signal point in each signal region are also shown.

	CRW-Comp	CRZ-Comp	CRW-Comp-1c	CRZ-Comp-1c	VR-Comp	VR-Comp-1c
Z+jets	0.33 ± 0.12	26 ± 6	0.65 ± 0.18	38 ± 7	48 ± 12	48 ± 13
W+jets	41 ± 10	–	89 ± 11	–	71 ± 25	32 ± 11
Other	22 ± 6	3.9 ± 1.2	15 ± 4	4.0 ± 1.1	21 ± 6	2.8 ± 0.8
Total SM	63 ± 8	30 ± 5	105 ± 10	42 ± 6	139 ± 27	83 ± 17
Observed	63	30	105	42	141	76

	SR-Comp1	SR-Comp2	SR-Comp3	SR-Comp-1c
Z+jets	0.9 ± 0.4	1.6 ± 0.9	3.1 ± 0.9	4.3 ± 1.2
W+jets	2.2 ± 1.0	1.3 ± 0.7	0.9 ± 0.6	2.8 ± 0.9
Other	0.56 ± 0.19	0.62 ± 0.20	1.04 ± 0.34	0.68 ± 0.29
Total SM	3.7 ± 1.2	3.5 ± 1.2	5.0 ± 1.2	7.9 ± 1.7
Observed	3	6	8	12
$m(\tilde{t}_1, \tilde{\chi}_1^0)$=(600, 550) GeV	6.1 ± 1.3			
$m(\tilde{t}_1, \tilde{\chi}_1^0)$=(550, 470) GeV		6.0 ± 0.8		
$m(\tilde{t}_1, \tilde{\chi}_1^0)$=(550, 375) GeV			7.9 ± 2.1	
$m(\tilde{t}_1, \tilde{\chi}_1^0)$=(450, 430) GeV				11.2 ± 1.7

Table 9: Summary of the extracted normalization factors when considering only the likelihood in the control regions for the High-Mass (HM) regions, the Compressed regions that require two c-tagged jets (Comp), and the Compressed regions requiring exactly one c-tagged jet (Comp-1c). Uncertainties include both the statistical and systematic components but do not include the extrapolation into the signal region, which can reduce the total uncertainty. The W+jets normalization factors have larger uncertainties because of the larger effect of theoretical uncertainties.

Region	Normalization factor
HM Z+jets	1.0 ± 0.4
Comp Z+jets	1.0 ± 0.4
Comp-1c Z+jets	1.1 ± 0.4
HM W+jets	1.4 ± 0.6
Comp W+jets	1.3 ± 0.7
Comp-1c W+jets	1.6 ± 0.7

limits on the production cross-section for both the minimal and Yang–Mills coupling scenarios are shown in Figure 11, with the theoretical cross-section at LO and the $\pm 1\sigma$ interval (encompassing the effects of PDF, α_{s}, renormalization and factorization scale variations) shown in blue.

A model-independent fit is performed for signal regions with the least stringent requirements: SR-HM1, SR-Comp3, and SR-HM-Disc. For the model-independent interpretation, the SM background estimates are fit to the observed yields in both the CRs and SRs, testing for the potential presence of any BSM events in the SRs. The observed cross-section limit, $\langle\epsilon\sigma\rangle^{95}_{\mathrm{obs}}$, is calculating by dividing the observed limit on the

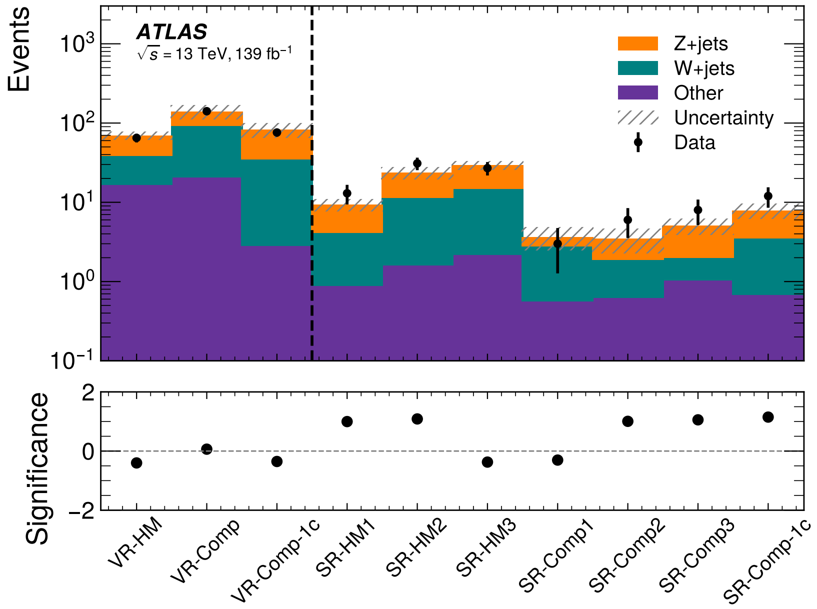

Figure 6: Comparison of event yields for the data (points) and SM expectation (stacked histograms) in all signal and validation regions after the background-only fits. The hatched uncertainty band around the SM prediction represents the total uncertainty, i.e. combining the detector-related and theory-based systematic uncertainties and the MC statistical uncertainties. The significance of the difference between the data and the SM background prediction, calculated with the profile-likelihood method described in Ref. [92] and using the total uncertainty, is shown in the bottom panel. Processes with top quarks and multiple vector bosons are included in "Other".

signal strength, S^{95}_{obs}, by the integrated luminosity. These limits on the number of BSM events are shown in Table 10 and can be reinterpreted for a generic BSM model by calculating the identification efficiency and detector acceptance for the model of interest.

Table 10: Model-independent upper limits on the BSM event yields and cross-sections. The $\langle\epsilon\sigma\rangle^{95}_{\mathrm{obs}}$ is the observed upper limit on the visible BSM cross-section at 95% CL, and S^{95}_{obs} is the observed upper limit on the number of BSM events. Similarly, S^{95}_{exp} is the expected upper limit on the number of BSM events but it is computed assuming that the observed number of events is identical to the number of background events. The discovery p-value ($p_{\mathrm{obs}}(S = 0)$), which tests the compatibility of the observed data with the background-only (zero signal yield) hypothesis relative to fluctuations of the background, is shown in the last column.

Signal Region	$\langle\epsilon\sigma\rangle^{95}_{\mathrm{obs}}$ [fb]	S^{95}_{obs}	S^{95}_{exp}	$p_{\mathrm{obs}}(S = 0)$
SR-HM1	0.09	12.8	$9.7^{+4.2}_{-2.9}$	0.19
SR-HM-Disc	0.36	50.7	34^{+13}_{-9}	0.09
SR-Comp3	0.07	9.2	$6.5^{+3.2}_{-2.0}$	0.15
SR-Comp-1c	0.08	11.6	$8.0^{+3.8}_{-2.4}$	0.13

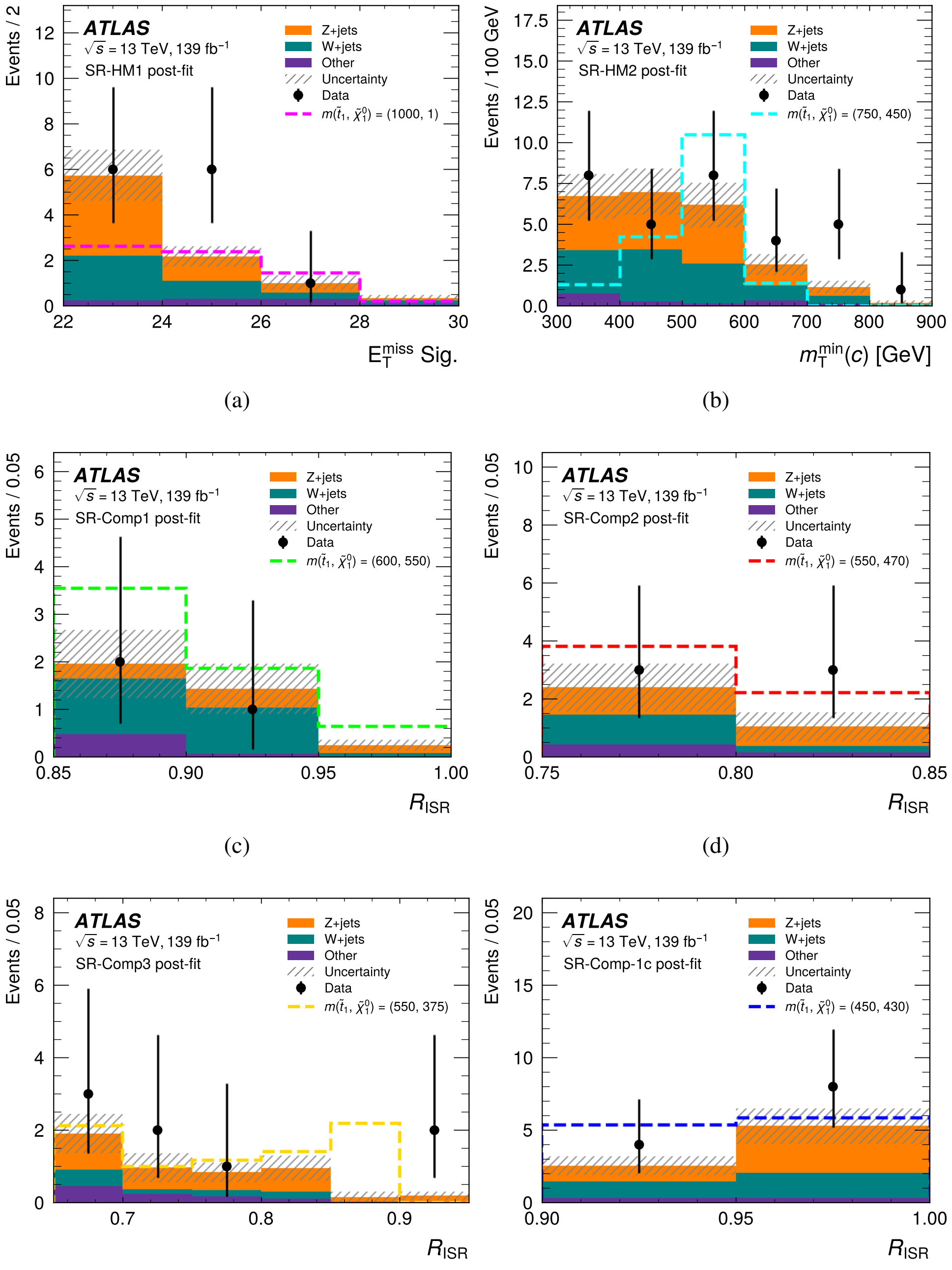

(a) (b)

(c) (d)

(e) (f)

Figure 7: Distributions for the signal regions showing the data (points) and the expected backgrounds (stacked histograms), after simultaneously fitting all the control regions. The histograms are binned in the key variables for each signal region: (a) $E_{\mathrm{T}}^{\mathrm{miss}}$ Sig. for SR-HM1, (b) $m_{\mathrm{T}}^{\mathrm{min}}(c)$ for SR-HM2, (c) R_{ISR} for SR-Comp1, (d) R_{ISR} for SR-Comp2, (e) R_{ISR} for SR-Comp3, and (f) R_{ISR} for SR-Comp-1c. The hatched band is the total systematic uncertainty for the expected backgrounds. Distributions of representative $\tilde{t}_1\bar{\tilde{t}}_1$ signals for different mass assumptions (or similar) are shown as dashed lines using pre-fit signal contributions. Processes with top quarks and multiple vector bosons are included in “Other”. The right-most bin in each histogram does not include the overflow entry but the x-axis range is chosen to include all observed data.

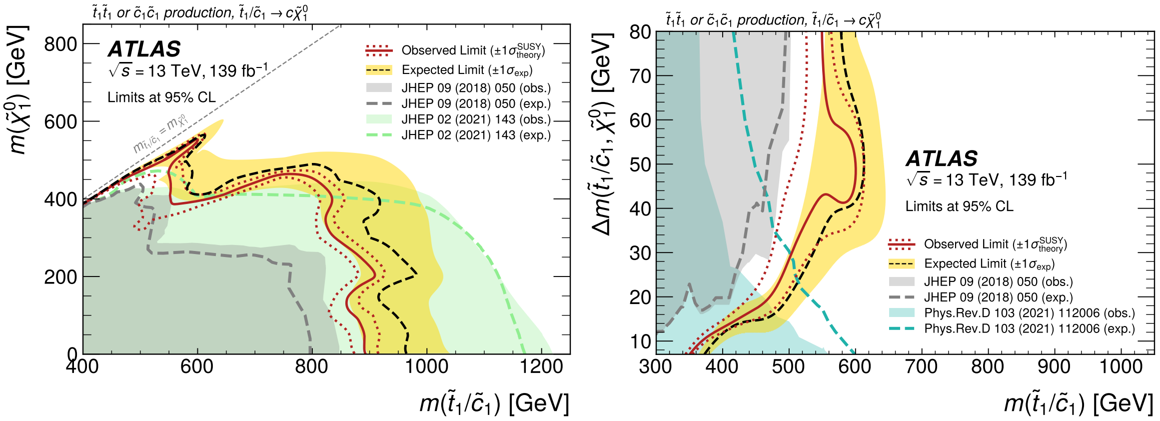

(a) (b)

Figure 8: Exclusion limits at 95% CL for pair production of top squarks decaying into charm quarks and neutralinos. The expected limit is shown as a dashed line while the $\pm 1\sigma$ interval is shown as a yellow band. The observed limit is shown as a red line and the effect of varying the signal cross-section by $\pm 1\sigma$ of its predicted theoretical uncertainty is shown as red dashed lines. The contours are shown as two-dimensional projections for masses of squarks and neutralinos (a) and their differences (b). The exclusion contour from the previous ATLAS result that used charm tagging (Ref. [30]) is shown as a grey-dashed line (expected) and grey-filled contour (observed). For (a), the single-squark-production exclusion contour from the ATLAS squarks and gluinos search that did not utilize charm tagging (Ref. [33]) is shown as a green-dashed line (expected) and green-filled contour (observed), while for (b), the contour from the ATLAS single-jet search (Ref. [32]) is shown as a cyan-dashed line (expected) and cyan-filled contour (observed).

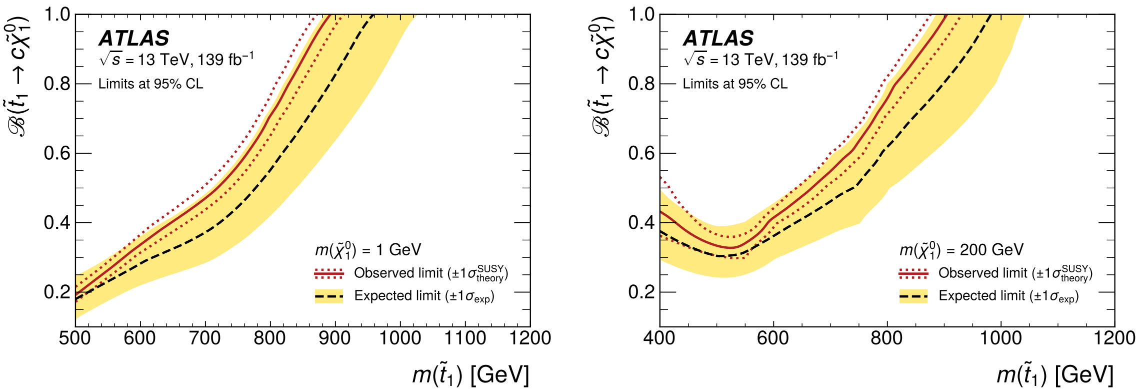

(a) (b)

Figure 9: The expected and observed exclusion contours for pair production of top squarks decaying into top or charm quarks and neutralinos. The contours are shown as two-dimensional projections in the plane of the squark mass and assumed branching fraction, whose value is varied between 0 (all decays to $t + \tilde{\chi}_1^0$) and 1 (all decays to $c + \tilde{\chi}_1^0$). The mass of the neutralino is fixed to either (a) 1 GeV or (b) 200 GeV. The cross-section limits for the contours are calculated by combining the signal regions as discussed earlier in the paper. The branching fractions above and masses below the lines (high branching fraction and low mass, and thus high production cross-section) are excluded. The expected limit is shown as a dashed line, while the $\pm 1\sigma$ interval is shown as a yellow band. The observed limit is shown as a red line and the effect of varying the signal cross-section by $\pm 1\sigma$ of its predicted theoretical uncertainty is shown as red dashed lines.

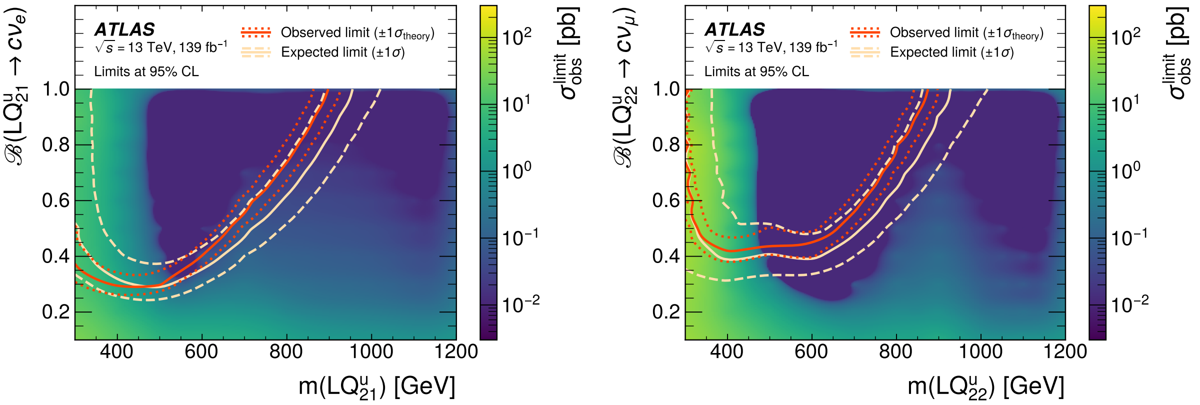

(a) (b)

Figure 10: Expected (white) and observed (red) exclusion limits at 95% CL for up-type scalar LQs coupled to (a) first- and (b) second-generation leptons. The observed upper limit on the production cross-section is plotted on the z-axis as a function of (a) $\mathcal{B}(\text{LQ}^{\text{u}} \to c\nu_e)$ with the alternative decay being $\text{LQ}^{\text{u}} \to s + e$ and (b) $\mathcal{B}(\text{LQ}^{\text{u}} \to c\nu_\mu)$ with the alternative decay being $\text{LQ}^{\text{u}} \to s + \mu$ (y-axis) and the leptoquark masses (x-axis). The branching fractions above and masses below the lines (high branching fraction and low mass, and thus high production cross-section) are excluded. The $\pm 1\sigma$ interval of the expected limit is shown as dashed white lines while the effect of varying the signal cross-section by $\pm 1\sigma$ of its predicted theoretical uncertainty is shown as red dashed lines.

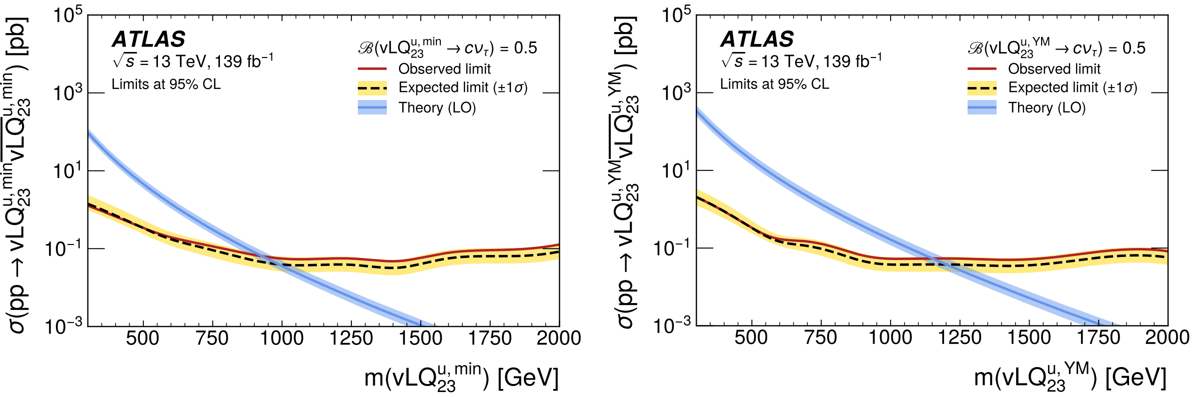

(a) (b)

Figure 11: Expected (dashed) and observed (solid) cross-section upper limits as a function of leptoquark mass for $U(1)$ vector-LQ models in the (a) minimal and (b) Yang–Mills coupling scenarios with $\beta_{23} = 1$, corresponding to a branching fraction $\mathcal{B}(\text{vLQ}^{\text{u}}_{23} \to c\nu_\tau) = 0.5$. The $\pm 1\sigma$ interval of the expected limit is shown as a yellow band. The theoretical prediction and its $\pm 1\sigma$ interval band are shown in blue.

8 Conclusion

This paper presents a search targeting BSM models contributing to final states with missing transverse momentum and charm-tagged jets, based on a 139 fb^{-1} dataset of proton–proton collisions at $\sqrt{s} = 13$ TeV recorded by the ATLAS experiment at the LHC. The observed experimental data are found to agree with the SM background estimate. The results are interpreted as upper limits at 95% CL on the production cross-section of selected SUSY and leptoquark models and as model-independent upper limits on the production cross-section for BSM particles. Top/charm squark masses are excluded up to ~900 GeV, assuming each squark decays into a charm quark and an LSP. This is a ~100 GeV improvement on the previous ATLAS search that used c-tagging. The increase in sensitivity is driven by the larger experimental dataset, the sophisticated design of the signal regions (which includes different strategies for large and small mass splittings between the top squark and the LSP), and improvements in c-tagging. The search also excludes, for the first time at the LHC, scalar leptoquarks with a mass below 900 GeV that decay into a charm quark and either a first- or second-generation neutrino. Finally, vector-leptoquark models in the minimal and Yang–Mills coupling scenarios are excluded at 95% CL up to masses of 950 GeV and 1150 GeV, respectively, assuming a branching fraction of $\mathcal{B}(\text{vLQ}_{23}^{\text{u}} \rightarrow c\nu_\tau) = 0.5$.

Acknowledgements

We thank CERN for the very successful operation of the LHC and its injectors, as well as the support staff at CERN and at our institutions worldwide without whom ATLAS could not be operated efficiently.

The crucial computing support from all WLCG partners is acknowledged gratefully, in particular from CERN, the ATLAS Tier-1 facilities at TRIUMF/SFU (Canada), NDGF (Denmark, Norway, Sweden), CC-IN2P3 (France), KIT/GridKA (Germany), INFN-CNAF (Italy), NL-T1 (Netherlands), PIC (Spain), RAL (UK) and BNL (USA), the Tier-2 facilities worldwide and large non-WLCG resource providers. Major contributors of computing resources are listed in Ref. [94].

We gratefully acknowledge the support of ANPCyT, Argentina; YerPhI, Armenia; ARC, Australia; BMWFW and FWF, Austria; ANAS, Azerbaijan; CNPq and FAPESP, Brazil; NSERC, NRC and CFI, Canada; CERN; ANID, Chile; CAS, MOST and NSFC, China; Minciencias, Colombia; MEYS CR, Czech Republic; DNRF and DNSRC, Denmark; IN2P3-CNRS and CEA-DRF/IRFU, France; SRNSFG, Georgia; BMBF, HGF and MPG, Germany; GSRI, Greece; RGC and Hong Kong SAR, China; ISF and Benoziyo Center, Israel; INFN, Italy; MEXT and JSPS, Japan; CNRST, Morocco; NWO, Netherlands; RCN, Norway; MNiSW, Poland; FCT, Portugal; MNE/IFA, Romania; MESTD, Serbia; MSSR, Slovakia; ARIS and MVZI, Slovenia; DSI/NRF, South Africa; MICIU/AEI, Spain; SRC and Wallenberg Foundation, Sweden; SERI, SNSF and Cantons of Bern and Geneva, Switzerland; NSTC, Taipei; TENMAK, Türkiye; STFC/UKRI, United Kingdom; DOE and NSF, United States of America.

Individual groups and members have received support from BCKDF, CANARIE, CRC and DRAC, Canada; CERN-CZ, FORTE and PRIMUS, Czech Republic; COST, ERC, ERDF, Horizon 2020, ICSC-NextGenerationEU and Marie Skłodowska-Curie Actions, European Union; Investissements d'Avenir Labex, Investissements d'Avenir Idex and ANR, France; DFG and AvH Foundation, Germany; Herakleitos, Thales and Aristeia programmes co-financed by EU-ESF and the Greek NSRF, Greece; BSF-NSF and MINERVA, Israel; Norwegian Financial Mechanism 2014-2021, Norway; NCN and NAWA, Poland; La Caixa Banking Foundation, CERCA Programme Generalitat de Catalunya and PROMETEO and GenT

Programmes Generalitat Valenciana, Spain; Göran Gustafssons Stiftelse, Sweden; The Royal Society and Leverhulme Trust, United Kingdom.

In addition, individual members wish to acknowledge support from CERN: European Organization for Nuclear Research (CERN PJAS); Chile: Agencia Nacional de Investigación y Desarrollo (FONDECYT 1190886, FONDECYT 1230812, FONDECYT 1230987); China: Chinese Ministry of Science and Technology (MOST-2023YFA1605700), National Natural Science Foundation of China (NSFC - 12175119, NSFC 12275265, NSFC-12075060); Czech Republic: Czech Science Foundation (GACR - 24-11373S), Ministry of Education Youth and Sports (FORTE CZ.02.01.01/00/22_008/0004632), PRIMUS Research Programme (PRIMUS/21/SCI/017); EU: H2020 European Research Council (ERC - 101002463); European Union: European Research Council (ERC - 948254, ERC 101089007), Horizon 2020 Framework Programme (MUCCA - CHIST-ERA-19-XAI-00), European Union, Future Artificial Intelligence Research (FAIR-NextGenerationEU PE00000013), Italian Center for High Performance Computing, Big Data and Quantum Computing (ICSC, NextGenerationEU); France: Agence Nationale de la Recherche (ANR-20-CE31-0013, ANR-21-CE31-0013, ANR-21-CE31-0022, ANR-22-EDIR-0002), Investissements d'Avenir Labex (ANR-11-LABX-0012); Germany: Baden-Württemberg Stiftung (BW Stiftung-Postdoc Eliteprogramme), Deutsche Forschungsgemeinschaft (DFG - 469666862, DFG - CR 312/5-2); Italy: Istituto Nazionale di Fisica Nucleare (ICSC, NextGenerationEU), Ministero dell'Università e della Ricerca (PRIN - 20223N7F8K - PNRR M4.C2.1.1); Japan: Japan Society for the Promotion of Science (JSPS KAKENHI JP21H05085, JSPS KAKENHI JP22H01227, JSPS KAKENHI JP22H04944, JSPS KAKENHI JP22KK0227); Netherlands: Netherlands Organisation for Scientific Research (NWO Veni 2020 - VI.Veni.202.179); Norway: Research Council of Norway (RCN-314472); Poland: Ministry of Science and Higher Education (IDUB AGH, POB8, D4 no 9722), Polish National Agency for Academic Exchange (PPN/PPO/2020/1/00002/U/00001), Polish National Science Centre (NCN 2021/42/E/ST2/00350, NCN OPUS nr 2022/47/B/ST2/03059, NCN UMO-2019/34/E/ST2/00393, UMO-2020/37/B/ST2/01043, UMO-2021/40/C/ST2/00187, UMO-2022/47/O/ST2/00148, UMO-2023/49/B/ST2/04085); Slovenia: Slovenian Research Agency (ARIS grant J1-3010); Spain: Generalitat Valenciana (Artemisa, FEDER, IDIFEDER/2018/048), Ministry of Science and Innovation (MCIN & NextGenEU PCI2022-135018-2, MICIN & FEDER PID2021-125273NB, RYC2019-028510-I, RYC2020-030254-I, RYC2021-031273-I, RYC2022-038164-I), PROMETEO and GenT Programmes Generalitat Valenciana (CIDEGENT/2019/023, CIDEGENT/2019/027); Sweden: Swedish Research Council (Swedish Research Council 2023-04654, VR 2018-00482, VR 2022-03845, VR 2022-04683, VR 2023-03403, VR grant 2021-03651), Knut and Alice Wallenberg Foundation (KAW 2018.0157, KAW 2018.0458, KAW 2019.0447, KAW 2022.0358); Switzerland: Swiss National Science Foundation (SNSF - PCEFP2_194658); United Kingdom: Leverhulme Trust (Leverhulme Trust RPG-2020-004), Royal Society (NIF-R1-231091); United States of America: U.S. Department of Energy (ECA DE-AC02-76SF00515), Neubauer Family Foundation.

References

[1] Y. Golfand and E. Likhtman,
Extension of the Algebra of Poincare Group Generators and Violation of P Invariance,
JETP Lett. **13** (1971) 323, [Pisma Zh. Eksp. Teor. Fiz. **13** (1971) 452].

[2] D. Volkov and V. Akulov, *Is the neutrino a goldstone particle?* Phys. Lett. B **46** (1973) 109.

[3] J. Wess and B. Zumino, *Supergauge transformations in four dimensions*,
Nucl. Phys. B **70** (1974) 39.

[4] J. Wess and B. Zumino, *Supergauge invariant extension of quantum electrodynamics*, Nucl. Phys. B **78** (1974) 1.

[5] S. Ferrara and B. Zumino, *Supergauge invariant Yang-Mills theories*, Nucl. Phys. B **79** (1974) 413.

[6] A. Salam and J. Strathdee, *Super-symmetry and non-Abelian gauges*, Phys. Lett. B **51** (1974) 353.

[7] N. Sakai, *Naturalness in supersymmetric GUTS*, Z. Phys. C **11** (1981) 153.

[8] S. Dimopoulos, S. Raby, and F. Wilczek, *Supersymmetry and the scale of unification*, Phys. Rev. D **24** (1981) 1681.

[9] L. E. Ibáñez and G. G. Ross, *Low-energy predictions in supersymmetric grand unified theories*, Phys. Lett. B **105** (1981) 439.

[10] S. Dimopoulos and H. Georgi, *Softly broken supersymmetry and SU(5)*, Nucl. Phys. B **193** (1981) 150.

[11] G. R. Farrar and P. Fayet, *Phenomenology of the production, decay, and detection of new hadronic states associated with supersymmetry*, Phys. Lett. B **76** (1978) 575.

[12] H. Goldberg, *Constraint on the Photino Mass from Cosmology*, Phys. Rev. Lett. **50** (1983) 1419, Erratum: Phys. Rev. Lett. **103** (2009) 099905.

[13] J. Ellis, J. Hagelin, D. V. Nanopoulos, K. A. Olive, and M. Srednicki, *Supersymmetric relics from the big bang*, Nucl. Phys. B **238** (1984) 453.

[14] R. Mahbubani, M. Papucci, G. Perez, J. T. Ruderman, and A. Weiler, *Light Nondegenerate Squarks at the LHC*, Phys. Rev. Lett. **110** (2013) 151804, arXiv: `1212.3328 [hep-ph]`.

[15] R. Gröber, M. Mühlleitner, E. Popenda, and A. Wlotzka, *Light stop decays into $Wb\tilde{\chi}_1^0$ near the kinematic threshold*, Phys. Lett. B **747** (2015) 144, arXiv: `1502.05935 [hep-ph]`.

[16] S. Dimopoulos and L. Susskind, *Mass without scalars*, Nucl. Phys. B **155** (1979) 237.

[17] S. Dimopoulos, *Technicoloured signatures*, Nucl. Phys. B **168** (1980) 69.

[18] E. Eichten and K. Lane, *Dynamical breaking of weak interaction symmetries*, Phys. Lett. B **90** (1980) 125.

[19] V. Angelopoulos et al., *Search for new quarks suggested by the superstring*, Nucl. Phys. B **292** (1987) 59.

[20] W. Buchmüller and D. Wyler, *Constraints on SU(5)-type leptoquarks*, Phys. Lett. B **177** (1986) 377.

[21] J. C. Pati and A. Salam, *Lepton number as the fourth "color"*, Phys. Rev. D **10** (1 1974) 275.

[22] H. Georgi and S. L. Glashow, *Unity of All Elementary-Particle Forces*, Phys. Rev. Lett. **32** (8 1974) 438.

[23] B. Diaz, M. Schmaltz, and Y.-M. Zhong, *The leptoquark Hunter's guide: Pair production*, JHEP **10** (2017) 097, arXiv: `1706.05033 [hep-ph]`.

[24] A. Belyaev, C. Leroy, R. Mehdiyev, and A. Pukhov, *Leptoquark single and pair production at LHC with CalcHEP/CompHEP in the complete model*, JHEP **09** (2005) 005.

[25] A. Belyaev, C. Leroy, R. Mehdiyev, and A. Pukhov, *Leptoquark single and pair production at LHC with CalcHEP/CompHEP in the complete model*, JHEP **09** (2005) 005, arXiv: `hep-ph/0502067`.

[26] J. Blumlein, E. Boos, and A. Kryukov, *Leptoquark pair production in hadronic interactions*, Z. Phys. C **76** (1997) 137, arXiv: `hep-ph/9610408`.

[27] T. Mandal, S. Mitra, and S. Seth, *Pair Production of Scalar Leptoquarks at the LHC to NLO Parton Shower Accuracy*, Phys. Rev. D **93** (2016) 035018, arXiv: `1506.07369 [hep-ph]`.

[28] M. Krämer, T. Plehn, M. Spira, and P. M. Zerwas, *Pair production of scalar leptoquarks at the CERN LHC*, Phys. Rev. D **71** (2005) 057503, arXiv: `hep-ph/0411038`.

[29] M. Krämer, T. Plehn, M. Spira, and P. M. Zerwas, *Pair production of scalar leptoquarks at the Fermilab Tevatron*, Phys. Rev. Lett. **79** (1997) 341, arXiv: `hep-ph/9704322`.

[30] ATLAS Collaboration, *Search for supersymmetry in final states with charm jets and missing transverse momentum in 13 TeV pp collisions with the ATLAS detector*, JHEP **09** (2018) 050, arXiv: `1805.01649 [hep-ex]`.

[31] P. Jackson and C. Rogan, *Recursive Jigsaw Reconstruction: HEP event analysis in the presence of kinematic and combinatoric ambiguities*, Phys. Rev. D **96** (2017) 112007, arXiv: `1705.10733 [hep-ph]`.

[32] ATLAS Collaboration, *Search for new phenomena in events with an energetic jet and missing transverse momentum in pp collisions at $\sqrt{s} = 13$ TeV with the ATLAS detector*, Phys. Rev. D **103** (2021) 112006, arXiv: `2102.10874 [hep-ex]`.

[33] ATLAS Collaboration, *Search for squarks and gluinos in final states with jets and missing transverse momentum using 139 fb^{-1} of $\sqrt{s} = 13$ TeV pp collision data with the ATLAS detector*, JHEP **02** (2021) 143, arXiv: `2010.14293 [hep-ex]`.

[34] ATLAS Collaboration, *A search for top-squark pair production, in final states containing a top quark, a charm quark and missing transverse momentum, using the 139 fb^{-1} of pp collision data collected by the ATLAS detector*, JHEP **07** (2024) 250, arXiv: `2402.12137 [hep-ex]`.

[35] CMS Collaboration, *Search for top squark production in fully hadronic final states in proton–proton collisions at $\sqrt{s} = 13$ TeV*, Phys. Rev. D **104** (2021) 052001, arXiv: `2103.01290 [hep-ex]`.

[36] ATLAS Collaboration, *The ATLAS Experiment at the CERN Large Hadron Collider*, JINST **3** (2008) S08003.

[37] ATLAS Collaboration, *ATLAS Insertable B-Layer: Technical Design Report*, ATLAS-TDR-19; CERN-LHCC-2010-013, 2010, URL: `https://cds.cern.ch/record/1291633`, Addendum: ATLAS-TDR-19-ADD-1; CERN-LHCC-2012-009, 2012, URL: `https://cds.cern.ch/record/1451888`.

[38] B. Abbott et al., *Production and integration of the ATLAS Insertable B-Layer*, JINST **13** (2018) T05008, arXiv: `1803.00844 [physics.ins-det]`.

[39] G. Avoni et al., *The new LUCID-2 detector for luminosity measurement and monitoring in ATLAS*, JINST **13** (2018) P07017.

[40] ATLAS Collaboration, *Performance of the ATLAS trigger system in 2015*, Eur. Phys. J. C **77** (2017) 317, arXiv: `1611.09661 [hep-ex]`.

[41] ATLAS Collaboration, *Software and computing for Run 3 of the ATLAS experiment at the LHC*, (2024), arXiv: `2404.06335 [hep-ex]`.

[42] ATLAS Collaboration, *ATLAS data quality operations and performance for 2015–2018 data-taking*, JINST **15** (2020) P04003, arXiv: `1911.04632 [physics.ins-det]`.

[43] ATLAS Collaboration, *Luminosity determination in pp collisions at $\sqrt{s} = 13$ TeV using the ATLAS detector at the LHC*, ATLAS-CONF-2019-021, 2019, URL: `https://cds.cern.ch/record/2677054`.

[44] G. Avoni et al., *The new LUCID-2 detector for luminosity measurement and monitoring in ATLAS*, JINST **13** (2018) P07017.

[45] ATLAS Collaboration, *Performance of the missing transverse momentum triggers for the ATLAS detector during Run-2 data taking*, JHEP **08** (2020) 080, arXiv: `2005.09554 [hep-ex]`.

[46] ATLAS Collaboration, *The ATLAS Simulation Infrastructure*, Eur. Phys. J. C **70** (2010) 823, arXiv: `1005.4568 [physics.ins-det]`.

[47] S. Agostinelli et al., *GEANT4 – a simulation toolkit*, Nucl. Instrum. Meth. A **506** (2003) 250.

[48] ATLAS Collaboration, *The new Fast Calorimeter Simulation in ATLAS*, ATL-SOFT-PUB-2018-002, 2018, URL: `https://cds.cern.ch/record/2630434`.

[49] T. Gleisberg et al., *Event generation with SHERPA 1.1*, JHEP **02** (2009) 007, arXiv: `0811.4622 [hep-ph]`.

[50] D. J. Lange, *The EvtGen particle decay simulation package*, Nucl. Instrum. Meth. A **462** (2001) 152.

[51] NNPDF Collaboration, R. D. Ball, et al., *Parton distributions for the LHC run II*, JHEP **04** (2015) 040, arXiv: `1410.8849 [hep-ph]`.

[52] ATLAS Collaboration, *Modelling and computational improvements to the simulation of single vector-boson plus jet processes for the ATLAS experiment*, JHEP **08** (2022) 089, arXiv: `2112.09588 [hep-ex]`.

[53] J. Alwall et al., *The automated computation of tree-level and next-to-leading order differential cross sections, and their matching to parton shower simulations*, JHEP **07** (2014) 079, arXiv: `1405.0301 [hep-ph]`.

[54] T. Sjöstrand et al., *An introduction to PYTHIA 8.2*, Comput. Phys. Commun. **191** (2015) 159, arXiv: `1410.3012 [hep-ph]`.

[55] ATLAS Collaboration, *ATLAS Pythia 8 tunes to 7 TeV data*, ATL-PHYS-PUB-2014-021, 2014, URL: `https://cds.cern.ch/record/1966419`.

[56] S. Alioli, P. Nason, C. Oleari, and E. Re, *A general framework for implementing NLO calculations in shower Monte Carlo programs: the POWHEG BOX*, JHEP **06** (2010) 043, arXiv: `1002.2581 [hep-ph]`.

[57] M. Czakon, P. Fiedler, and A. Mitov, *Total Top-Quark Pair-Production Cross Section at Hadron Colliders Through $O(\alpha_S^4)$*, Phys. Rev. Lett. **110** (2013) 252004, arXiv: `1303.6254 [hep-ph]`.

[58] M. Czakon and A. Mitov, *NNLO corrections to top pair production at hadron colliders: the quark-gluon reaction*, JHEP **01** (2013) 080, arXiv: `1210.6832 [hep-ph]`.

[59] M. Czakon and A. Mitov, *NNLO corrections to top-pair production at hadron colliders: the all-fermionic scattering channels*, JHEP **12** (2012) 054, arXiv: `1207.0236 [hep-ph]`.

[60] P. Bärnreuther, M. Czakon, and A. Mitov, *Percent-Level-Precision Physics at the Tevatron: Next-to-Next-to-Leading Order QCD Corrections to $q\bar{q} \to t\bar{t} + X$*, Phys. Rev. Lett. **109** (2012) 132001, arXiv: `1204.5201 [hep-ph]`.

[61] M. Cacciari, M. Czakon, M. Mangano, A. Mitov, and P. Nason, *Top-pair production at hadron colliders with next-to-next-to-leading logarithmic soft-gluon resummation*, Phys. Lett. B **710** (2012) 612, arXiv: `1111.5869 [hep-ph]`.

[62] M. Czakon and A. Mitov, *Top++: A program for the calculation of the top-pair cross-section at hadron colliders*, Comput. Phys. Commun. **185** (2014) 2930, arXiv: `1112.5675 [hep-ph]`.

[63] N. Kidonakis, *Next-to-next-to-leading-order collinear and soft gluon corrections for t-channel single top quark production*, Phys. Rev. D **83** (2011) 091503, arXiv: `1103.2792 [hep-ph]`.

[64] N. Kidonakis, *Two-loop soft anomalous dimensions for single top quark associated production with a W^- or H^-*, Phys. Rev. D **82** (2010) 054018, arXiv: `1005.4451 [hep-ph]`.

[65] N. Kidonakis, *Next-to-next-to-leading logarithm resummation for s-channel single top quark production*, Phys. Rev. D **81** (2010) 054028, arXiv: `1001.5034 [hep-ph]`.

[66] E. Bothmann et al., *Event generation with Sherpa 2.2*, SciPost Phys. **7** (2019) 034, arXiv: `1905.09127 [hep-ph]`.

[67] W. Beenakker, C. Borschensky, M. Krämer, A. Kulesza, and E. Laenen, *NNLL-fast: predictions for coloured supersymmetric particle production at the LHC with threshold and Coulomb resummation*, JHEP **12** (2016) 133, arXiv: `1607.07741 [hep-ph]`.

[68] W. Beenakker, M. Krämer, T. Plehn, M. Spira, and P. M. Zerwas, *Stop production at hadron colliders*, Nucl. Phys. B **515** (1998) 3, arXiv: `hep-ph/9710451`.

[69] W. Beenakker et al., *Supersymmetric top and bottom squark production at hadron colliders*, JHEP **08** (2010) 098, arXiv: `1006.4771 [hep-ph]`.

[70] W. Beenakker et al., *NNLL resummation for stop pair-production at the LHC*, JHEP **05** (2016) 153, arXiv: `1601.02954 [hep-ph]`.

[71] C. Borschensky, B. Fuks, A. Kulesza, and D. Schwartländer, *Scalar leptoquark pair production at hadron colliders*, Phys. Rev. D **101** (2020) 115017, arXiv: `2002.08971 [hep-ph]`.

[72] ATLAS Collaboration, *Vertex Reconstruction Performance of the ATLAS Detector at $\sqrt{s} = 13$ TeV*, ATL-PHYS-PUB-2015-026, 2015, URL: `https://cds.cern.ch/record/2037717`.

[73] M. Cacciari, G. P. Salam, and G. Soyez, *The anti-k_t jet clustering algorithm*, JHEP **04** (2008) 063, arXiv: `0802.1189 [hep-ph]`.

[74] M. Cacciari, G. P. Salam, and G. Soyez, *FastJet user manual*, Eur. Phys. J. C **72** (2012) 1896, arXiv: `1111.6097 [hep-ph]`.

[75] ATLAS Collaboration, *Jet reconstruction and performance using particle flow with the ATLAS Detector*, Eur. Phys. J. C **77** (2017) 466, arXiv: `1703.10485 [hep-ex]`.

[76] ATLAS Collaboration, *Jet energy scale and resolution measured in proton–proton collisions at* $\sqrt{s} = 13$ *TeV with the ATLAS detector*, Eur. Phys. J. C **81** (2021) 689, arXiv: `2007.02645 [hep-ex]`.

[77] ATLAS Collaboration, E_T^{miss} *performance in the ATLAS detector using 2015–2016 LHC* pp *collisions*, ATLAS-CONF-2018-023, 2018, URL: `https://cds.cern.ch/record/2625233`.

[78] ATLAS Collaboration, *Performance of pile-up mitigation techniques for jets in* pp *collisions at* $\sqrt{s} = 8$ *TeV using the ATLAS detector*, Eur. Phys. J. C **76** (2016) 581, arXiv: `1510.03823 [hep-ex]`.

[79] ATLAS Collaboration, *ATLAS flavour-tagging algorithms for the LHC Run 2* pp *collision dataset*, Eur. Phys. J. C **83** (2023) 681, arXiv: `2211.16345 [physics.data-an]`.

[80] ATLAS Collaboration, *Measurement of the* c*-jet mistagging efficiency in* $t\bar{t}$ *events using* pp *collision data at* $\sqrt{s} = 13$ *TeV collected with the ATLAS detector*, Eur. Phys. J. C **82** (2022) 95, arXiv: `2109.10627 [hep-ex]`.

[81] ATLAS Collaboration, *ATLAS* b*-jet identification performance and efficiency measurement with* $t\bar{t}$ *events in* pp *collisions at* $\sqrt{s} = 13$ *TeV*, Eur. Phys. J. C **79** (2019) 970, arXiv: `1907.05120 [hep-ex]`.

[82] ATLAS Collaboration, *Calibration of the light-flavour jet mistagging efficiency of the* b*-tagging algorithms with* Z*+jets events using* $139\,fb^{-1}$ *of ATLAS proton–proton collision data at* $\sqrt{s} = 13$ *TeV*, Eur. Phys. J. C **83** (2023) 728, arXiv: `2301.06319 [hep-ex]`.

[83] ATLAS Collaboration, *Electron and photon performance measurements with the ATLAS detector using the 2015–2017 LHC proton–proton collision data*, JINST **14** (2019) P12006, arXiv: `1908.00005 [hep-ex]`.

[84] ATLAS Collaboration, *Muon reconstruction and identification efficiency in ATLAS using the full Run 2* pp *collision data set at* $\sqrt{s} = 13$ *TeV*, Eur. Phys. J. C **81** (2021) 578, arXiv: `2012.00578 [hep-ex]`.

[85] ATLAS Collaboration, *Reconstruction, Energy Calibration, and Identification of Hadronically Decaying Tau Leptons in the ATLAS Experiment for Run-2 of the LHC*, ATL-PHYS-PUB-2015-045, 2015, URL: `https://cds.cern.ch/record/2064383`.

[86] ATLAS Collaboration, *Identification of hadronic tau lepton decays using neural networks in the ATLAS experiment*, ATL-PHYS-PUB-2019-033, 2019, URL: `https://cds.cern.ch/record/2688062`.

[87] ATLAS Collaboration, *The performance of missing transverse momentum reconstruction and its significance with the ATLAS detector using* $140\,fb^{-1}$ *of* $\sqrt{s} = 13$ *TeV* pp *collisions*, (2024), arXiv: `2402.05858 [hep-ex]`.

[88] ATLAS Collaboration, *Object-based missing transverse momentum significance in the ATLAS Detector*, ATLAS-CONF-2018-038, 2018, URL: `https://cds.cern.ch/record/2630948`.

[89] ATLAS Collaboration, *Searches for new phenomena in events with two leptons, jets, and missing transverse momentum in* $139\,fb^{-1}$ *of* $\sqrt{s} = 13$ *TeV* pp *collisions with the ATLAS detector*, Eur. Phys. J. C **83** (2023) 515, arXiv: `2204.13072 [hep-ex]`.

[90] ATLAS Collaboration,
Measurements of inclusive and differential fiducial cross-sections of $t\bar{t}$ production with additional heavy-flavour jets in proton–proton collisions at $\sqrt{s} = 13$ TeV with the ATLAS detector,
JHEP **04** (2019) 046, arXiv: `1811.12113 [hep-ex]`.

[91] G. Cowan, K. Cranmer, E. Gross, and O. Vitells,
Asymptotic formulae for likelihood-based tests of new physics, Eur. Phys. J. C **71** (2011) 1554, arXiv: `1007.1727 [physics.data-an]`, Erratum: Eur. Phys. J. C **73** (2013) 2501.

[92] R. D. Cousins, J. T. Linnemann, and J. Tucker,
Evaluation of three methods for calculating statistical significance when incorporating a systematic uncertainty into a test of the background-only hypothesis for a Poisson process,
Nucl. Instrum. Meth. A **595** (2008) 480, arXiv: `physics/0702156 [physics.data-an]`.

[93] A. L. Read, *Presentation of search results: the CL_S technique*, J. Phys. G **28** (2002) 2693.

[94] ATLAS Collaboration, *ATLAS Computing Acknowledgements*, ATL-SOFT-PUB-2023-001, 2023, URL: `https://cds.cern.ch/record/2869272`.

The ATLAS Collaboration

G. Aad[104], E. Aakvaag[17], B. Abbott[123], S. Abdelhameed[119a], K. Abeling[56], N.J. Abicht[50], S.H. Abidi[30], M. Aboelela[45], A. Aboulhorma[36e], H. Abramowicz[155], H. Abreu[154], Y. Abulaiti[120], B.S. Acharya[70a,70b,l], A. Ackermann[64a], C. Adam Bourdarios[4], L. Adamczyk[87a], S.V. Addepalli[27], M.J. Addison[103], J. Adelman[118], A. Adiguzel[22c], T. Adye[137], A.A. Affolder[139], Y. Afik[40], M.N. Agaras[13], J. Agarwala[74a,74b], A. Aggarwal[102], C. Agheorghiesei[28c], F. Ahmadov[39,z], W.S. Ahmed[106], S. Ahuja[97], X. Ai[63e], G. Aielli[77a,77b], A. Aikot[166], M. Ait Tamlihat[36e], B. Aitbenchikh[36a], M. Akbiyik[102], T.P.A. Åkesson[100], A.V. Akimov[38], D. Akiyama[171], N.N. Akolkar[25], S. Aktas[22a], K. Al Khoury[42], G.L. Alberghi[24b], J. Albert[168], P. Albicocco[54], G.L. Albouy[61], S. Alderweireldt[53], Z.L. Alegria[124], M. Aleksa[37], I.N. Aleksandrov[39], C. Alexa[28b], T. Alexopoulos[10], F. Alfonsi[24b], M. Algren[57], M. Alhroob[170], B. Ali[135], H.M.J. Ali[93], S. Ali[32], S.W. Alibocus[94], M. Aliev[34c], G. Alimonti[72a], W. Alkakhi[56], C. Allaire[67], B.M.M. Allbrooke[150], J.F. Allen[53], C.A. Allendes Flores[140f], P.P. Allport[21], A. Aloisio[73a,73b], F. Alonso[92], C. Alpigiani[142], Z.M.K. Alsolami[93], M. Alvarez Estevez[101], A. Alvarez Fernandez[102], M. Alves Cardoso[57], M.G. Alviggi[73a,73b], M. Aly[103], Y. Amaral Coutinho[84b], A. Ambler[106], C. Amelung[37], M. Amerl[103], C.G. Ames[111], D. Amidei[108], K.J. Amirie[158], S.P. Amor Dos Santos[133a], K.R. Amos[166], S. An[85], V. Ananiev[128], C. Anastopoulos[143], T. Andeen[11], J.K. Anders[37], A.C. Anderson[60], S.Y. Andrean[48a,48b], A. Andreazza[72a,72b], S. Angelidakis[9], A. Angerami[42], A.V. Anisenkov[38], A. Annovi[75a], C. Antel[57], E. Antipov[149], M. Antonelli[54], F. Anulli[76a], M. Aoki[85], T. Aoki[157], M.A. Aparo[150], L. Aperio Bella[49], C. Appelt[19], A. Apyan[27], S.J. Arbiol Val[88], C. Arcangeletti[54], A.T.H. Arce[52], E. Arena[94], J-F. Arguin[110], S. Argyropoulos[55], J.-H. Arling[49], O. Arnaez[4], H. Arnold[149], G. Artoni[76a,76b], H. Asada[113], K. Asai[121], S. Asai[157], N.A. Asbah[37], R.A. Ashby Pickering[170], K. Assamagan[30], R. Astalos[29a], K.S.V. Astrand[100], S. Atashi[162], R.J. Atkin[34a], M. Atkinson[165], H. Atmani[36f], P.A. Atmasiddha[131], K. Augsten[135], S. Auricchio[73a,73b], A.D. Auriol[21], V.A. Austrup[103], G. Avolio[37], K. Axiotis[57], G. Azuelos[110,ae], D. Babal[29b], H. Bachacou[138], K. Bachas[156,p], A. Bachiu[35], F. Backman[48a,48b], A. Badea[40], T.M. Baer[108], P. Bagnaia[76a,76b], M. Bahmani[19], D. Bahner[55], K. Bai[126], J.T. Baines[137], L. Baines[96], O.K. Baker[175], E. Bakos[16], D. Bakshi Gupta[8], L.E. Balabram Filho[84b], V. Balakrishnan[123], R. Balasubramanian[117], E.M. Baldin[38], P. Balek[87a], E. Ballabene[24b,24a], F. Balli[138], L.M. Baltes[64a], W.K. Balunas[33], J. Balz[102], I. Bamwidhi[119b], E. Banas[88], M. Bandieramonte[132], A. Bandyopadhyay[25], S. Bansal[25], L. Barak[155], M. Barakat[49], E.L. Barberio[107], D. Barberis[58b,58a], M. Barbero[104], M.Z. Barel[117], K.N. Barends[34a], T. Barillari[112], M-S. Barisits[37], T. Barklow[147], P. Baron[125], D.A. Baron Moreno[103], A. Baroncelli[63a], A.J. Barr[129], J.D. Barr[98], F. Barreiro[101], J. Barreiro Guimarães da Costa[14], U. Barron[155], M.G. Barros Teixeira[133a], S. Barsov[38], F. Bartels[64a], R. Bartoldus[147], A.E. Barton[93], P. Bartos[29a], A. Basan[102], M. Baselga[50], A. Bassalat[67,b], M.J. Basso[159a], S. Bataju[45], R. Bate[167], R.L. Bates[60], S. Batlamous[101], B. Batool[145], M. Battaglia[139], D. Battulga[19], M. Bauce[76a,76b], M. Bauer[80], P. Bauer[25], L.T. Bazzano Hurrell[31], J.B. Beacham[52], T. Beau[130], J.Y. Beaucamp[92], P.H. Beauchemin[161], P. Bechtle[25], H.P. Beck[20,o], K. Becker[170], A.J. Beddall[83], V.A. Bednyakov[39], C.P. Bee[149], L.J. Beemster[16], T.A. Beermann[37], M. Begalli[84d], M. Begel[30], A. Behera[149], J.K. Behr[49], J.F. Beirer[37], F. Beisiegel[25], M. Belfkir[119b], G. Bella[155], L. Bellagamba[24b], A. Bellerive[35], P. Bellos[21], K. Beloborodov[38], D. Benchekroun[36a], F. Bendebba[36a], Y. Benhammou[155], K.C. Benkendorfer[62], L. Beresford[49], M. Beretta[54], E. Bergeaas Kuutmann[164], N. Berger[4], B. Bergmann[135], J. Beringer[18a], G. Bernardi[5], C. Bernius[147], F.U. Bernlochner[25], F. Bernon[37,104], A. Berrocal Guardia[13], T. Berry[97], P. Berta[136], A. Berthold[51], S. Bethke[112], A. Betti[76a,76b], A.J. Bevan[96], N.K. Bhalla[55], S. Bhatta[149], D.S. Bhattacharya[169], P. Bhattarai[147], K.D. Bhide[55], V.S. Bhopatkar[124], R.M. Bianchi[132], G. Bianco[24b,24a], O. Biebel[111], R. Bielski[126], M. Biglietti[78a], C.S. Billingsley[45], M. Bindi[56], A. Bingul[22b], C. Bini[76a,76b], A. Biondini[94], G.A. Bird[33], M. Birman[172], M. Biros[136], S. Biryukov[150], T. Bisanz[50], E. Bisceglie[44b,44a], J.P. Biswal[137], D. Biswas[145], I. Bloch[49], A. Blue[60], U. Blumenschein[96], J. Blumenthal[102], V.S. Bobrovnikov[38], M. Boehler[55], B. Boehm[169], D. Bogavac[37], A.G. Bogdanchikov[38], C. Bohm[48a], V. Boisvert[97], P. Bokan[37], T. Bold[87a], M. Bomben[5], M. Bona[96], M. Boonekamp[138], C.D. Booth[97], A.G. Borbély[60], I.S. Bordulev[38], H.M. Borecka-Bielska[110], G. Borissov[93], D. Bortoletto[129], D. Boscherini[24b], M. Bosman[13], J.D. Bossio Sola[37], K. Bouaouda[36a], N. Bouchhar[166], L. Boudet[4], J. Boudreau[132], E.V. Bouhova-Thacker[93], D. Boumediene[41], R. Bouquet[58b,58a], A. Boveia[122], J. Boyd[37], D. Boye[30], I.R. Boyko[39], L. Bozianu[57], J. Bracinik[21], N. Brahimi[4], G. Brandt[174], O. Brandt[33], F. Braren[49], B. Brau[105], J.E. Brau[126], R. Brener[172], L. Brenner[117], R. Brenner[164], S. Bressler[172], G. Brianti[79a,79b], D. Britton[60], D. Britzger[112], I. Brock[25], R. Brock[109], G. Brooijmans[42], E.M. Brooks[159b], E. Brost[30], L.M. Brown[168], L.E. Bruce[62], T.L. Bruckler[129], P.A. Bruckman de Renstrom[88], B. Brüers[49], A. Bruni[24b], G. Bruni[24b], M. Bruschi[24b], N. Bruscino[76a,76b], T. Buanes[17], Q. Buat[142], D. Buchin[112], A.G. Buckley[60], O. Bulekov[38], B.A. Bullard[147], S. Burdin[94], C.D. Burgard[50], A.M. Burger[37], B. Burghgrave[8], O. Burlayenko[55], J. Burleson[165], J.T.P. Burr[33], J.C. Burzynski[146], E.L. Busch[42], V. Büscher[102], P.J. Bussey[60], J.M. Butler[26], C.M. Buttar[60], J.M. Butterworth[98], W. Buttinger[137], C.J. Buxo Vazquez[109], A.R. Buzykaev[38], S. Cabrera Urbán[166], L. Cadamuro[67], D. Caforio[59], H. Cai[132], Y. Cai[14,114c], Y. Cai[114a], V.M.M. Cairo[37], O. Cakir[3a], N. Calace[37], P. Calafiura[18a], G. Calderini[130], P. Calfayan[69], G. Callea[60], L.P. Caloba[84b], D. Calvet[41], S. Calvet[41], M. Calvetti[75a,75b], R. Camacho Toro[130], S. Camarda[37], D. Camarero Munoz[27], P. Camarri[77a,77b], M.T. Camerlingo[73a,73b], D. Cameron[37], C. Camincher[168], M. Campanelli[98], A. Camplani[43], V. Canale[73a,73b], A.C. Canbay[3a], E. Canonero[97], J. Cantero[166], Y. Cao[165], F. Capocasa[27], M. Capua[44b,44a], A. Carbone[72a,72b], R. Cardarelli[77a], J.C.J. Cardenas[8], G. Carducci[44b,44a], T. Carli[37], G. Carlino[73a], J.I. Carlotto[13], B.T. Carlson[132,q], E.M. Carlson[168,159a], J. Carmignani[94], L. Carminati[72a,72b], A. Carnelli[138], M. Carnesale[76a,76b], S. Caron[116], E. Carquin[140f], S. Carrá[72a], G. Carratta[24b,24a], A.M. Carroll[126], T.M. Carter[53], M.P. Casado[13,i], M. Caspar[49], F.L. Castillo[4], L. Castillo Garcia[13], V. Castillo Gimenez[166], N.F. Castro[133a,133e], A. Catinaccio[37], J.R. Catmore[128], T. Cavaliere[4], V. Cavaliere[30], N. Cavalli[24b,24a], L.J. Caviedes Betancourt[23b], Y.C. Cekmecelioglu[49], E. Celebi[83], S. Cella[37], F. Celli[129], M.S. Centonze[71a,71b], V. Cepaitis[57], K. Cerny[125], A.S. Cerqueira[84a], A. Cerri[150], L. Cerrito[77a,77b], F. Cerutti[18a], B. Cervato[145], A. Cervelli[24b], G. Cesarini[54], S.A. Cetin[83], D. Chakraborty[118], J. Chan[18a], W.Y. Chan[157], J.D. Chapman[33], E. Chapon[138], B. Chargeishvili[153b], D.G. Charlton[21], M. Chatterjee[20], C. Chauhan[136], Y. Che[114a], S. Chekanov[6], S.V. Chekulaev[159a], G.A. Chelkov[39,a], A. Chen[108], B. Chen[155], B. Chen[168], H. Chen[114a], H. Chen[30], J. Chen[63c], J. Chen[146], M. Chen[129], S. Chen[157], S.J. Chen[114a], X. Chen[63c,138], X. Chen[15,ad], Y. Chen[63a], C.L. Cheng[173], H.C. Cheng[65a], S. Cheong[147], A. Cheplakov[39], E. Cheremushkina[49], E. Cherepanova[117], R. Cherkaoui El Moursli[36e], E. Cheu[7], K. Cheung[66], L. Chevalier[138], V. Chiarella[54], G. Chiarelli[75a], N. Chiedde[104], G. Chiodini[71a], A.S. Chisholm[21], A. Chitan[28b], M. Chitishvili[166], M.V. Chizhov[39,r],

K. Choi[11], Y. Chou[142], E.Y.S. Chow[116], K.L. Chu[172], M.C. Chu[65a], X. Chu[14,114c],
Z. Chubinidze[54], J. Chudoba[134], J.J. Chwastowski[88], D. Cieri[112], K.M. Ciesla[87a],
V. Cindro[95], A. Ciocio[18a], F. Cirotto[73a,73b], Z.H. Citron[172], M. Citterio[72a], D.A. Ciubotaru[28b],
A. Clark[57], P.J. Clark[53], N. Clarke Hall[98], C. Clarry[158], J.M. Clavijo Columbie[49],
S.E. Clawson[49], C. Clement[48a,48b], Y. Coadou[104], M. Cobal[70a,70c], A. Coccaro[58b],
R.F. Coelho Barrue[133a], R. Coelho Lopes De Sa[105], S. Coelli[72a], B. Cole[42], J. Collot[61],
P. Conde Muiño[133a,133g], M.P. Connell[34c], S.H. Connell[34c], E.I. Conroy[129], F. Conventi[73a,af],
H.G. Cooke[21], A.M. Cooper-Sarkar[129], F.A. Corchia[24b,24a], A. Cordeiro Oudot Choi[130],
L.D. Corpe[41], M. Corradi[76a,76b], F. Corriveau[106,x], A. Cortes-Gonzalez[19], M.J. Costa[166],
F. Costanza[4], D. Costanzo[143], B.M. Cote[122], J. Couthures[4], G. Cowan[97], K. Cranmer[173],
D. Cremonini[24b,24a], S. Crépé-Renaudin[61], F. Crescioli[130], M. Cristinziani[145],
M. Cristoforetti[79a,79b], V. Croft[117], J.E. Crosby[124], G. Crosetti[44b,44a], A. Cueto[101], H. Cui[98],
Z. Cui[7], W.R. Cunningham[60], F. Curcio[166], J.R. Curran[53], P. Czodrowski[37],
M.M. Czurylo[37], M.J. Da Cunha Sargedas De Sousa[58b,58a], J.V. Da Fonseca Pinto[84b],
C. Da Via[103], W. Dabrowski[87a], T. Dado[50], S. Dahbi[152], T. Dai[108], D. Dal Santo[20],
C. Dallapiccola[105], M. Dam[43], G. D'amen[30], V. D'Amico[111], J. Damp[102], J.R. Dandoy[35],
D. Dannheim[37], M. Danninger[146], V. Dao[149], G. Darbo[58b], S.J. Das[30,ag], F. Dattola[49],
S. D'Auria[72a,72b], A. D'Avanzo[73a,73b], C. David[34a], T. Davidek[136], I. Dawson[96],
H.A. Day-hall[135], K. De[8], R. De Asmundis[73a], N. De Biase[49], S. De Castro[24b,24a],
N. De Groot[116], P. de Jong[117], H. De la Torre[118], A. De Maria[114a], A. De Salvo[76a],
U. De Sanctis[77a,77b], F. De Santis[71a,71b], A. De Santo[150], J.B. De Vivie De Regie[61],
D.V. Dedovich[39], J. Degens[94], A.M. Deiana[45], F. Del Corso[24b,24a], J. Del Peso[101],
F. Del Rio[64a], L. Delagrange[130], F. Deliot[138], C.M. Delitzsch[50], M. Della Pietra[73a,73b],
D. Della Volpe[57], A. Dell'Acqua[37], L. Dell'Asta[72a,72b], M. Delmastro[4], P.A. Delsart[61],
S. Demers[175], M. Demichev[39], S.P. Denisov[38], L. D'Eramo[41], D. Derendarz[88], F. Derue[130],
P. Dervan[94], K. Desch[25], C. Deutsch[25], F.A. Di Bello[58b,58a], A. Di Ciaccio[77a,77b],
L. Di Ciaccio[4], A. Di Domenico[76a,76b], C. Di Donato[73a,73b], A. Di Girolamo[37],
G. Di Gregorio[37], A. Di Luca[79a,79b], B. Di Micco[78a,78b], R. Di Nardo[78a,78b], K.F. Di Petrillo[40],
M. Diamantopoulou[35], F.A. Dias[117], T. Dias Do Vale[146], M.A. Diaz[140a,140b],
F.G. Diaz Capriles[25], A.R. Didenko[39], M. Didenko[166], E.B. Diehl[108], S. Díez Cornell[49],
C. Diez Pardos[145], C. Dimitriadi[164], A. Dimitrievska[21], J. Dingfelder[25], T. Dingley[129],
I-M. Dinu[28b], S.J. Dittmeier[64b], F. Dittus[37], M. Divisek[136], F. Djama[104], T. Djobava[153b],
C. Doglioni[103,100], A. Dohnalova[29a], J. Dolejsi[136], Z. Dolezal[136], K. Domijan[87a],
K.M. Dona[40], M. Donadelli[84d], B. Dong[109], J. Donini[41], A. D'Onofrio[73a,73b],
M. D'Onofrio[94], J. Dopke[137], A. Doria[73a], N. Dos Santos Fernandes[133a], P. Dougan[103],
M.T. Dova[92], A.T. Doyle[60], M.A. Draguet[129], E. Dreyer[172], I. Drivas-koulouris[10],
M. Drnevich[120], M. Drozdova[57], D. Du[63a], T.A. du Pree[117], F. Dubinin[38], M. Dubovsky[29a],
E. Duchovni[172], G. Duckeck[111], O.A. Ducu[28b], D. Duda[53], A. Dudarev[37], E.R. Duden[27],
M. D'uffizi[103], L. Duflot[67], M. Dührssen[37], I. Duminica[28g], A.E. Dumitriu[28b],
M. Dunford[64a], S. Dungs[50], K. Dunne[48a,48b], A. Duperrin[104], H. Duran Yildiz[3a],
M. Düren[59], A. Durglishvili[153b], B.L. Dwyer[118], G.I. Dyckes[18a], M. Dyndal[87a],
B.S. Dziedzic[37], Z.O. Earnshaw[150], G.H. Eberwein[129], B. Eckerova[29a], S. Eggebrecht[56],
E. Egidio Purcino De Souza[130], L.F. Ehrke[57], G. Eigen[17], K. Einsweiler[18a], T. Ekelof[164],
P.A. Ekman[100], S. El Farkh[36b], Y. El Ghazali[36b], H. El Jarrari[37], A. El Moussaouy[36a],
V. Ellajosyula[164], M. Ellert[164], F. Ellinghaus[174], N. Ellis[37], J. Elmsheuser[30], M. Elsawy[119a],
M. Elsing[37], D. Emeliyanov[137], Y. Enari[157], I. Ene[18a], S. Epari[13], P.A. Erland[88],
D. Ernani Martins Neto[88], M. Errenst[174], M. Escalier[67], C. Escobar[166], E. Etzion[155],

G. Evans[133a], H. Evans[69], L.S. Evans[97], A. Ezhilov[38], S. Ezzarqtouni[36a], F. Fabbri[24b,24a], L. Fabbri[24b,24a], G. Facini[98], V. Fadeyev[139], R.M. Fakhrutdinov[38], D. Fakoudis[102], S. Falciano[76a], L.F. Falda Ulhoa Coelho[37], F. Fallavollita[112], G. Falsetti[44b,44a], J. Faltova[136], C. Fan[165], Y. Fan[14], Y. Fang[14,114c], M. Fanti[72a,72b], M. Faraj[70a,70b], Z. Farazpay[99], A. Farbin[8], A. Farilla[78a], T. Farooque[109], S.M. Farrington[53], F. Fassi[36e], D. Fassouliotis[9], M. Faucci Giannelli[77a,77b], W.J. Fawcett[33], L. Fayard[67], P. Federic[136], P. Federicova[134], O.L. Fedin[38,a], M. Feickert[173], L. Feligioni[104], D.E. Fellers[126], C. Feng[63b], M. Feng[15], Z. Feng[117], M.J. Fenton[162], L. Ferencz[49], R.A.M. Ferguson[93], S.I. Fernandez Luengo[140f], P. Fernandez Martinez[13], M.J.V. Fernoux[104], J. Ferrando[93], A. Ferrari[164], P. Ferrari[117,116], R. Ferrari[74a], D. Ferrere[57], C. Ferretti[108], D. Fiacco[76a,76b], F. Fiedler[102], P. Fiedler[135], A. Filipčič[95], E.K. Filmer[1], F. Filthaut[116], M.C.N. Fiolhais[133a,133c,c], L. Fiorini[166], W.C. Fisher[109], T. Fitschen[103], P.M. Fitzhugh[138], I. Fleck[145], P. Fleischmann[108], T. Flick[174], M. Flores[34d,ab], L.R. Flores Castillo[65a], L. Flores Sanz De Acedo[37], F.M. Follega[79a,79b], N. Fomin[33], J.H. Foo[158], A. Formica[138], A.C. Forti[103], E. Fortin[37], A.W. Fortman[18a], M.G. Foti[18a], L. Fountas[9,j], D. Fournier[67], H. Fox[93], P. Francavilla[75a,75b], S. Francescato[62], S. Franchellucci[57], M. Franchini[24b,24a], S. Franchino[64a], D. Francis[37], L. Franco[116], V. Franco Lima[37], L. Franconi[49], M. Franklin[62], G. Frattari[27], Y.Y. Frid[155], J. Friend[60], N. Fritzsche[51], A. Froch[55], D. Froidevaux[37], J.A. Frost[129], Y. Fu[63a], S. Fuenzalida Garrido[140f], M. Fujimoto[104], K.Y. Fung[65a], E. Furtado De Simas Filho[84e], M. Furukawa[157], J. Fuster[166], A. Gaa[56], A. Gabrielli[24b,24a], A. Gabrielli[158], P. Gadow[37], G. Gagliardi[58b,58a], L.G. Gagnon[18a], S. Gaid[163], S. Galantzan[155], E.J. Gallas[129], B.J. Gallop[137], K.K. Gan[122], S. Ganguly[157], Y. Gao[53], F.M. Garay Walls[140a,140b], B. Garcia[30], C. García[166], A. Garcia Alonso[117], A.G. Garcia Caffaro[175], J.E. García Navarro[166], M. Garcia-Sciveres[18a], G.L. Gardner[131], R.W. Gardner[40], N. Garelli[161], D. Garg[81], R.B. Garg[147], J.M. Gargan[53], C.A. Garner[158], C.M. Garvey[34a], V.K. Gassmann[161], G. Gaudio[74a], V. Gautam[13], P. Gauzzi[76a,76b], J. Gavranovic[95], I.L. Gavrilenko[38], A. Gavrilyuk[38], C. Gay[167], G. Gaycken[126], E.N. Gazis[10], A.A. Geanta[28b], C.M. Gee[139], A. Gekow[122], C. Gemme[58b], M.H. Genest[61], A.D. Gentry[115], S. George[97], W.F. George[21], T. Geralis[47], P. Gessinger-Befurt[37], M.E. Geyik[174], M. Ghani[170], K. Ghorbanian[96], A. Ghosal[145], A. Ghosh[162], A. Ghosh[7], B. Giacobbe[24b], S. Giagu[76a,76b], T. Giani[117], A. Giannini[63a], S.M. Gibson[97], M. Gignac[139], D.T. Gil[87b], A.K. Gilbert[87a], B.J. Gilbert[42], D. Gillberg[35], G. Gilles[117], L. Ginabat[130], D.M. Gingrich[2,ae], M.P. Giordani[70a,70c], P.F. Giraud[138], G. Giugliarelli[70a,70c], D. Giugni[72a], F. Giuli[37], I. Gkialas[9,j], L.K. Gladilin[38], C. Glasman[101], G.R. Gledhill[126], G. Glemža[49], M. Glisic[126], I. Gnesi[44b,e], Y. Go[30], M. Goblirsch-Kolb[37], B. Gocke[50], D. Godin[110], B. Gokturk[22a], S. Goldfarb[107], T. Golling[57], M.G.D. Gololo[34g], D. Golubkov[38], J.P. Gombas[109], A. Gomes[133a,133b], G. Gomes Da Silva[145], A.J. Gomez Delegido[166], R. Gonçalo[133a], L. Gonella[21], A. Gongadze[153c], F. Gonnella[21], J.L. Gonski[147], R.Y. González Andana[53], S. González de la Hoz[166], R. Gonzalez Lopez[94], C. Gonzalez Renteria[18a], M.V. Gonzalez Rodrigues[49], R. Gonzalez Suarez[164], S. Gonzalez-Sevilla[57], L. Goossens[37], B. Gorini[37], E. Gorini[71a,71b], A. Gorišek[95], T.C. Gosart[131], A.T. Goshaw[52], M.I. Gostkin[39], S. Goswami[124], C.A. Gottardo[37], S.A. Gotz[111], M. Gouighri[36b], V. Goumarre[49], A.G. Goussiou[142], N. Govender[34c], I. Grabowska-Bold[87a], K. Graham[35], E. Gramstad[128], S. Grancagnolo[71a,71b], C.M. Grant[1,138], P.M. Gravila[28f], F.G. Gravili[71a,71b], H.M. Gray[18a], M. Greco[71a,71b], M.J. Green[1], C. Grefe[25], A.S. Grefsrud[17], I.M. Gregor[49], K.T. Greif[162], P. Grenier[147], S.G. Grewe[112], A.A. Grillo[139], K. Grimm[32], S. Grinstein[13,t], J.-F. Grivaz[67], E. Gross[172], J. Grosse-Knetter[56], J.C. Grundy[129], L. Guan[108], J.G.R. Guerrero Rojas[166], G. Guerrieri[70a,70c], R. Gugel[102], J.A.M. Guhit[108], A. Guida[19], E. Guilloton[170], S. Guindon[37], F. Guo[14,114c], J. Guo[63c], L. Guo[49], Y. Guo[108], R. Gupta[132], S. Gurbuz[25], S.S. Gurdasani[55], G. Gustavino[76a,76b], P. Gutierrez[123], L.F. Gutierrez Zagazeta[131], M. Gutsche[51], C. Gutschow[98], C. Gwenlan[129], C.B. Gwilliam[94], E.S. Haaland[128], A. Haas[120], M. Habedank[49], C. Haber[18a], H.K. Hadavand[8], A. Hadef[51], S. Hadzic[112], A.I. Hagan[93], J.J. Hahn[145], E.H. Haines[98], M. Haleem[169], J. Haley[124], J.J. Hall[143], G.D. Hallewell[104], L. Halser[20], K. Hamano[168], M. Hamer[25], G.N. Hamity[53], E.J. Hampshire[97], J. Han[63b], K. Han[63a], L. Han[114a], L. Han[63a], S. Han[18a], Y.F. Han[158], K. Hanagaki[85], M. Hance[139], D.A. Hangal[42], H. Hanif[146], M.D. Hank[131], J.B. Hansen[43], P.H. Hansen[43], K. Hara[160], D. Harada[57], T. Harenberg[174], S. Harkusha[38], M.L. Harris[105], Y.T. Harris[129], J. Harrison[13], N.M. Harrison[122], P.F. Harrison[170], N.M. Hartman[112], N.M. Hartmann[111], R.Z. Hasan[97,137], Y. Hasegawa[144], S. Hassan[17], R. Hauser[109], C.M. Hawkes[21], R.J. Hawkings[37], Y. Hayashi[157], S. Hayashida[113], D. Hayden[109], C. Hayes[108], R.L. Hayes[117], C.P. Hays[129], J.M. Hays[96], H.S. Hayward[94], F. He[63a], M. He[14,114c], Y. He[141], Y. He[49], Y. He[98], N.B. Heatley[96], V. Hedberg[100], A.L. Heggelund[128], N.D. Hehir[96,*], C. Heidegger[55], K.K. Heidegger[55], J. Heilman[35], S. Heim[49], T. Heim[18a], J.G. Heinlein[131], J.J. Heinrich[126], L. Heinrich[112,ac], J. Hejbal[134], A. Held[173], S. Hellesund[17], C.M. Helling[167], S. Hellman[48a,48b], R.C.W. Henderson[93], L. Henkelmann[33], A.M. Henriques Correia[37], H. Herde[100], Y. Hernández Jiménez[149], L.M. Herrmann[25], T. Herrmann[51], G. Herten[55], R. Hertenberger[111], L. Hervas[37], M.E. Hesping[102], N.P. Hessey[159a], M. Hidaoui[36b], N. Hidic[136], E. Hill[158], S.J. Hillier[21], J.R. Hinds[109], F. Hinterkeuser[25], M. Hirose[127], S. Hirose[160], D. Hirschbuehl[174], T.G. Hitchings[103], B. Hiti[95], J. Hobbs[149], R. Hobincu[28e], N. Hod[172], M.C. Hodgkinson[143], B.H. Hodkinson[129], A. Hoecker[37], D.D. Hofer[108], J. Hofer[49], T. Holm[25], M. Holzbock[112], L.B.A.H. Hommels[33], B.P. Honan[103], J.J. Hong[69], J. Hong[63c], T.M. Hong[132], B.H. Hooberman[165], W.H. Hopkins[6], M.C. Hoppesch[165], Y. Horii[113], S. Hou[152], A.S. Howard[95], J. Howarth[60], J. Hoya[6], M. Hrabovsky[125], A. Hrynevich[49], T. Hryn'ova[4], P.J. Hsu[66], S.-C. Hsu[142], T. Hsu[67], M. Hu[18a], Q. Hu[63a], S. Huang[65b], X. Huang[14,114c], Y. Huang[143], Y. Huang[102], Y. Huang[14], Z. Huang[103], Z. Hubacek[135], M. Huebner[25], F. Huegging[25], T.B. Huffman[129], C.A. Hugli[49], M. Huhtinen[37], S.K. Huiberts[17], R. Hulsken[106], N. Huseynov[12,g], J. Huston[109], J. Huth[62], R. Hyneman[147], G. Iacobucci[57], G. Iakovidis[30], L. Iconomidou-Fayard[67], J.P. Iddon[37], P. Iengo[73a,73b], R. Iguchi[157], Y. Iiyama[157], T. Iizawa[129], Y. Ikegami[85], N. Ilic[158], H. Imam[36a], M. Ince Lezki[57], T. Ingebretsen Carlson[48a,48b], J.M. Inglis[96], G. Introzzi[74a,74b], M. Iodice[78a], V. Ippolito[76a,76b], R.K. Irwin[94], M. Ishino[157], W. Islam[173], C. Issever[19,49], S. Istin[22a,ai], H. Ito[171], R. Iuppa[79a,79b], A. Ivina[172], J.M. Izen[46], V. Izzo[73a], P. Jacka[134], P. Jackson[1], C.S. Jagfeld[111], G. Jain[159a], P. Jain[49], K. Jakobs[55], T. Jakoubek[172], J. Jamieson[60], W. Jang[157], M. Javurkova[105], P. Jawahar[103], L. Jeanty[126], J. Jejelava[153a,aa], P. Jenni[55,f], C.E. Jessiman[35], C. Jia[63b], J. Jia[149], X. Jia[62], X. Jia[14,114c], Z. Jia[114a], C. Jiang[53], S. Jiggins[49], J. Jimenez Pena[13], S. Jin[114a], A. Jinaru[28b], O. Jinnouchi[141], P. Johansson[143], K.A. Johns[7], J.W. Johnson[139], D.M. Jones[150], E. Jones[49], P. Jones[33], R.W.L. Jones[93], T.J. Jones[94], H.L. Joos[56,37], R. Joshi[122], J. Jovicevic[16], X. Ju[18a], J.J. Junggeburth[105], T. Junkermann[64a], A. Juste Rozas[13,t], M.K. Juzek[88], S. Kabana[140e], A. Kaczmarska[88], M. Kado[112], H. Kagan[122], M. Kagan[147], A. Kahn[131], C. Kahra[102], T. Kaji[157], E. Kajomovitz[154], N. Kakati[172], I. Kalaitzidou[55], C.W. Kalderon[30], N.J. Kang[139], D. Kar[34g], K. Karava[129], M.J. Kareem[159b], E. Karentzos[55], O. Karkout[117], S.N. Karpov[39], Z.M. Karpova[39], V. Kartvelishvili[93], A.N. Karyukhin[38], E. Kasimi[156], J. Katzy[49], S. Kaur[35], K. Kawade[144], M.P. Kawale[123], C. Kawamoto[89], T. Kawamoto[63a], E.F. Kay[37], F.I. Kaya[161],

S. Kazakos[109], V.F. Kazanin[38], Y. Ke[149], J.M. Keaveney[34a], R. Keeler[168], G.V. Kehris[62], J.S. Keller[35], A.S. Kelly[98], J.J. Kempster[150], P.D. Kennedy[102], O. Kepka[134], B.P. Kerridge[137], S. Kersten[174], B.P. Kerševan[95], L. Keszeghova[29a], S. Ketabchi Haghighat[158], R.A. Khan[132], A. Khanov[124], A.G. Kharlamov[38], T. Kharlamova[38], E.E. Khoda[142], M. Kholodenko[38], T.J. Khoo[19], G. Khoriauli[169], J. Khubua[153b,*], Y.A.R. Khwaira[130], B. Kibirige[34g], D. Kim[6], D.W. Kim[48a,48b], Y.K. Kim[40], N. Kimura[98], M.K. Kingston[56], A. Kirchhoff[56], C. Kirfel[25], F. Kirfel[25], J. Kirk[137], A.E. Kiryunin[112], C. Kitsaki[10], O. Kivernyk[25], M. Klassen[161], C. Klein[35], L. Klein[169], M.H. Klein[45], S.B. Klein[57], U. Klein[94], P. Klimek[37], A. Klimentov[30], T. Klioutchnikova[37], P. Kluit[117], S. Kluth[112], E. Kneringer[80], T.M. Knight[158], A. Knue[50], R. Kobayashi[89], D. Kobylianskii[172], S.F. Koch[129], M. Kocian[147], P. Kodyš[136], D.M. Koeck[126], P.T. Koenig[25], T. Koffas[35], O. Kolay[51], I. Koletsou[4], T. Komarek[88], K. Köneke[55], A.X.Y. Kong[1], T. Kono[121], N. Konstantinidis[98], P. Kontaxakis[57], B. Konya[100], R. Kopeliansky[42], S. Koperny[87a], K. Korcyl[88], K. Kordas[156,d], A. Korn[98], S. Korn[56], I. Korolkov[13], N. Korotkova[38], B. Kortman[117], O. Kortner[112], S. Kortner[112], W.H. Kostecka[118], V.V. Kostyukhin[145], A. Kotsokechagia[138], A. Kotwal[52], A. Koulouris[37], A. Kourkoumeli-Charalampidi[74a,74b], C. Kourkoumelis[9], E. Kourlitis[112,ac], O. Kovanda[126], R. Kowalewski[168], W. Kozanecki[138], A.S. Kozhin[38], V.A. Kramarenko[38], G. Kramberger[95], P. Kramer[102], M.W. Krasny[130], A. Krasznahorkay[37], A.C. Kraus[118], J.W. Kraus[174], J.A. Kremer[49], T. Kresse[51], L. Kretschmann[174], J. Kretzschmar[94], K. Kreul[19], P. Krieger[158], S. Krishnamurthy[105], M. Krivos[136], K. Krizka[21], K. Kroeninger[50], H. Kroha[112], J. Kroll[134], J. Kroll[131], K.S. Krowpman[109], U. Kruchonak[39], H. Krüger[25], N. Krumnack[82], M.C. Kruse[52], O. Kuchinskaia[38], S. Kuday[3a], S. Kuehn[37], R. Kuesters[55], T. Kuhl[49], V. Kukhtin[39], Y. Kulchitsky[38,a], S. Kuleshov[140d,140b], M. Kumar[34g], N. Kumari[49], P. Kumari[159b], A. Kupco[134], T. Kupfer[50], A. Kupich[38], O. Kuprash[55], H. Kurashige[86], L.L. Kurchaninov[159a], O. Kurdysh[67], Y.A. Kurochkin[38], A. Kurova[38], M. Kuze[141], A.K. Kvam[105], J. Kvita[125], T. Kwan[106], N.G. Kyriacou[108], L.A.O. Laatu[104], C. Lacasta[166], F. Lacava[76a,76b], H. Lacker[19], D. Lacour[130], N.N. Lad[98], E. Ladygin[39], A. Lafarge[41], B. Laforge[130], T. Lagouri[175], F.Z. Lahbabi[36a], S. Lai[56], J.E. Lambert[168], S. Lammers[69], W. Lampl[7], C. Lampoudis[156,d], G. Lamprinoudis[102], A.N. Lancaster[118], E. Lançon[30], U. Landgraf[55], M.P.J. Landon[96], V.S. Lang[55], O.K.B. Langrekken[128], A.J. Lankford[162], F. Lanni[37], K. Lantzsch[25], A. Lanza[74a], J.F. Laporte[138], T. Lari[72a], F. Lasagni Manghi[24b], M. Lassnig[37], V. Latonova[134], A. Laurier[154], S.D. Lawlor[143], Z. Lawrence[103], R. Lazaridou[170], M. Lazzaroni[72a,72b], B. Le[103], E.M. Le Boulicaut[52], L.T. Le Pottier[18a], B. Leban[24b,24a], A. Lebedev[82], M. LeBlanc[103], F. Ledroit-Guillon[61], S.C. Lee[152], S. Lee[48a,48b], T.F. Lee[94], L.L. Leeuw[34c], H.P. Lefebvre[97], M. Lefebvre[168], C. Leggett[18a], G. Lehmann Miotto[37], M. Leigh[57], W.A. Leight[105], W. Leinonen[116], A. Leisos[156,s], M.A.L. Leite[84c], C.E. Leitgeb[19], R. Leitner[136], K.J.C. Leney[45], T. Lenz[25], S. Leone[75a], C. Leonidopoulos[53], A. Leopold[148], R. Les[109], C.G. Lester[33], M. Levchenko[38], J. Levêque[4], L.J. Levinson[172], G. Levrini[24b,24a], M.P. Lewicki[88], C. Lewis[142], D.J. Lewis[4], A. Li[5], B. Li[63b], C. Li[63a], C-Q. Li[112], H. Li[63a], H. Li[63b], H. Li[114a], H. Li[15], H. Li[63b], J. Li[63c], K. Li[142], L. Li[63c], M. Li[14,114c], S. Li[14,114c], S. Li[63d,63c], T. Li[5], X. Li[106], Z. Li[129], Z. Li[157], Z. Li[14,114c], S. Liang[14,114c], Z. Liang[14], M. Liberatore[138], B. Liberti[77a], K. Lie[65c], J. Lieber Marin[84e], H. Lien[69], H. Lin[108], K. Lin[109], R.E. Lindley[7], J.H. Lindon[2], J. Ling[62], E. Lipeles[131], A. Lipniacka[17], A. Lister[167], J.D. Little[69], B. Liu[14], B.X. Liu[114b], D. Liu[63d,63c], E.H.L. Liu[21], J.B. Liu[63a], J.K.K. Liu[33], K. Liu[63d], K. Liu[63d,63c], M. Liu[63a], M.Y. Liu[63a], P. Liu[14], Q. Liu[63d,142,63c], X. Liu[63a], X. Liu[63b], Y. Liu[114b,114c], Y.L. Liu[63b], Y.W. Liu[63a],

J. Llorente Merino[146], S.L. Lloyd[96], E.M. Lobodzinska[49], P. Loch[7], T. Lohse[19],
K. Lohwasser[143], E. Loiacono[49], M. Lokajicek[134,*], J.D. Lomas[21], J.D. Long[165],
I. Longarini[162], R. Longo[165], I. Lopez Paz[68], A. Lopez Solis[49], N. Lorenzo Martinez[4],
A.M. Lory[111], M. Losada[119a], G. Löschcke Centeno[150], O. Loseva[38], X. Lou[48a,48b],
X. Lou[14,114c], A. Lounis[67], P.A. Love[93], G. Lu[14,114c], M. Lu[67], S. Lu[131], Y.J. Lu[66],
H.J. Lubatti[142], C. Luci[76a,76b], F.L. Lucio Alves[114a], F. Luehring[69], I. Luise[149],
O. Lukianchuk[67], O. Lundberg[148], B. Lund-Jensen[148,*], N.A. Luongo[6], M.S. Lutz[37],
A.B. Lux[26], D. Lynn[30], R. Lysak[134], E. Lytken[100], V. Lyubushkin[39], T. Lyubushkina[39],
M.M. Lyukova[149], M.Firdaus M. Soberi[53], H. Ma[30], K. Ma[63a], L.L. Ma[63b], W. Ma[63a],
Y. Ma[124], J.C. MacDonald[102], P.C. Machado De Abreu Farias[84e], R. Madar[41], T. Madula[98],
J. Maeda[86], T. Maeno[30], H. Maguire[143], V. Maiboroda[138], A. Maio[133a,133b,133d], K. Maj[87a],
O. Majersky[49], S. Majewski[126], N. Makovec[67], V. Maksimovic[16], B. Malaescu[130],
Pa. Malecki[88], V.P. Maleev[38], F. Malek[61,n], M. Mali[95], D. Malito[97], U. Mallik[81,*],
S. Maltezos[10], S. Malyukov[39], J. Mamuzic[13], G. Mancini[54], M.N. Mancini[27], G. Manco[74a,74b],
J.P. Mandalia[96], S.S. Mandarry[150], I. Mandić[95], L. Manhaes de Andrade Filho[84a],
I.M. Maniatis[172], J. Manjarres Ramos[91], D.C. Mankad[172], A. Mann[111], S. Manzoni[37],
L. Mao[63c], X. Mapekula[34c], A. Marantis[156,s], G. Marchiori[5], M. Marcisovsky[134],
C. Marcon[72a], M. Marinescu[21], S. Marium[49], M. Marjanovic[123], A. Markhoos[55],
M. Markovitch[67], E.J. Marshall[93], Z. Marshall[18a], S. Marti-Garcia[166], J. Martin[98],
T.A. Martin[137], V.J. Martin[53], B. Martin dit Latour[17], L. Martinelli[76a,76b], M. Martinez[13,t],
P. Martinez Agullo[166], V.I. Martinez Outschoorn[105], P. Martinez Suarez[13], S. Martin-Haugh[137],
G. Martinovicova[136], V.S. Martoiu[28b], A.C. Martyniuk[98], A. Marzin[37], D. Mascione[79a,79b],
L. Masetti[102], T. Mashimo[157], J. Masik[103], A.L. Maslennikov[38], P. Massarotti[73a,73b],
P. Mastrandrea[75a,75b], A. Mastroberardino[44b,44a], T. Masubuchi[157], T. Mathisen[164],
J. Matousek[136], N. Matsuzawa[157], J. Maurer[28b], A.J. Maury[67], B. Maček[95], D.A. Maximov[38],
A.E. May[103], R. Mazini[152], I. Maznas[118], M. Mazza[109], S.M. Mazza[139], E. Mazzeo[72a,72b],
C. Mc Ginn[30], J.P. Mc Gowan[168], S.P. Mc Kee[108], C.C. McCracken[167], E.F. McDonald[107],
A.E. McDougall[117], J.A. Mcfayden[150], R.P. McGovern[131], R.P. Mckenzie[34g],
T.C. Mclachlan[49], D.J. Mclaughlin[98], S.J. McMahon[137], C.M. Mcpartland[94],
R.A. McPherson[168,x], S. Mehlhase[111], A. Mehta[94], D. Melini[166], B.R. Mellado Garcia[34g],
A.H. Melo[56], F. Meloni[49], A.M. Mendes Jacques Da Costa[103], H.Y. Meng[158], L. Meng[93],
S. Menke[112], M. Mentink[37], E. Meoni[44b,44a], G. Mercado[118], S. Merianos[156],
C. Merlassino[70a,70c], L. Merola[73a,73b], C. Meroni[72a,72b], J. Metcalfe[6], A.S. Mete[6],
E. Meuser[102], C. Meyer[69], J-P. Meyer[138], R.P. Middleton[137], L. Mijović[53],
G. Mikenberg[172], M. Mikestikova[134], M. Mikuž[95], H. Mildner[102], A. Milic[37],
D.W. Miller[40], E.H. Miller[147], L.S. Miller[35], A. Milov[172], D.A. Milstead[48a,48b], T. Min[114a],
A.A. Minaenko[38], I.A. Minashvili[153b], L. Mince[60], A.I. Mincer[120], B. Mindur[87a],
M. Mineev[39], Y. Mino[89], L.M. Mir[13], M. Miralles Lopez[60], M. Mironova[18a], A. Mishima[157],
M.C. Missio[116], A. Mitra[170], V.A. Mitsou[166], Y. Mitsumori[113], O. Miu[158],
P.S. Miyagawa[96], T. Mkrtchyan[64a], M. Mlinarevic[98], T. Mlinarevic[98], M. Mlynarikova[37],
S. Mobius[20], P. Mogg[111], M.H. Mohamed Farook[115], A.F. Mohammed[14,114c], S. Mohapatra[42],
G. Mokgatitswane[34g], L. Moleri[172], B. Mondal[145], S. Mondal[135], K. Mönig[49],
E. Monnier[104], L. Monsonis Romero[166], J. Montejo Berlingen[13], M. Montella[122],
F. Montereali[78a,78b], F. Monticelli[92], S. Monzani[70a,70c], N. Morange[67],
A.L. Moreira De Carvalho[49], M. Moreno Llácer[166], C. Moreno Martinez[57], P. Morettini[58b],
S. Morgenstern[37], M. Morii[62], M. Morinaga[157], F. Morodei[76a,76b], L. Morvaj[37],
P. Moschovakos[37], B. Moser[37], M. Mosidze[153b], T. Moskalets[45], P. Moskvitina[116],

J. Moss[32,k], P. Moszkowicz[87a], A. Moussa[36d], E.J.W. Moyse[105], O. Mtintsilana[34g],
S. Muanza[104], J. Mueller[132], D. Muenstermann[93], R. Müller[37], G.A. Mullier[164],
A.J. Mullin[33], J.J. Mullin[131], D.P. Mungo[158], D. Munoz Perez[166], F.J. Munoz Sanchez[103],
M. Murin[103], W.J. Murray[170,137], M. Muškinja[95], C. Mwewa[30], A.G. Myagkov[38,a],
A.J. Myers[8], G. Myers[108], M. Myska[135], B.P. Nachman[18a], O. Nackenhorst[50], K. Nagai[129],
K. Nagano[85], J.L. Nagle[30,ag], E. Nagy[104], A.M. Nairz[37], Y. Nakahama[85], K. Nakamura[85],
K. Nakkalil[5], H. Nanjo[127], E.A. Narayanan[115], I. Naryshkin[38], L. Nasella[72a,72b],
M. Naseri[35], S. Nasri[119b], C. Nass[25], G. Navarro[23a], J. Navarro-Gonzalez[166], R. Nayak[155],
A. Nayaz[19], P.Y. Nechaeva[38], S. Nechaeva[24b,24a], F. Nechansky[49], L. Nedic[129], T.J. Neep[21],
A. Negri[74a,74b], M. Negrini[24b], C. Nellist[117], C. Nelson[106], K. Nelson[108], S. Nemecek[134],
M. Nessi[37,h], M.S. Neubauer[165], F. Neuhaus[102], J. Neundorf[49], P.R. Newman[21],
C.W. Ng[132], Y.W.Y. Ng[49], B. Ngair[119a], H.D.N. Nguyen[110], R.B. Nickerson[129],
R. Nicolaidou[138], J. Nielsen[139], M. Niemeyer[56], J. Niermann[56], N. Nikiforou[37],
V. Nikolaenko[38,a], I. Nikolic-Audit[130], K. Nikolopoulos[21], P. Nilsson[30], I. Ninca[49],
G. Ninio[155], A. Nisati[76a], N. Nishu[2], R. Nisius[112], J-E. Nitschke[51], E.K. Nkadimeng[34g],
T. Nobe[157], T. Nommensen[151], M.B. Norfolk[143], B.J. Norman[35], M. Noury[36a], J. Novak[95],
T. Novak[95], L. Novotny[135], R. Novotny[115], L. Nozka[125], K. Ntekas[162],
N.M.J. Nunes De Moura Junior[84b], J. Ocariz[130], A. Ochi[86], I. Ochoa[133a], S. Oerdek[49,u],
J.T. Offermann[40], A. Ogrodnik[136], A. Oh[103], C.C. Ohm[148], H. Oide[85], R. Oishi[157],
M.L. Ojeda[49], Y. Okumura[157], L.F. Oleiro Seabra[133a], I. Oleksiyuk[57], S.A. Olivares Pino[140d],
G. Oliveira Correa[13], D. Oliveira Damazio[30], D. Oliveira Goncalves[84a], J.L. Oliver[162],
Ö.O. Öncel[55], A.P. O'Neill[20], A. Onofre[133a,133e], P.U.E. Onyisi[11], M.J. Oreglia[40],
G.E. Orellana[92], D. Orestano[78a,78b], N. Orlando[13], R.S. Orr[158], L.M. Osojnak[131],
R. Ospanov[63a], G. Otero y Garzon[31], H. Otono[90], P.S. Ott[64a], G.J. Ottino[18a], M. Ouchrif[36d],
F. Ould-Saada[128], T. Ovsiannikova[142], M. Owen[60], R.E. Owen[137], V.E. Ozcan[22a],
F. Ozturk[88], N. Ozturk[8], S. Ozturk[83], H.A. Pacey[129], A. Pacheco Pages[13],
C. Padilla Aranda[13], G. Padovano[76a,76b], S. Pagan Griso[18a], G. Palacino[69], A. Palazzo[71a,71b],
J. Pampel[25], J. Pan[175], T. Pan[65a], D.K. Panchal[11], C.E. Pandini[117], J.G. Panduro Vazquez[137],
H.D. Pandya[1], H. Pang[15], P. Pani[49], G. Panizzo[70a,70c], L. Panwar[130], L. Paolozzi[57],
S. Parajuli[165], A. Paramonov[6], C. Paraskevopoulos[54], D. Paredes Hernandez[65b],
A. Pareti[74a,74b], K.R. Park[42], T.H. Park[158], M.A. Parker[33], F. Parodi[58b,58a], E.W. Parrish[118],
V.A. Parrish[53], J.A. Parsons[42], U. Parzefall[55], B. Pascual Dias[110], L. Pascual Dominguez[101],
E. Pasqualucci[76a], S. Passaggio[58b], F. Pastore[97], P. Patel[88], U.M. Patel[52], J.R. Pater[103],
T. Pauly[37], C.I. Pazos[161], J. Pearkes[147], M. Pedersen[128], R. Pedro[133a], S.V. Peleganchuk[38],
O. Penc[37], E.A. Pender[53], G.D. Penn[175], K.E. Penski[111], M. Penzin[38], B.S. Peralva[84d],
A.P. Pereira Peixoto[142], L. Pereira Sanchez[147], D.V. Perepelitsa[30,ag], G. Perera[105],
E. Perez Codina[159a], M. Perganti[10], H. Pernegger[37], S. Perrella[76a,76b], O. Perrin[41],
K. Peters[49], R.F.Y. Peters[103], B.A. Petersen[37], T.C. Petersen[43], E. Petit[104], V. Petousis[135],
C. Petridou[156,d], T. Petru[136], A. Petrukhin[145], M. Pettee[18a], A. Petukhov[38], K. Petukhova[37],
R. Pezoa[140f], L. Pezzotti[37], G. Pezzullo[175], T.M. Pham[173], T. Pham[107], P.W. Phillips[137],
G. Piacquadio[149], E. Pianori[18a], F. Piazza[126], R. Piegaia[31], D. Pietreanu[28b],
A.D. Pilkington[103], M. Pinamonti[70a,70c], J.L. Pinfold[2], B.C. Pinheiro Pereira[133a],
A.E. Pinto Pinoargote[138,138], L. Pintucci[70a,70c], K.M. Piper[150], A. Pirttikoski[57], D.A. Pizzi[35],
L. Pizzimento[65b], A. Pizzini[117], M.-A. Pleier[30], V. Pleskot[136], E. Plotnikova[39], G. Poddar[96],
R. Poettgen[100], L. Poggioli[130], I. Pokharel[56], S. Polacek[136], G. Polesello[74a],
A. Poley[146,159a], A. Polini[24b], C.S. Pollard[170], Z.B. Pollock[122], E. Pompa Pacchi[76a,76b],
N.I. Pond[98], D. Ponomarenko[116], L. Pontecorvo[37], S. Popa[28a], G.A. Popeneciu[28d],

A. Poreba[37], D.M. Portillo Quintero[159a], S. Pospisil[135], M.A. Postill[143], P. Postolache[28c], K. Potamianos[170], P.A. Potepa[87a], I.N. Potrap[39], C.J. Potter[33], H. Potti[151], J. Poveda[166], M.E. Pozo Astigarraga[37], A. Prades Ibanez[166], J. Pretel[55], D. Price[103], M. Primavera[71a], M.A. Principe Martin[101], R. Privara[125], T. Procter[60], M.L. Proffitt[142], N. Proklova[131], K. Prokofiev[65c], G. Proto[112], J. Proudfoot[6], M. Przybycien[87a], W.W. Przygoda[87b], A. Psallidas[47], J.E. Puddefoot[143], D. Pudzha[55], D. Pyatiizbyantseva[38], J. Qian[108], D. Qichen[103], Y. Qin[13], T. Qiu[53], A. Quadt[56], M. Queitsch-Maitland[103], G. Quetant[57], R.P. Quinn[167], G. Rabanal Bolanos[62], D. Rafanoharana[55], F. Raffaeli[77a,77b], F. Ragusa[72a,72b], J.L. Rainbolt[40], J.A. Raine[57], S. Rajagopalan[30], E. Ramakoti[38], I.A. Ramirez-Berend[35], K. Ran[49,114c], D.S. Rankin[131], N.P. Rapheeha[34g], H. Rasheed[28b], V. Raskina[130], D.F. Rassloff[64a], A. Rastogi[18a], S. Rave[102], S. Ravera[58b,58a], B. Ravina[56], I. Ravinovich[172], M. Raymond[37], A.L. Read[128], N.P. Readioff[143], D.M. Rebuzzi[74a,74b], G. Redlinger[30], A.S. Reed[112], K. Reeves[27], J.A. Reidelsturz[174], D. Reikher[155], A. Rej[50], C. Rembser[37], M. Renda[28b], F. Renner[49], A.G. Rennie[162], A.L. Rescia[49], S. Resconi[72a], M. Ressegotti[58b,58a], S. Rettie[37], J.G. Reyes Rivera[109], E. Reynolds[18a], O.L. Rezanova[38], P. Reznicek[136], H. Riani[36d], N. Ribaric[93], E. Ricci[79a,79b], R. Richter[112], S. Richter[48a,48b], E. Richter-Was[87b], M. Ridel[130], S. Ridouani[36d], P. Rieck[120], P. Riedler[37], E.M. Riefel[48a,48b], J.O. Rieger[117], M. Rijssenbeek[149], M. Rimoldi[37], L. Rinaldi[24b,24a], P. Rincke[56,164], T.T. Rinn[30], M.P. Rinnagel[111], G. Ripellino[164], I. Riu[13], J.C. Rivera Vergara[168], F. Rizatdinova[124], E. Rizvi[96], B.R. Roberts[18a], S.H. Robertson[106,x], D. Robinson[33], C.M. Robles Gajardo[140f], M. Robles Manzano[102], A. Robson[60], A. Rocchi[77a,77b], C. Roda[75a,75b], S. Rodriguez Bosca[37], Y. Rodriguez Garcia[23a], A. Rodriguez Rodriguez[55], A.M. Rodríguez Vera[118], S. Roe[37], J.T. Roemer[37], A.R. Roepe-Gier[139], O. Røhne[128], R.A. Rojas[105], C.P.A. Roland[130], J. Roloff[30], A. Romaniouk[38], E. Romano[74a,74b], M. Romano[24b], A.C. Romero Hernandez[165], N. Rompotis[94], L. Roos[130], S. Rosati[76a], B.J. Rosser[40], E. Rossi[129], E. Rossi[73a,73b], L.P. Rossi[62], L. Rossini[55], R. Rosten[122], M. Rotaru[28b], B. Rottler[55], C. Rougier[91], D. Rousseau[67], D. Rousso[49], A. Roy[165], S. Roy-Garand[158], A. Rozanov[104], Z.M.A. Rozario[60], Y. Rozen[154], A. Rubio Jimenez[166], A.J. Ruby[94], V.H. Ruelas Rivera[19], T.A. Ruggeri[1], A. Ruggiero[129], A. Ruiz-Martinez[166], A. Rummler[37], Z. Rurikova[55], N.A. Rusakovich[39], H.L. Russell[168], G. Russo[76a,76b], J.P. Rutherfoord[7], S. Rutherford Colmenares[33], M. Rybar[136], E.B. Rye[128], A. Ryzhov[45], J.A. Sabater Iglesias[57], P. Sabatini[166], H.F-W. Sadrozinski[139], F. Safai Tehrani[76a], B. Safarzadeh Samani[137], S. Saha[1], M. Sahinsoy[112], A. Saibel[166], M. Saimpert[138], M. Saito[157], T. Saito[157], A. Sala[72a,72b], D. Salamani[37], A. Salnikov[147], J. Salt[166], A. Salvador Salas[155], D. Salvatore[44b,44a], F. Salvatore[150], A. Salzburger[37], D. Sammel[55], E. Sampson[93], D. Sampsonidis[156,d], D. Sampsonidou[126], J. Sánchez[166], V. Sanchez Sebastian[166], H. Sandaker[128], C.O. Sander[49], J.A. Sandesara[105], M. Sandhoff[174], C. Sandoval[23b], L. Sanfilippo[64a], D.P.C. Sankey[137], T. Sano[89], A. Sansoni[54], L. Santi[37,76b], C. Santoni[41], H. Santos[133a,133b], A. Santra[172], E. Sanzani[24b,24a], K.A. Saoucha[163], J.G. Saraiva[133a,133d], J. Sardain[7], O. Sasaki[85], K. Sato[160], C. Sauer[64b], E. Sauvan[4], P. Savard[158,ae], R. Sawada[157], C. Sawyer[137], L. Sawyer[99], C. Sbarra[24b], A. Sbrizzi[24b,24a], T. Scanlon[98], J. Schaarschmidt[142], U. Schäfer[102], A.C. Schaffer[67,45], D. Schaile[111], R.D. Schamberger[149], C. Scharf[19], M.M. Schefer[20], V.A. Schegelsky[38], D. Scheirich[136], M. Schernau[162], C. Scheulen[56], C. Schiavi[58b,58a], M. Schioppa[44b,44a], B. Schlag[147], K.E. Schleicher[55], S. Schlenker[37], J. Schmeing[174], M.A. Schmidt[174], K. Schmieden[102], C. Schmitt[102], N. Schmitt[102], S. Schmitt[49], L. Schoeffel[138], A. Schoening[64b], P.G. Scholer[35], E. Schopf[129], M. Schott[25], J. Schovancova[37], S. Schramm[57], T. Schroer[57], H-C. Schultz-Coulon[64a], M. Schumacher[55], B.A. Schumm[139], Ph. Schune[138], A.J. Schuy[142], H.R. Schwartz[139], A. Schwartzman[147], T.A. Schwarz[108], Ph. Schwemling[138], R. Schwienhorst[109], F.G. Sciacca[20], A. Sciandra[30], G. Sciolla[27], F. Scuri[75a], C.D. Sebastiani[94], K. Sedlaczek[118], S.C. Seidel[115], A. Seiden[139], B.D. Seidlitz[42], C. Seitz[49], J.M. Seixas[84b], G. Sekhniaidze[73a], L. Selem[61], N. Semprini-Cesari[24b,24a], D. Sengupta[57], V. Senthilkumar[166], L. Serin[67], M. Sessa[77a,77b], H. Severini[123], F. Sforza[58b,58a], A. Sfyrla[57], Q. Sha[14], E. Shabalina[56], A.H. Shah[33], R. Shaheen[148], J.D. Shahinian[131], D. Shaked Renous[172], L.Y. Shan[14], M. Shapiro[18a], A. Sharma[37], A.S. Sharma[167], P. Sharma[81], P.B. Shatalov[38], K. Shaw[150], S.M. Shaw[103], Q. Shen[63c], D.J. Sheppard[146], P. Sherwood[98], L. Shi[98], X. Shi[14], C.O. Shimmin[175], J.D. Shinner[97], I.P.J. Shipsey[129,*], S. Shirabe[90], M. Shiyakova[39,v], M.J. Shochet[40], D.R. Shope[128], B. Shrestha[123], S. Shrestha[122,ah], M.J. Shroff[168], P. Sicho[134], A.M. Sickles[165], E. Sideras Haddad[34g], A.C. Sidley[117], A. Sidoti[24b], F. Siegert[51], Dj. Sijacki[16], F. Sili[92], J.M. Silva[53], I. Silva Ferreira[84b], M.V. Silva Oliveira[30], S.B. Silverstein[48a], S. Simion[67], R. Simoniello[37], E.L. Simpson[103], H. Simpson[150], L.R. Simpson[108], N.D. Simpson[100], S. Simsek[83], S. Sindhu[56], P. Sinervo[158], S. Singh[158], S. Sinha[49], S. Sinha[103], M. Sioli[24b,24a], I. Siral[37], E. Sitnikova[49], J. Sjölin[48a,48b], A. Skaf[56], E. Skorda[21], P. Skubic[123], M. Slawinska[88], V. Smakhtin[172], B.H. Smart[137], S.Yu. Smirnov[38], Y. Smirnov[38], L.N. Smirnova[38,a], O. Smirnova[100], A.C. Smith[42], D.R. Smith[162], E.A. Smith[40], H.A. Smith[129], J.L. Smith[103], R. Smith[147], M. Smizanska[93], K. Smolek[135], A.A. Snesarev[38], S.R. Snider[158], H.L. Snoek[117], S. Snyder[30], R. Sobie[168,x], A. Soffer[155], C.A. Solans Sanchez[37], E.Yu. Soldatov[38], U. Soldevila[166], A.A. Solodkov[38], S. Solomon[27], A. Soloshenko[39], K. Solovieva[55], O.V. Solovyanov[41], P. Sommer[37], A. Sonay[13], W.Y. Song[159b], A. Sopczak[135], A.L. Sopio[98], F. Sopkova[29b], J.D. Sorenson[115], I.R. Sotarriva Alvarez[141], V. Sothilingam[64a], O.J. Soto Sandoval[140c,140b], S. Sottocornola[69], R. Soualah[163], Z. Soumaimi[36e], D. South[49], N. Soybelman[172], S. Spagnolo[71a,71b], M. Spalla[112], D. Sperlich[55], G. Spigo[37], S. Spinali[93], B. Spisso[73a,73b], D.P. Spiteri[60], M. Spousta[136], E.J. Staats[35], R. Stamen[64a], A. Stampekis[21], M. Standke[25], E. Stanecka[88], W. Stanek-Maslouska[49], M.V. Stange[51], B. Stanislaus[18a], M.M. Stanitzki[49], B. Stapf[49], E.A. Starchenko[38], G.H. Stark[139], J. Stark[91], P. Staroba[134], P. Starovoitov[64a], S. Stärz[106], R. Staszewski[88], G. Stavropoulos[47], A. Stefl[37], P. Steinberg[30], B. Stelzer[146,159a], H.J. Stelzer[132], O. Stelzer-Chilton[159a], H. Stenzel[59], T.J. Stevenson[150], G.A. Stewart[37], J.R. Stewart[124], M.C. Stockton[37], G. Stoicea[28b], M. Stolarski[133a], S. Stonjek[112], A. Straessner[51], J. Strandberg[148], S. Strandberg[48a,48b], M. Stratmann[174], M. Strauss[123], T. Strebler[104], P. Strizenec[29b], R. Ströhmer[169], D.M. Strom[126], R. Stroynowski[45], A. Strubig[48a,48b], S.A. Stucci[30], B. Stugu[17], J. Stupak[123], N.A. Styles[49], D. Su[147], S. Su[63a], W. Su[63d], X. Su[63a], D. Suchy[29a], K. Sugizaki[157], V.V. Sulin[38], M.J. Sullivan[94], D.M.S. Sultan[129], L. Sultanaliyeva[38], S. Sultansoy[3b], T. Sumida[89], S. Sun[173], O. Sunneborn Gudnadottir[164], N. Sur[104], M.R. Sutton[150], H. Suzuki[160], M. Svatos[134], M. Swiatlowski[159a], T. Swirski[169], I. Sykora[29a], M. Sykora[136], T. Sykora[136], D. Ta[102], K. Tackmann[49,u], A. Taffard[162], R. Tafirout[159a], J.S. Tafoya Vargas[67], Y. Takubo[85], M. Talby[104], A.A. Talyshev[38], K.C. Tam[65b], N.M. Tamir[155], A. Tanaka[157], J. Tanaka[157], R. Tanaka[67], M. Tanasini[149], Z. Tao[167], S. Tapia Araya[140f], S. Tapprogge[102], A. Tarek Abouelfadl Mohamed[109], S. Tarem[154], K. Tariq[14], G. Tarna[28b], G.F. Tartarelli[72a], M.J. Tartarin[91], P. Tas[136], M. Tasevsky[134], E. Tassi[44b,44a], A.C. Tate[165], G. Tateno[157], Y. Tayalati[36e,w], G.N. Taylor[107], W. Taylor[159b], R. Teixeira De Lima[147], P. Teixeira-Dias[97], J.J. Teoh[158], K. Terashi[157], J. Terron[101], S. Terzo[13], M. Testa[54], R.J. Teuscher[158,x], A. Thaler[80], O. Theiner[57], N. Themistokleous[53], T. Theveneaux-Pelzer[104], O. Thielmann[174], D.W. Thomas[97], J.P. Thomas[21], E.A. Thompson[18a], P.D. Thompson[21], E. Thomson[131], R.E. Thornberry[45], C. Tian[63a], Y. Tian[56], V. Tikhomirov[38,a], Yu.A. Tikhonov[38], S. Timoshenko[38], D. Timoshyn[136], E.X.L. Ting[1], P. Tipton[175], A. Tishelman-Charny[30], S.H. Tlou[34g], K. Todome[141], S. Todorova-Nova[136], S. Todt[51], L. Toffolin[70a,70c], M. Togawa[85], J. Tojo[90], S. Tokár[29a], K. Tokushuku[85], O. Toldaiev[69], R. Tombs[33], M. Tomoto[85,113], L. Tompkins[147,m], K.W. Topolnicki[87b], E. Torrence[126], H. Torres[91], E. Torró Pastor[166], M. Toscani[31], C. Tosciri[40], M. Tost[11], D.R. Tovey[143], I.S. Trandafir[28b], T. Trefzger[169], A. Tricoli[30], I.M. Trigger[159a], S. Trincaz-Duvoid[130], D.A. Trischuk[27], B. Trocmé[61], A. Tropina[39], L. Truong[34c], M. Trzebinski[88], A. Trzupek[88], F. Tsai[149], M. Tsai[108], A. Tsiamis[156,d], P.V. Tsiareshka[38], S. Tsigaridas[159a], A. Tsirigotis[156,s], V. Tsiskaridze[158], E.G. Tskhadadze[153a], M. Tsopoulou[156], Y. Tsujikawa[89], I.I. Tsukerman[38], V. Tsulaia[18a], S. Tsuno[85], K. Tsuri[121], D. Tsybychev[149], Y. Tu[65b], A. Tudorache[28b], V. Tudorache[28b], A.N. Tuna[62], S. Turchikhin[58b,58a], I. Turk Cakir[3a], R. Turra[72a], T. Turtuvshin[39,y], P.M. Tuts[42], S. Tzamarias[156,d], E. Tzovara[102], F. Ukegawa[160], P.A. Ulloa Poblete[140c,140b], E.N. Umaka[30], G. Unal[37], A. Undrus[30], G. Unel[162], J. Urban[29b], P. Urrejola[140a], G. Usai[8], R. Ushioda[141], M. Usman[110], Z. Uysal[83], V. Vacek[135], B. Vachon[106], T. Vafeiadis[37], A. Vaitkus[98], C. Valderanis[111], E. Valdes Santurio[48a,48b], M. Valente[159a], S. Valentinetti[24b,24a], A. Valero[166], E. Valiente Moreno[166], A. Vallier[91], J.A. Valls Ferrer[166], D.R. Van Arneman[117], T.R. Van Daalen[142], A. Van Der Graaf[50], P. Van Gemmeren[6], M. Van Rijnbach[37], S. Van Stroud[98], I. Van Vulpen[117], P. Vana[136], M. Vanadia[77a,77b], W. Vandelli[37], E.R. Vandewall[124], D. Vannicola[155], L. Vannoli[54], R. Vari[76a], E.W. Varnes[7], C. Varni[18b], T. Varol[152], D. Varouchas[67], L. Varriale[166], K.E. Varvell[151], M.E. Vasile[28b], L. Vaslin[85], G.A. Vasquez[168], A. Vasyukov[39], L.M. Vaughan[124], R. Vavricka[102], T. Vazquez Schroeder[37], J. Veatch[32], V. Vecchio[103], M.J. Veen[105], I. Veliscek[30], L.M. Veloce[158], F. Veloso[133a,133c], S. Veneziano[76a], A. Ventura[71a,71b], S. Ventura Gonzalez[138], A. Verbytskyi[112], M. Verducci[75a,75b], C. Vergis[96], M. Verissimo De Araujo[84b], W. Verkerke[117], J.C. Vermeulen[117], C. Vernieri[147], M. Vessella[105], M.C. Vetterli[146,ae], A. Vgenopoulos[102], N. Viaux Maira[140f], T. Vickey[143], O.E. Vickey Boeriu[143], G.H.A. Viehhauser[129], L. Vigani[64b], M. Villa[24b,24a], M. Villaplana Perez[166], E.M. Villhauer[53], E. Vilucchi[54], M.G. Vincter[35], A. Visibile[117], C. Vittori[37], I. Vivarelli[24b,24a], E. Voevodina[112], F. Vogel[111], J.C. Voigt[51], P. Vokac[135], Yu. Volkotrub[87b], J. Von Ahnen[49], E. Von Toerne[25], B. Vormwald[37], V. Vorobel[136], K. Vorobev[38], M. Vos[166], K. Voss[145], M. Vozak[117], L. Vozdecky[123], N. Vranjes[16], M. Vranjes Milosavljevic[16], M. Vreeswijk[117], N.K. Vu[63d,63c], R. Vuillermet[37], O. Vujinovic[102], I. Vukotic[40], S. Wada[160], C. Wagner[105], J.M. Wagner[18a], W. Wagner[174], S. Wahdan[174], H. Wahlberg[92], M. Wakida[113], J. Walder[137], R. Walker[111], W. Walkowiak[145], A. Wall[131], E.J. Wallin[100], T. Wamorkar[6], A.Z. Wang[139], C. Wang[102], C. Wang[11], H. Wang[18a], J. Wang[65c], P. Wang[98], R. Wang[62], R. Wang[6], S.M. Wang[152], S. Wang[63b], S. Wang[14], T. Wang[63a], W.T. Wang[81], W. Wang[14], X. Wang[114a], X. Wang[165], X. Wang[63c], Y. Wang[63d], Y. Wang[114a], Y. Wang[63a], Z. Wang[108], Z. Wang[63d,52,63c], Z. Wang[108], A. Warburton[106], R.J. Ward[21], N. Warrack[60], S. Waterhouse[97], A.T. Watson[21], H. Watson[60], M.F. Watson[21], E. Watton[60,137], G. Watts[142], B.M. Waugh[98], J.M. Webb[55], C. Weber[30], H.A. Weber[19], M.S. Weber[20], S.M. Weber[64a], C. Wei[63a], Y. Wei[55], A.R. Weidberg[129], E.J. Weik[120], J. Weingarten[50], C. Weiser[55], C.J. Wells[49], T. Wenaus[30], B. Wendland[50], T. Wengler[37], N.S. Wenke[112], N. Wermes[25], M. Wessels[64a], A.M. Wharton[93], A.S. White[62], A. White[8], M.J. White[1], D. Whiteson[162], L. Wickremasinghe[127], W. Wiedenmann[173], M. Wielers[137], C. Wiglesworth[43], D.J. Wilbern[123], H.G. Wilkens[37], J.J.H. Wilkinson[33], D.M. Williams[42], H.H. Williams[131], S. Williams[33], S. Willocq[105], B.J. Wilson[103], P.J. Windischhofer[40], F.I. Winkel[31], F. Winklmeier[126], B.T. Winter[55], J.K. Winter[103], M. Wittgen[147], M. Wobisch[99], T. Wojtkowski[61], Z. Wolffs[117], J. Wollrath[162], M.W. Wolter[88], H. Wolters[133a,133c], M.C. Wong[139], E.L. Woodward[42], S.D. Worm[49], B.K. Wosiek[88], K.W. Woźniak[88], S. Wozniewski[56], K. Wraight[60], C. Wu[21], M. Wu[114b], M. Wu[116], S.L. Wu[173], X. Wu[57], Y. Wu[63a], Z. Wu[4], J. Wuerzinger[112,ac], T.R. Wyatt[103], B.M. Wynne[53], S. Xella[43], L. Xia[114a], M. Xia[15], M. Xie[63a], S. Xin[14,114c], A. Xiong[126], J. Xiong[18a], D. Xu[14], H. Xu[63a], L. Xu[63a], R. Xu[131], T. Xu[108], Y. Xu[15], Z. Xu[53], Z. Xu[114a], B. Yabsley[151], S. Yacoob[34a], Y. Yamaguchi[141], E. Yamashita[157], H. Yamauchi[160], T. Yamazaki[18a], Y. Yamazaki[86], J. Yan[63c], S. Yan[60], Z. Yan[105], H.J. Yang[63c,63d], H.T. Yang[63a], S. Yang[63a], T. Yang[65c], X. Yang[37], X. Yang[14], Y. Yang[45], Y. Yang[63a], Z. Yang[63a], W-M. Yao[18a], H. Ye[114a], H. Ye[56], J. Ye[14], S. Ye[30], X. Ye[63a], Y. Yeh[98], I. Yeletskikh[39], B. Yeo[18b], M.R. Yexley[98], T.P. Yildirim[129], P. Yin[42], K. Yorita[171], S. Younas[28b], C.J.S. Young[37], C. Young[147], C. Yu[14,114c], Y. Yu[63a], J. Yuan[14,114c], M. Yuan[108], R. Yuan[63d,63c], L. Yue[98], M. Zaazoua[63a], B. Zabinski[88], E. Zaid[53], Z.K. Zak[88], T. Zakareishvili[166], S. Zambito[57], J.A. Zamora Saa[140d,140b], J. Zang[157], D. Zanzi[55], O. Zaplatilek[135], C. Zeitnitz[174], H. Zeng[14], J.C. Zeng[165], D.T. Zenger Jr[27], O. Zenin[38], T. Ženiš[29a], S. Zenz[96], S. Zerradi[36a], D. Zerwas[67], M. Zhai[14,114c], D.F. Zhang[143], J. Zhang[63b], J. Zhang[6], K. Zhang[14,114c], L. Zhang[63a], L. Zhang[114a], P. Zhang[14,114c], R. Zhang[173], S. Zhang[108], S. Zhang[91], T. Zhang[157], X. Zhang[63c], X. Zhang[63b], Y. Zhang[63c], Y. Zhang[98], Y. Zhang[114a], Z. Zhang[18a], Z. Zhang[63b], Z. Zhang[67], H. Zhao[142], T. Zhao[63b], Y. Zhao[139], Z. Zhao[63a], Z. Zhao[63a], A. Zhemchugov[39], J. Zheng[114a], K. Zheng[165], X. Zheng[63a], Z. Zheng[147], D. Zhong[165], B. Zhou[108], H. Zhou[7], N. Zhou[63c], Y. Zhou[15], Y. Zhou[114a], Y. Zhou[7], C.G. Zhu[63b], J. Zhu[108], X. Zhu[63d], Y. Zhu[63c], Y. Zhu[63a], X. Zhuang[14], K. Zhukov[38], N.I. Zimine[39], J. Zinsser[64b], M. Ziolkowski[145], L. Živković[16], A. Zoccoli[24b,24a], K. Zoch[62], T.G. Zorbas[143], O. Zormpa[47], W. Zou[42], L. Zwalinski[37].

[1]Department of Physics, University of Adelaide, Adelaide; Australia.
[2]Department of Physics, University of Alberta, Edmonton AB; Canada.
[3](a)Department of Physics, Ankara University, Ankara;(b)Division of Physics, TOBB University of Economics and Technology, Ankara; Türkiye.
[4]LAPP, Université Savoie Mont Blanc, CNRS/IN2P3, Annecy; France.
[5]APC, Université Paris Cité, CNRS/IN2P3, Paris; France.
[6]High Energy Physics Division, Argonne National Laboratory, Argonne IL; United States of America.
[7]Department of Physics, University of Arizona, Tucson AZ; United States of America.
[8]Department of Physics, University of Texas at Arlington, Arlington TX; United States of America.
[9]Physics Department, National and Kapodistrian University of Athens, Athens; Greece.
[10]Physics Department, National Technical University of Athens, Zografou; Greece.
[11]Department of Physics, University of Texas at Austin, Austin TX; United States of America.
[12]Institute of Physics, Azerbaijan Academy of Sciences, Baku; Azerbaijan.
[13]Institut de Física d'Altes Energies (IFAE), Barcelona Institute of Science and Technology, Barcelona; Spain.
[14]Institute of High Energy Physics, Chinese Academy of Sciences, Beijing; China.
[15]Physics Department, Tsinghua University, Beijing; China.
[16]Institute of Physics, University of Belgrade, Belgrade; Serbia.
[17]Department for Physics and Technology, University of Bergen, Bergen; Norway.
[18](a)Physics Division, Lawrence Berkeley National Laboratory, Berkeley CA;(b)University of California,

Berkeley CA; United States of America.
[19]Institut für Physik, Humboldt Universität zu Berlin, Berlin; Germany.
[20]Albert Einstein Center for Fundamental Physics and Laboratory for High Energy Physics, University of Bern, Bern; Switzerland.
[21]School of Physics and Astronomy, University of Birmingham, Birmingham; United Kingdom.
[22](a)Department of Physics, Bogazici University, Istanbul;(b)Department of Physics Engineering, Gaziantep University, Gaziantep;(c)Department of Physics, Istanbul University, Istanbul; Türkiye.
[23](a)Facultad de Ciencias y Centro de Investigaciónes, Universidad Antonio Nariño, Bogotá;(b)Departamento de Física, Universidad Nacional de Colombia, Bogotá; Colombia.
[24](a)Dipartimento di Fisica e Astronomia A. Righi, Università di Bologna, Bologna;(b)INFN Sezione di Bologna; Italy.
[25]Physikalisches Institut, Universität Bonn, Bonn; Germany.
[26]Department of Physics, Boston University, Boston MA; United States of America.
[27]Department of Physics, Brandeis University, Waltham MA; United States of America.
[28](a)Transilvania University of Brasov, Brasov;(b)Horia Hulubei National Institute of Physics and Nuclear Engineering, Bucharest;(c)Department of Physics, Alexandru Ioan Cuza University of Iasi, Iasi;(d)National Institute for Research and Development of Isotopic and Molecular Technologies, Physics Department, Cluj-Napoca;(e)National University of Science and Technology Politechnica, Bucharest;(f)West University in Timisoara, Timisoara;(g)Faculty of Physics, University of Bucharest, Bucharest; Romania.
[29](a)Faculty of Mathematics, Physics and Informatics, Comenius University, Bratislava;(b)Department of Subnuclear Physics, Institute of Experimental Physics of the Slovak Academy of Sciences, Kosice; Slovak Republic.
[30]Physics Department, Brookhaven National Laboratory, Upton NY; United States of America.
[31]Universidad de Buenos Aires, Facultad de Ciencias Exactas y Naturales, Departamento de Física, y CONICET, Instituto de Física de Buenos Aires (IFIBA), Buenos Aires; Argentina.
[32]California State University, CA; United States of America.
[33]Cavendish Laboratory, University of Cambridge, Cambridge; United Kingdom.
[34](a)Department of Physics, University of Cape Town, Cape Town;(b)iThemba Labs, Western Cape;(c)Department of Mechanical Engineering Science, University of Johannesburg, Johannesburg;(d)National Institute of Physics, University of the Philippines Diliman (Philippines);(e)University of South Africa, Department of Physics, Pretoria;(f)University of Zululand, KwaDlangezwa;(g)School of Physics, University of the Witwatersrand, Johannesburg; South Africa.
[35]Department of Physics, Carleton University, Ottawa ON; Canada.
[36](a)Faculté des Sciences Ain Chock, Université Hassan II de Casablanca;(b)Faculté des Sciences, Université Ibn-Tofail, Kénitra;(c)Faculté des Sciences Semlalia, Université Cadi Ayyad, LPHEA-Marrakech;(d)LPMR, Faculté des Sciences, Université Mohamed Premier, Oujda;(e)Faculté des sciences, Université Mohammed V, Rabat;(f)Institute of Applied Physics, Mohammed VI Polytechnic University, Ben Guerir; Morocco.
[37]CERN, Geneva; Switzerland.
[38]Affiliated with an institute covered by a cooperation agreement with CERN.
[39]Affiliated with an international laboratory covered by a cooperation agreement with CERN.
[40]Enrico Fermi Institute, University of Chicago, Chicago IL; United States of America.
[41]LPC, Université Clermont Auvergne, CNRS/IN2P3, Clermont-Ferrand; France.
[42]Nevis Laboratory, Columbia University, Irvington NY; United States of America.
[43]Niels Bohr Institute, University of Copenhagen, Copenhagen; Denmark.
[44](a)Dipartimento di Fisica, Università della Calabria, Rende;(b)INFN Gruppo Collegato di Cosenza, Laboratori Nazionali di Frascati; Italy.

[45]Physics Department, Southern Methodist University, Dallas TX; United States of America.
[46]Physics Department, University of Texas at Dallas, Richardson TX; United States of America.
[47]National Centre for Scientific Research "Demokritos", Agia Paraskevi; Greece.
[48](a)Department of Physics, Stockholm University;(b)Oskar Klein Centre, Stockholm; Sweden.
[49]Deutsches Elektronen-Synchrotron DESY, Hamburg and Zeuthen; Germany.
[50]Fakultät Physik , Technische Universität Dortmund, Dortmund; Germany.
[51]Institut für Kern- und Teilchenphysik, Technische Universität Dresden, Dresden; Germany.
[52]Department of Physics, Duke University, Durham NC; United States of America.
[53]SUPA - School of Physics and Astronomy, University of Edinburgh, Edinburgh; United Kingdom.
[54]INFN e Laboratori Nazionali di Frascati, Frascati; Italy.
[55]Physikalisches Institut, Albert-Ludwigs-Universität Freiburg, Freiburg; Germany.
[56]II. Physikalisches Institut, Georg-August-Universität Göttingen, Göttingen; Germany.
[57]Département de Physique Nucléaire et Corpusculaire, Université de Genève, Genève; Switzerland.
[58](a)Dipartimento di Fisica, Università di Genova, Genova;(b)INFN Sezione di Genova; Italy.
[59]II. Physikalisches Institut, Justus-Liebig-Universität Giessen, Giessen; Germany.
[60]SUPA - School of Physics and Astronomy, University of Glasgow, Glasgow; United Kingdom.
[61]LPSC, Université Grenoble Alpes, CNRS/IN2P3, Grenoble INP, Grenoble; France.
[62]Laboratory for Particle Physics and Cosmology, Harvard University, Cambridge MA; United States of America.
[63](a)Department of Modern Physics and State Key Laboratory of Particle Detection and Electronics, University of Science and Technology of China, Hefei;(b)Institute of Frontier and Interdisciplinary Science and Key Laboratory of Particle Physics and Particle Irradiation (MOE), Shandong University, Qingdao;(c)School of Physics and Astronomy, Shanghai Jiao Tong University, Key Laboratory for Particle Astrophysics and Cosmology (MOE), SKLPPC, Shanghai;(d)Tsung-Dao Lee Institute, Shanghai;(e)School of Physics, Zhengzhou University; China.
[64](a)Kirchhoff-Institut für Physik, Ruprecht-Karls-Universität Heidelberg, Heidelberg;(b)Physikalisches Institut, Ruprecht-Karls-Universität Heidelberg, Heidelberg; Germany.
[65](a)Department of Physics, Chinese University of Hong Kong, Shatin, N.T., Hong Kong;(b)Department of Physics, University of Hong Kong, Hong Kong;(c)Department of Physics and Institute for Advanced Study, Hong Kong University of Science and Technology, Clear Water Bay, Kowloon, Hong Kong; China.
[66]Department of Physics, National Tsing Hua University, Hsinchu; Taiwan.
[67]IJCLab, Université Paris-Saclay, CNRS/IN2P3, 91405, Orsay; France.
[68]Centro Nacional de Microelectrónica (IMB-CNM-CSIC), Barcelona; Spain.
[69]Department of Physics, Indiana University, Bloomington IN; United States of America.
[70](a)INFN Gruppo Collegato di Udine, Sezione di Trieste, Udine;(b)ICTP, Trieste;(c)Dipartimento Politecnico di Ingegneria e Architettura, Università di Udine, Udine; Italy.
[71](a)INFN Sezione di Lecce;(b)Dipartimento di Matematica e Fisica, Università del Salento, Lecce; Italy.
[72](a)INFN Sezione di Milano;(b)Dipartimento di Fisica, Università di Milano, Milano; Italy.
[73](a)INFN Sezione di Napoli;(b)Dipartimento di Fisica, Università di Napoli, Napoli; Italy.
[74](a)INFN Sezione di Pavia;(b)Dipartimento di Fisica, Università di Pavia, Pavia; Italy.
[75](a)INFN Sezione di Pisa;(b)Dipartimento di Fisica E. Fermi, Università di Pisa, Pisa; Italy.
[76](a)INFN Sezione di Roma;(b)Dipartimento di Fisica, Sapienza Università di Roma, Roma; Italy.
[77](a)INFN Sezione di Roma Tor Vergata;(b)Dipartimento di Fisica, Università di Roma Tor Vergata, Roma; Italy.
[78](a)INFN Sezione di Roma Tre;(b)Dipartimento di Matematica e Fisica, Università Roma Tre, Roma; Italy.
[79](a)INFN-TIFPA;(b)Università degli Studi di Trento, Trento; Italy.

[80]Universität Innsbruck, Department of Astro and Particle Physics, Innsbruck; Austria.
[81]University of Iowa, Iowa City IA; United States of America.
[82]Department of Physics and Astronomy, Iowa State University, Ames IA; United States of America.
[83]Istinye University, Sariyer, Istanbul; Türkiye.
[84](a)Departamento de Engenharia Elétrica, Universidade Federal de Juiz de Fora (UFJF), Juiz de Fora;(b)Universidade Federal do Rio De Janeiro COPPE/EE/IF, Rio de Janeiro;(c)Instituto de Física, Universidade de São Paulo, São Paulo;(d)Rio de Janeiro State University, Rio de Janeiro;(e)Federal University of Bahia, Bahia; Brazil.
[85]KEK, High Energy Accelerator Research Organization, Tsukuba; Japan.
[86]Graduate School of Science, Kobe University, Kobe; Japan.
[87](a)AGH University of Krakow, Faculty of Physics and Applied Computer Science, Krakow;(b)Marian Smoluchowski Institute of Physics, Jagiellonian University, Krakow; Poland.
[88]Institute of Nuclear Physics Polish Academy of Sciences, Krakow; Poland.
[89]Faculty of Science, Kyoto University, Kyoto; Japan.
[90]Research Center for Advanced Particle Physics and Department of Physics, Kyushu University, Fukuoka ; Japan.
[91]L2IT, Université de Toulouse, CNRS/IN2P3, UPS, Toulouse; France.
[92]Instituto de Física La Plata, Universidad Nacional de La Plata and CONICET, La Plata; Argentina.
[93]Physics Department, Lancaster University, Lancaster; United Kingdom.
[94]Oliver Lodge Laboratory, University of Liverpool, Liverpool; United Kingdom.
[95]Department of Experimental Particle Physics, Jožef Stefan Institute and Department of Physics, University of Ljubljana, Ljubljana; Slovenia.
[96]School of Physics and Astronomy, Queen Mary University of London, London; United Kingdom.
[97]Department of Physics, Royal Holloway University of London, Egham; United Kingdom.
[98]Department of Physics and Astronomy, University College London, London; United Kingdom.
[99]Louisiana Tech University, Ruston LA; United States of America.
[100]Fysiska institutionen, Lunds universitet, Lund; Sweden.
[101]Departamento de Física Teorica C-15 and CIAFF, Universidad Autónoma de Madrid, Madrid; Spain.
[102]Institut für Physik, Universität Mainz, Mainz; Germany.
[103]School of Physics and Astronomy, University of Manchester, Manchester; United Kingdom.
[104]CPPM, Aix-Marseille Université, CNRS/IN2P3, Marseille; France.
[105]Department of Physics, University of Massachusetts, Amherst MA; United States of America.
[106]Department of Physics, McGill University, Montreal QC; Canada.
[107]School of Physics, University of Melbourne, Victoria; Australia.
[108]Department of Physics, University of Michigan, Ann Arbor MI; United States of America.
[109]Department of Physics and Astronomy, Michigan State University, East Lansing MI; United States of America.
[110]Group of Particle Physics, University of Montreal, Montreal QC; Canada.
[111]Fakultät für Physik, Ludwig-Maximilians-Universität München, München; Germany.
[112]Max-Planck-Institut für Physik (Werner-Heisenberg-Institut), München; Germany.
[113]Graduate School of Science and Kobayashi-Maskawa Institute, Nagoya University, Nagoya; Japan.
[114](a)Department of Physics, Nanjing University, Nanjing;(b)School of Science, Shenzhen Campus of Sun Yat-sen University;(c)University of Chinese Academy of Science (UCAS), Beijing; China.
[115]Department of Physics and Astronomy, University of New Mexico, Albuquerque NM; United States of America.
[116]Institute for Mathematics, Astrophysics and Particle Physics, Radboud University/Nikhef, Nijmegen; Netherlands.

[117]Nikhef National Institute for Subatomic Physics and University of Amsterdam, Amsterdam; Netherlands.
[118]Department of Physics, Northern Illinois University, DeKalb IL; United States of America.
[119](a)New York University Abu Dhabi, Abu Dhabi;(b)United Arab Emirates University, Al Ain; United Arab Emirates.
[120]Department of Physics, New York University, New York NY; United States of America.
[121]Ochanomizu University, Otsuka, Bunkyo-ku, Tokyo; Japan.
[122]Ohio State University, Columbus OH; United States of America.
[123]Homer L. Dodge Department of Physics and Astronomy, University of Oklahoma, Norman OK; United States of America.
[124]Department of Physics, Oklahoma State University, Stillwater OK; United States of America.
[125]Palacký University, Joint Laboratory of Optics, Olomouc; Czech Republic.
[126]Institute for Fundamental Science, University of Oregon, Eugene, OR; United States of America.
[127]Graduate School of Science, Osaka University, Osaka; Japan.
[128]Department of Physics, University of Oslo, Oslo; Norway.
[129]Department of Physics, Oxford University, Oxford; United Kingdom.
[130]LPNHE, Sorbonne Université, Université Paris Cité, CNRS/IN2P3, Paris; France.
[131]Department of Physics, University of Pennsylvania, Philadelphia PA; United States of America.
[132]Department of Physics and Astronomy, University of Pittsburgh, Pittsburgh PA; United States of America.
[133](a)Laboratório de Instrumentação e Física Experimental de Partículas - LIP, Lisboa;(b)Departamento de Física, Faculdade de Ciências, Universidade de Lisboa, Lisboa;(c)Departamento de Física, Universidade de Coimbra, Coimbra;(d)Centro de Física Nuclear da Universidade de Lisboa, Lisboa;(e)Departamento de Física, Universidade do Minho, Braga;(f)Departamento de Física Teórica y del Cosmos, Universidad de Granada, Granada (Spain);(g)Departamento de Física, Instituto Superior Técnico, Universidade de Lisboa, Lisboa; Portugal.
[134]Institute of Physics of the Czech Academy of Sciences, Prague; Czech Republic.
[135]Czech Technical University in Prague, Prague; Czech Republic.
[136]Charles University, Faculty of Mathematics and Physics, Prague; Czech Republic.
[137]Particle Physics Department, Rutherford Appleton Laboratory, Didcot; United Kingdom.
[138]IRFU, CEA, Université Paris-Saclay, Gif-sur-Yvette; France.
[139]Santa Cruz Institute for Particle Physics, University of California Santa Cruz, Santa Cruz CA; United States of America.
[140](a)Departamento de Física, Pontificia Universidad Católica de Chile, Santiago;(b)Millennium Institute for Subatomic physics at high energy frontier (SAPHIR), Santiago;(c)Instituto de Investigación Multidisciplinario en Ciencia y Tecnología, y Departamento de Física, Universidad de La Serena;(d)Universidad Andres Bello, Department of Physics, Santiago;(e)Instituto de Alta Investigación, Universidad de Tarapacá, Arica;(f)Departamento de Física, Universidad Técnica Federico Santa María, Valparaíso; Chile.
[141]Department of Physics, Institute of Science, Tokyo; Japan.
[142]Department of Physics, University of Washington, Seattle WA; United States of America.
[143]Department of Physics and Astronomy, University of Sheffield, Sheffield; United Kingdom.
[144]Department of Physics, Shinshu University, Nagano; Japan.
[145]Department Physik, Universität Siegen, Siegen; Germany.
[146]Department of Physics, Simon Fraser University, Burnaby BC; Canada.
[147]SLAC National Accelerator Laboratory, Stanford CA; United States of America.
[148]Department of Physics, Royal Institute of Technology, Stockholm; Sweden.

[149]Departments of Physics and Astronomy, Stony Brook University, Stony Brook NY; United States of America.
[150]Department of Physics and Astronomy, University of Sussex, Brighton; United Kingdom.
[151]School of Physics, University of Sydney, Sydney; Australia.
[152]Institute of Physics, Academia Sinica, Taipei; Taiwan.
[153](a)E. Andronikashvili Institute of Physics, Iv. Javakhishvili Tbilisi State University, Tbilisi;(b)High Energy Physics Institute, Tbilisi State University, Tbilisi;(c)University of Georgia, Tbilisi; Georgia.
[154]Department of Physics, Technion, Israel Institute of Technology, Haifa; Israel.
[155]Raymond and Beverly Sackler School of Physics and Astronomy, Tel Aviv University, Tel Aviv; Israel.
[156]Department of Physics, Aristotle University of Thessaloniki, Thessaloniki; Greece.
[157]International Center for Elementary Particle Physics and Department of Physics, University of Tokyo, Tokyo; Japan.
[158]Department of Physics, University of Toronto, Toronto ON; Canada.
[159](a)TRIUMF, Vancouver BC;(b)Department of Physics and Astronomy, York University, Toronto ON; Canada.
[160]Division of Physics and Tomonaga Center for the History of the Universe, Faculty of Pure and Applied Sciences, University of Tsukuba, Tsukuba; Japan.
[161]Department of Physics and Astronomy, Tufts University, Medford MA; United States of America.
[162]Department of Physics and Astronomy, University of California Irvine, Irvine CA; United States of America.
[163]University of Sharjah, Sharjah; United Arab Emirates.
[164]Department of Physics and Astronomy, University of Uppsala, Uppsala; Sweden.
[165]Department of Physics, University of Illinois, Urbana IL; United States of America.
[166]Instituto de Física Corpuscular (IFIC), Centro Mixto Universidad de Valencia - CSIC, Valencia; Spain.
[167]Department of Physics, University of British Columbia, Vancouver BC; Canada.
[168]Department of Physics and Astronomy, University of Victoria, Victoria BC; Canada.
[169]Fakultät für Physik und Astronomie, Julius-Maximilians-Universität Würzburg, Würzburg; Germany.
[170]Department of Physics, University of Warwick, Coventry; United Kingdom.
[171]Waseda University, Tokyo; Japan.
[172]Department of Particle Physics and Astrophysics, Weizmann Institute of Science, Rehovot; Israel.
[173]Department of Physics, University of Wisconsin, Madison WI; United States of America.
[174]Fakultät für Mathematik und Naturwissenschaften, Fachgruppe Physik, Bergische Universität Wuppertal, Wuppertal; Germany.
[175]Department of Physics, Yale University, New Haven CT; United States of America.
[a] Also Affiliated with an institute covered by a cooperation agreement with CERN.
[b] Also at An-Najah National University, Nablus; Palestine.
[c] Also at Borough of Manhattan Community College, City University of New York, New York NY; United States of America.
[d] Also at Center for Interdisciplinary Research and Innovation (CIRI-AUTH), Thessaloniki; Greece.
[e] Also at Centro Studi e Ricerche Enrico Fermi; Italy.
[f] Also at CERN, Geneva; Switzerland.
[g] Also at CMD-AC UNEC Research Center, Azerbaijan State University of Economics (UNEC); Azerbaijan.
[h] Also at Département de Physique Nucléaire et Corpusculaire, Université de Genève, Genève; Switzerland.
[i] Also at Departament de Fisica de la Universitat Autonoma de Barcelona, Barcelona; Spain.
[j] Also at Department of Financial and Management Engineering, University of the Aegean, Chios; Greece.

[k] Also at Department of Physics, California State University, Sacramento; United States of America.
[l] Also at Department of Physics, King's College London, London; United Kingdom.
[m] Also at Department of Physics, Stanford University, Stanford CA; United States of America.
[n] Also at Department of Physics, Stellenbosch University; South Africa.
[o] Also at Department of Physics, University of Fribourg, Fribourg; Switzerland.
[p] Also at Department of Physics, University of Thessaly; Greece.
[q] Also at Department of Physics, Westmont College, Santa Barbara; United States of America.
[r] Also at Faculty of Physics, Sofia University, 'St. Kliment Ohridski', Sofia; Bulgaria.
[s] Also at Hellenic Open University, Patras; Greece.
[t] Also at Institucio Catalana de Recerca i Estudis Avancats, ICREA, Barcelona; Spain.
[u] Also at Institut für Experimentalphysik, Universität Hamburg, Hamburg; Germany.
[v] Also at Institute for Nuclear Research and Nuclear Energy (INRNE) of the Bulgarian Academy of Sciences, Sofia; Bulgaria.
[w] Also at Institute of Applied Physics, Mohammed VI Polytechnic University, Ben Guerir; Morocco.
[x] Also at Institute of Particle Physics (IPP); Canada.
[y] Also at Institute of Physics and Technology, Mongolian Academy of Sciences, Ulaanbaatar; Mongolia.
[z] Also at Institute of Physics, Azerbaijan Academy of Sciences, Baku; Azerbaijan.
[aa] Also at Institute of Theoretical Physics, Ilia State University, Tbilisi; Georgia.
[ab] Also at National Institute of Physics, University of the Philippines Diliman (Philippines); Philippines.
[ac] Also at Technical University of Munich, Munich; Germany.
[ad] Also at The Collaborative Innovation Center of Quantum Matter (CICQM), Beijing; China.
[ae] Also at TRIUMF, Vancouver BC; Canada.
[af] Also at Università di Napoli Parthenope, Napoli; Italy.
[ag] Also at University of Colorado Boulder, Department of Physics, Colorado; United States of America.
[ah] Also at Washington College, Chestertown, MD; United States of America.
[ai] Also at Yeditepe University, Physics Department, Istanbul; Türkiye.
[*] Deceased